The Dissertation Committee for Aimee Elizabeth Talarski certifies that this is the approved version of the following dissertation:

Genetic basis for ichthyotoxicity and osmoregulation in the euryhaline haptophyte, *Prymnesium parvum* **N. Carter**

Committee:

_____
John W. La Claire, II, Supervisor

_____
Deana Erdner

_____
Stanley Roux

_____
David Herrin

_____
Robert Jansen

Genetic basis for ichthyotoxicity and osmoregulation in the euryhaline haptophyte, *Prymnesium parvum* N. Carter

by

Aimee Elizabeth Talarski, B.S.; M.S.

Dissertation

Presented to the Faculty of the Graduate School of

The University of Texas at Austin

in Partial Fulfillment

of the Requirements

for the Degree of

Doctor of Philosophy

The University of Texas at Austin

May 2014

Dedication

This dissertation is dedicated in loving memory of my son, Bobby Talarski Hamza.

Acknowledgements

Genetic basis for ichthyotoxicity and osmoregulation in the euryhaline haptophyte, *Prymnesium parvum* N. Carter

Aimee Elizabeth Talarski, Ph.D.

The University of Texas at Austin, 2014

Supervisor: John W. La Claire, II

There is limited information currently available regarding the underlying physiological responses and molecular mechanisms of osmoregulation, acetate metabolism [in relation to the synthesis of glycerolipids, polyunsaturated fatty acids (PUFA), and ichthyotoxins], and transport in *Prymnesium parvum* N. Carter, a microalga that causes devastating harmful algal blooms (HAB) worldwide. This dissertation examines gene expression under environmental conditions that are associated with HAB formation, including phosphate limitation and low salinity, using microarrays and RNA sequencing (RNA-Seq). A comparative fatty acid methyl ester (FAME) analysis at 30 *vs*. 5 practical salinity units (psu) was performed to gain additional insight into acetate metabolism. The RNA-Seq analysis included a *de novo* assembly of the *P. parvum* transcriptome, generating 47,289 transcripts, of which 35.4% were identifiable. This permitted the evaluation of the expression of many more genes compared with the microarray analysis, which examined ~3,500 genes. Relevant candidate genes identified included those whose products are involved in osmolyte production, salinity stress, and ion transport. With respect to the putative synthesis of polyketide ichthyotoxins, 32 different polyketide synthase (PKS) transcripts were identified in the transcriptome assembly, none of which were differentially expressed. Hemolysin and monogalactosyldiacylglycerol synthase were downregulated at 30 *vs*. 5 psu, suggesting the increased presence of additional ichthyotoxins at the lower salinity. Evidence for several PUFA synthesis pathways was also revealed. Fatty acid compositions were

largely similar at the two salinities, containing relatively prominent quantities of the PUFA stearidonic acid, but compositions varied among strains. The transcription of genes whose products are associated with vesicular transport was elevated, and higher levels of extracellular prymnesins were observed in HAB-forming conditions. Thus, with regard to acetate metabolism, I have revealed evidence for the post-transcriptional regulation of the production of prymnesins and the contributory effects of hemolysin, monogalactosyldiacylglycerol, and PUFA towards ichthyotoxicity. Further, I propose that toxin transport is triggered in HAB-forming conditions, in which the toxins are actively being excreted. Collectively, these data shed light on the transcriptional responses that occur following alterations in phosphate availability and salinity, including those associated with the synthesis and delivery of a number of potential ichthyotoxins from *P. parvum*.

Table of Contents

List of Tables

List of Figures

Chapter 1: Introduction

1.1 THE ORGANISM

Prymnesium parvum is a globally distributed, unicellular isokont belonging to the phylum Haptophyta (Coleman, 1988; Guo *et al*., 1996; Johansson and Graneli, 1999; Barkoh *et al*., 2008). It is commonly referred to as the "golden alga" due to the preponderance of carotenoids in its plastids, which cause bodies of water to take on a golden hue during periods of bloom (Jeffrey and Wright, 1994; Olli and Trunov, 2007). It is mixotrophic, ingesting dissolved organic and particulate matter, including bacteria and protists, in addition to deriving energy from photosynthesis (Moestrup, 1994; Graneli and Carlsson, 1998; Baker *et al*., 2007; Burkholder *et al*., 2008; Lindehoff *et al*., 2009; Bowers *et al*., 2010). It is also euryhaline and has been shown to be able to adapt to media salinity levels ranging from 3 to 30 practical salinity units (psu), although it typically forms blooms in brackish waters (Larsen and Bryant, 1998; Graneli *et al*., 2012). These harmful algal blooms (HABs) have led to extensive fish kills worldwide (Otterstrøm and Steeman-Nielsen, 1940; Shilo, 1971; Holmquist and Willen, 1993). The consequential negative impact on the coastal marine ecosystem and associated economic problems for commercial aquaculture have prompted extensive studies on this organism. Much research on *P*. *parvum* HABs has been focused on the environmental causes of blooms, toxin identification, and bloom management (Guo *et al*., 1996; Johansson and Graneli, 1999; Graneli and Johansson, 2003; Sengco *et al*., 2005; Barkoh *et al*., 2008). For example, blooms typically coincide with abiotic and biotic stress events, including not only salt stress but also nutrient limitation (nitrogen and/or phosphate) and fluctuations in temperature and light intensity (Yariv and Hestrin, 1961; Shilo, 1967; Larsen *et al*., 1993; Stabell *et al*., 1993; Simonsen and Moestrup, 1997; Igarashi *et al*., 1999; Johansson and Graneli, 1999).

1.2 PRYMNESINS

The toxins that have long been thought to be responsible for the ichthyotoxicity of *P. parvum* HABs include prymnesins-1 and -2 (Fig. 1.1) (Yariv and Hestrin, 1961; Igarashi *et al.*, 1999; Sengco *et al.*, 2005), although recently, other compounds have also been suggested to play roles, including fatty acid amides, polyunsaturated fatty acids (PUFA), and galactolipids (Kozakai *et al.*, 1982; Henrikson *et al.*, 2010; Bertin *et al.*, 2012). Prymnesins in particular belong to a class of secondary metabolites called polyketides (Reich *et al.*, 1965; Igarashi *et al.*, 1996). Such secondary metabolites are not critical to the survival of an organism but may confer advantages, such as defense, predation, and competitor reduction as has been suggested for prymnesins (Driscoll *et al.*, 2013). Ichthyotoxicity is generally caused by increasing permeability of the gill cell membranes, leading to cell swelling and subsequent lysis and death (Yariv and Hestrin, 1961; Dafni and Shilo, 1966; Paster, 1973). Notably, *P. parvum* does not exhibit autotoxicity (Fistarol *et al.*, 2003). Prymnesins require cofactors for activation, such as Ca^{2+}, Mg^{2+}, and Na^+, and antibiotics, including streptomycin (Yariv and Hestrin, 1961; Ulitzur and Shilo, 1964; Sarig, 1989). The precise mechanisms that are involved in prymnesin synthesis and delivery remain to be delineated.

.
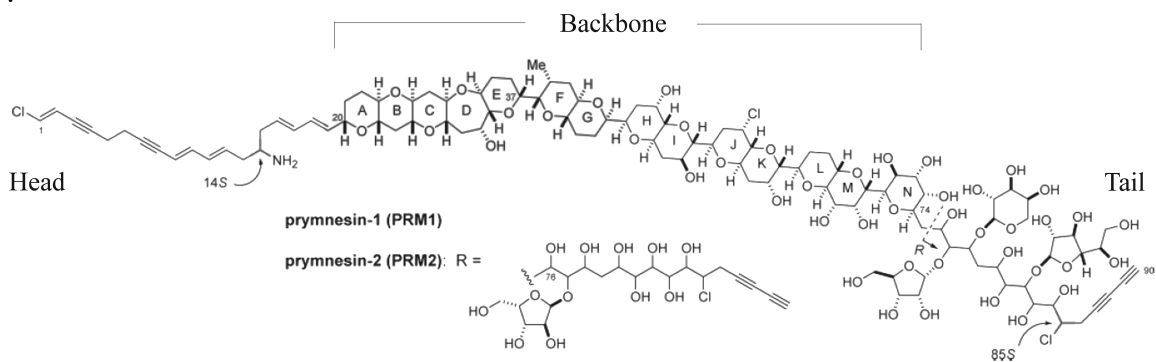
Figure 1.1   Structures of prymnesins-1 and -2 (insert). Reproduced with permission from Manning and La Claire (2010).

2

Structurally, the prymnesins are amphiphilic, glycosidic toxins that are 90 carbons in length and contain trans-1,6-transdioxadecaline units, conjugated double and triple bonds, and chlorine and nitrogen atoms (Igarashi *et al*., 1999). As polyketides, they possess the characteristic keto groups that are attached to many of their alternating carbon atoms. In prymnesins and a number of other polyketides, these keto groups are reduced to hydroxyl groups during biosynthesis (Hopwood and Sherman, 1990; Igarashi *et al*., 1999). Prymnesins are structurally similar to toxins that are produced by other algae utilizing modular type I polyketide synthase (PKS) enzymes, including maitotoxin and ciguatoxin in dinoflagellates, which both contain polycyclic ether moieties (Murata and Yasumoto, 2000).

1.2.1 Putative Role of PKS in Prymnesin Synthesis

Polyketides include a very diverse group of compounds with different functions depending on the side chains, chain lengths, and keto group positioning (Hopwood and Sherman, 1990). PKS enzymes include types I, II, and III. Type I PKS can be modular or iterative; the former possess enzymes that are arranged in distinct modules, while the latter contains the same catalytic domains but on a single polypeptide. Type II PKS is also iterative, but contains slight differences in its catalytic domains. Type III PKS is iterative and homodimeric, typically acting primarily as a condensing enzyme (Hopwood and Sherman, 1990; Shen, 2003). The polyketide prymnesins are thought to be synthesized by the PKS enzyme complex in an acetate-metabolism-related pathway (Cane and Walsh, 1999; Mann, 2001). Genes encoding type I PKS in particular have been isolated and sequenced from axenic *P*. *parvum* cultures (La Claire, 2006), and this enzyme is thought to be responsible for prymnesin synthesis. Type I PKS has also been detected in closely related organisms, including *Emiliana huxleyi* (John *et al*., 2008). This enzyme complex consists of modular, covalently linked proteins, and it synthesizes polyketides by successive Claisen condensations of malonyl-CoA-derived extender units

3

to carboxylic acid starter units in a manner that is very similar to fatty acid biosynthesis. The malonyl Co-A is formed from the carboxylation of acetyl-CoA and CO_2; thus, acetyl-CoA availability is critical to polyketide synthesis via PKS (Moore and Hertweck, 2001; Smith and Tsai, 2007).

1.3 ACETATE METABOLISM IN POLYKETIDE AND FATTY ACID BIOSYNTHESIS

Although acetyl-CoA is necessary for both fatty acid and polyketide biosynthesis, it cannot be transported across membranes. Thus, different subcellular compartments must independently synthesize their own pools for relevant metabolic processes. The plastid is the main site of fatty acid biosynthesis, where the acetyl-CoA is typically supplied by acetate and pyruvate via the actions of the pyruvate dehydrogenase complex and acetyl-CoA synthetase (Ke *et al.*, 2000; Oliver *et al.*, 2009). The cytosol is where fatty acid elongation primarily takes place, and cytoplasmic acetyl-CoA is typically supplied by citrate via the activity of ATP citrate lyase (Ke *et al.*, 2000; Fatland *et al.*, 2002; Khozin-Goldberg and Cohen, 2011). Other organelles that contain acetyl-CoA pools include the mitochondria, where acetyl-CoA may be converted to citrate and supplied to the tricarboxylic acid (TCA) cycle or be involved in fatty acid biosynthesis and breakdown, and peroxisomes, where fatty acids are broken down (Oliver *et al.*, 2009). Although the plastid is the main site of fatty acid biosynthesis by the enzyme fatty acid synthase (FAS) (Ohlrogge and Browse, 1995; Nikolau *et al.*, 2003; Joyard *et al.*, 2010), the site of prymnesin synthesis by PKS in *P. parvum* is unknown. It may occur in the chloroplast or cytosol, or alternatively, a precursor may be formed in the chloroplast that is exported to the endoplasmic reticulum (ER) for additional processing, as has been suggested to occur in the formation of the structurally similar brevetoxins in the dinoflagellate *Karenia brevis* (Huerlimann and Heimann, 2013; Van Dolah *et al.*, 2013). Thus, each sub-cellular site contains unique enzymes for the synthesis of acetyl-CoA, and

enzyme activities may be investigated at the transcriptional level in addition to those of the FAS and PKS enzymes, and their associated modules.

1.3.1 Modular Type I FAS Activities

The first committed step in fatty acid biosynthesis is the carboxylation of acetyl-CoA to form malonyl-CoA. Thus, it is a point of regulation for this pathway (Ohlrogge and Browse, 1995; Khozin-Goldberg and Cohen, 2011). The biosynthesis of fatty acids by the modular enzyme Type I FAS initiates with the transfer of a coenzyme A-linked starter unit to an acyl carrier protein (ACP) by an acyltransferase (AT). At this point, the growing chain is tethered to the enzymatic apparatus by a thioester linkage (Hopwood and Sherman, 1990; Kwan and Schulz, 2011). Next, ketosynthase (KS) extends the growing chain by decarboxylative condensation. The AT, KS, and ACP constitute the core catalytic domains, and the auxiliary domains, which are reductive elements, include ketoreductase (KR), dehydratase (DH), and enoyl reductase (ER). Following synthesis, the final fully reduced, aliphatic molecule is released from the enzymatic apparatus by a thioesterase (TE) (Cane and Walsh, 1999; Smith and Tsai, 2007; Korman *et al.*, 2010; Arakawa, 2012). FAS produces saturated acyl moieties with either 16 or 18 carbons, which are largely utilized to form glycerolipid membrane components. They also may be exported from the plastid for further modifications, such as elongation, desaturation, and phospholipid and triacylglycerol (TAG) formation in the ER (Ohlrogge and Browse, 1995; Cook, 1996; Huerlimann and Heimann, 2013).

1.3.2 Modular Type I PKS Activities

Modular Type I PKS differs from Type I FAS due to the variable compositions that may comprise its reductive domain (Fig 1.2). Additionally, it may contain a cyclase. Thus, Type I PKS is able to produce diverse output with varying reductive states

(Hopwood and Sherman, 1990; Kwan *et al*., 2011; Arakawa, 2012). This enzyme is also capable of using alternative starter and extender units, which further contributes to this variation (Moore and Hertweck, 2001; Chan *et al*., 2009). As a result, the final products of Type I PKS include a wide array of metabolites with an assortment of functionalities (Ohlrogge and Browse, 1995; Cook, 1996; Huerlimann and Heimann, 2013).
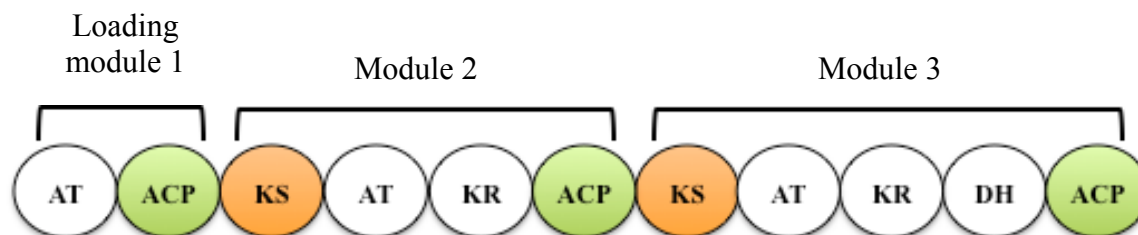
Figure 1.2   Example of modular type I PKS.

1.4 POSSIBLE MODES OF PRYMNESIN TRANSPORT

To be toxic to fish, the polyketide prymnesins must be out in the water column (Graneli *et al*., 2012). The path that prymnesins take to reach the extracellular environment is unknown. Actually, there is a lack of information concerning the mechanisms of excretion of similar polyketides in any HAB-forming algae. They may be actively extruded from *P. parvum* cells, be released from dying cells, or both. Due to the large sizes and amphipathic natures of the prymnesins, it is unlikely that they are simply diffused out of cells, although leakage from damaged cells might be possible. Many species, including plants, fungi, bacteria, and algae, use specific membrane transporters to accomplish the translocation of polyketides and other secondary metabolites (Callahan *et al*., 1999; Pfeifer and Khosla, 2001; Pearson *et al*., 2004; Yazaki, 2006; Chen *et al*., 2013; Masschelein *et al*., 2013). Alternatively, vesicle-mediated secretion is the preferred method for their export in other organisms (Kunst and Samuels, 2003; Lin *et al*., 2003;

Yazaki, 2006; Chanda *et al*., 2009; Reis *et al*., 2013). Notably, the sequestration of secondary metabolites into vesicles or vacuoles, for example, is commonly observed in a variety of eukaryotic organisms as a means of protecting cells from autotoxicity (McKey, 1979; Sirikantaramas *et al*., 2008). A similar compartmentalization of enzymes and intermediates that are involved in secondary metabolism have also been frequently reported (Chiou *et al*., 2004; Lee *et al*., 2004; Maggio-Hall *et al*., 2005; Chanda *et al*., 2009; Hong and Linz, 2009), suggesting the possibility of the involvement of several sub-cellular locations in prymnesin synthesis in *P*. *parvum*. Collectively, these data suggest that prymnesins may similarly be transported/exported via membrane transporters or a vesicle-mediated transport and secretion system in *P*. *parvum*.

1.4.1 Potential Role of Secretory Pathway in Prymnesin Secretion

The secretory system usually includes vesicles and vacuoles in addition to the ER, Golgi, endosomes, and plasma membrane (Chrispeels, 1991; Roze *et al*., 2011). The first step of secretion in the conventional pathway typically includes the sequestration of metabolites in the ER lumen, after which they traffic to the Golgi apparatus in (COPII-coated) vesicles. The metabolites are released into and pass through the Golgi and trans-Golgi network (TGN) and are again packaged into vesicles, which fuse with the plasma membrane and deposit their contents into the external environment (Neumann *et al*., 2003; Hawes and Satiat-Jeunemaitre, 2005; Peer, 2011) (Fig. 1.3). The fusion process is precipitated by the actions of tethering factors, which form loose links to connect the vesicle and target membrane (Latjinhouwers *et al*., 2005; Lupashin and Sztul, 2005). Tethering factors interact with various sub-cellular membranes and include the trafficking protein particle (TRAPP) complex, which is involved in ER-to-Golgi traffic, and the exocyst, which acts at the TGN and plasma membrane (Raymond *et al*., 1992; Sacher *et al*., 2001; Whyte and Munro, 2002). The tethering complexes are thought to activate small GTPases on the vesicle membrane, such as RAB, which facilitate the subsequent

7

vesicle docking and fusion (Batoko *et al*., 2000; Sacher *et al*., 2001; Sztul and Lupashin, 2006). ADP-ribosylation factor (ARF) is another regulatory protein that is involved in the recruitment of coat proteins, tethering complexes, and membrane remodeling enzymes (D'Souza-Schorey and Chavrier, 2006; Gillingham and Munro, 2007).

Vesicle fusion is mediated by interactions between soluble *N*-ethylmaleimide sensitive factor attachment receptor proteins (SNARES) that reside on the outer vesicle coat and cytosolic side of the plasma membrane (Moreau *et al*., 2006). Following fusion, contents are released outside of the cell. Cytoskeletal elements including actin and myosin have been linked to exocytosis and are thought to either aid in the expulsion of cargo through contractile force or to stabilize the fusion process, allowing for the release of vesicular contents. Vesicle mobility and direction also involve these two cytoskeletal proteins (Poste and Allison, 1973; Burridge and Phillips, 1975; Winsor and Schiebel, 1997; Deneka *et al*., 2003; Ojangu *et al*., 2007; Salgado *et al*., 2008; Nightingale *et al*., 2012). Elevations in cytosolic Ca^{2+} concentrations are known to induce exocytosis (Sutter *et al*., 2007). Some Ca^{2+}-dependent candidates that may be involved in the regulation of plant exocytosis include calmodulin, Ca^{2+}-dependent protein kinases, NADPH oxidases, actin-binding protein, synaptotagmin, and annexin (Cole and Fowler, 2006; Mortimer *et al*., 2008; Schapire *et al*., 2008).
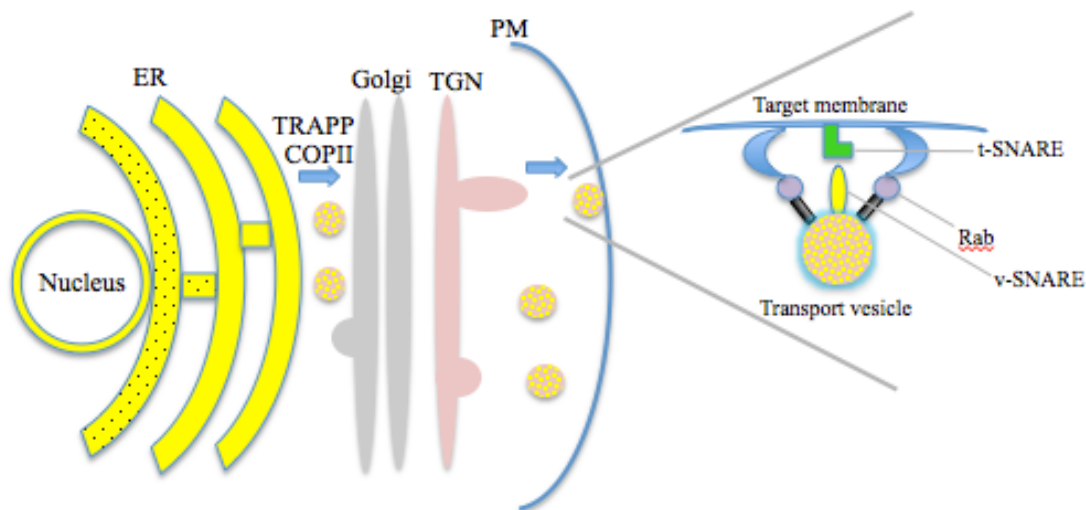
Figure 1.3 Conventional secretory pathway in eukaryotes. Arrows highlight path leading to exocytosis. Inset depicts close-up view of vesicle-target membrane interaction. PM- plasma membrane.

1.4.2 Potential Role of Membrane Transporters in Prymnesin Extrusion

In addition to vesicular transport, the sequestration and export of secondary metabolites have also been reported through the action of ATP-binding cassette (ABC) transporters. In fact, the genes encoding these transporters have been observed to be situated in close proximity to PKS genes and non-ribosomal peptide synthase (NRPS)/PKS hybrid genes in some organisms (Pfeifer and Khosla, 2001; Sun *et al.*, 2003; Pearson *et al.*, 2004; Martin *et al.*, 2005; Chen *et al.*, 2013; Masschelein *et al.*, 2013). Other transporters that have been observed to be clustered with secondary metabolite biosynthesis genes include the major facilitator superfamily, small multidrug resistance, resistance-nodulation-cell division, and drug/metabolite exporter (Paulsen *et al.*, 1996; Pao *et al.*, 1998; Daßler *et al.*, 2000; Putman *et al.*, 2000; Zheleznova *et al.*, 2000). Investigations into the proximity of these transporter genes to the secondary metabolite genes in addition to assessment of transporter activities strongly support their

involvement in secondary metabolite export. Additionally, some amphipathic secondary metabolites have been reported to utilize glutathione–S-transferase (GST) as a carrier to aid in membrane translocation (Marrs *et al*., 1995; Weisiger, 1996; Ishikawa *et al*., 1997; Rea *et al*., 1998; Walczak and Dean, 2000; Bartholomew *et al*., 2002; Kolukisaoglu *et al*., 2002). Multidrug resistance protein is typically the substrate preference for GST-conjugates, which is a family of drug transporters that includes ABC transporters (Bartholomew *et al*., 2002). Because there is a lack of knowledge regarding the transport and exudation of polyketides in toxic algae, investigations into this process are warranted.

1.5 MECHANISMS OF SALT TOLERANCE IN MARINE ALGAE

It has been established that hyposalinity stress promotes the extracellular accumulation of polyketides in *P. parvum* (Baker *et al.,* 2007 and 2009; Brooks *et al*., 2010; Freitag *et al*., 2011; Weissbach and Legrand, 2012). However, there is limited information describing the mechanisms that enable this microalga to adapt to euryhaline environments, and no information on how the prymnesins exit the cells, as already noted.

Salt tolerance in many euryhaline marine algae typically involves a two-phase process. First, cell volume is adjusted by the influx or efflux of water along the osmotic gradient. This typically occurs in a matter of seconds. Ionic adjustments also rapidly occur, mainly involving K^+, Na^+, and Cl^- (Kirst, 1989; Kobayashi *et al*., 2007). However, precise mechanisms of ionic adaptations to salt stress vary among algal species. Because excessive Na^+ concentrations are toxic to the cell, interfering with vital metabolic pathways, euryhaline and halotolerant plants and algae have developed strategies to effectively maintain homeostasis within the cell, such as the use of Na^+/H^+ antiporters to counteract excessive Na^+ uptake (Padan and Sculdiner, 1996; Inaba *et al*., 2001; Wutipraditkul *et al*., 2005). Excess Na^+ and Cl^- may also be compartmentalized (for example, into vacuoles) to decrease cytosolic ion levels and facilitate osmotic adjustment (Binzel *et al*., 1988; Niu *et al*., 1995). Notably, the initial influx of NaCl from the

external environment leads to the cytosolic accumulation of Ca^{2+}, which triggers stress signal transduction pathways, further facilitating salt adaptation (Perez-Prat *et al*., 1992; Mendoza *et al*., 1994; Knight *et al*., 1997). However, sustained increases in Ca^{2+} concentrations are also damaging to cells, so it is necessary to regain homeostasis, as well as to maintain balanced intracellular K^+ concentrations because these ions are necessary for performing essential cellular processes (Pick *et al*., 1986; Talebi *et al*., 2013). Ion homeostasis within cells is achieved through the activity of a variety of transporters, including plasma membrane and vacuolar H^+-ATPases and pyrophosphatases, Na^+- and Ca^{2+}-ATPases, secondary active transporters (antiporters and symporters), ion channels, and ABC transporters (Niu *et al*., 1995; Sze *et al*., 1999; Blumwald *et al*., 2000). It should be noted that *P*. *parvum* expresses a variety of types of ion and other transporters (La Claire, 2006; Beszteri *et al*., 2012).

Osmolytes are also important for salt-tolerant and euryhaline organisms to adapt to changing salinity levels. These compounds act as solutes to maintain osmotic balance in the cell, avoiding the accumulation of high concentrations of ions that would inhibit crucial metabolic processes (Brown and Simpson, 1972; Ford, 1984; Kobayashi *et al*., 2007). The main osmolyte that has been observed in haptophytic algae including *P*. *parvum* is β-(dimethylsulphonio)-propionate (DMSP), which is a tertiary sulfonium compound that is a precursor of dimethylsulfide (DMS) (Dickinson and Kirst, 1987; Steinke *et al*., 1998; Kobayashi *et al*., 2007). DMSP is usually associated with long-term salinity changes, particularly in hypersaline environments (Dickinson and Kirst, 1986; Young *et al*., 1987; Edwards *et al*., 1988). In marine algae, the pathway leading to DMSP synthesis has been elucidated, in which methionine undergoes transamination, reduction, methylation (which is carried out by an S-adenosylmethionine S-methyltransferase in *Enteromorpha intestinalis*), and oxidative decarboxylation reactions (Gage *et al*., 1997; Summers *et al*., 1998). Thus, the presence of this osmolyte contributes to the ability of *P*. *parvum* to adapt to fluctuating environmental salinity concentrations.

Hypersalinity has other metabolic effects. For example, it typically disrupts the activity of the photosynthetic apparatus, leading to decreased levels of light harvesting pigments (Schubert *et al*., 1993; Sayed, 2003; Kosova *et al*., 2011; Bhargava and Srivastava, 2013). CO_2 solubility is also reduced, which affects photosynthesis rates (Booth and Beardall, 1991; Moisander *et al*., 2002). Therefore, carbon acquisition-related activity may be enhanced in these conditions. Increased rates of photosynthetic CO_2 fixation and energy metabolism have also been observed in more salt-tolerant species, and carbon metabolism may likely be directed toward the synthesis of osmolytes (Takabe *et al*., 1988; Liska *et al*., 2004; Bhargava and Srivastava, 2013; Incharoensakdi and Waditee-Sirisattha, 2013). Membranes also are destabilized and undergo restructuring, affecting the solubility and transport of substrates and ions, as a potential means of enhancing salt tolerance. Additionally, membrane fluidity is often altered in the effort to maintain cell integrity, along with changes in membrane protein composition and abundance due to their syntheses and degradation (Lee *et al*., 1989; Singh *et al*., 2002; Katz *et al*., 2007). Increases in chaperone activity also typically occur, which stabilize and direct the transport and insertion of newly synthesized proteins. Further, the increased presence of ubiquitins is frequently observed, which regulate membrane protein stability and turnover. Finally, the upregulation of antioxidative stress enzymes has been observed as a secondary response to salt stress (Sunkar *et al*., 2003; Katz *et al*., 2007; Ashraf, 2009; Bhargava and Srivastava, 2013).

1.6 RESEARCH OBJECTIVES

This dissertation addresses the transcriptomic responses of *P. parvum* (UTEX 2797) to environmental stress conditions, including those of phosphate limitation and salinity. In particular, pathways involving salinity adaptation and osmoregulation were examined to obtain insight into relevant mechanisms that might confer euryhaline capabilities to this and likely other marine algae. Also, patterns of gene expression in

relation to acetate metabolism were investigated to elucidate relevant activities that occur as a result of abiotic stress, both globally and particularly in terms of prymnesin synthesis. The transcription of genes whose products are involved in transport-related processes were investigated as well, to obtain insight into potential mechanisms that may be used by this organism to deliver prymnesins to the external environment. Research objectives were accomplished using high-throughput techniques that allow for the evaluation of the expression of a large number of genes simultaneously, including DNA microarrays and RNA sequencing (RNA-Seq).

This research was conducted based on the notion that there would be significant differential gene expression occurring in treatment conditions (abiotic stress) *versus* control conditions and the prediction that altering growth conditions to induce abiotic stress would allow for the elucidation of candidate genes and mechanisms that are involved in osmoregulation and salinity adaptation, acetate metabolism and transport, and prymnesin production and secretion. Thus, my null hypothesis was that there would be no significant differences in gene expression between conditions.

In Chapter 2, microarrays were used to examine differential gene expression following the growth of *P. parvum* in both phosphate-deficient and phosphate-replete conditions. These arrays were printed in-house, and a unique working protocol was developed. Microarrays allowed for the simultaneous evaluation of the expression of approximately 3,500 genes. Although this experiment did not reveal the differential expression of any PKS genes, potential transcriptomic patterns in relation to acetate metabolism and transport began to emerge. Thus, a further and more extensive evaluation of gene expression in response to abiotic stress was desirable.

Chapter 3 is an expansion upon Chapter 2 where the number of transcripts that were able to be evaluated increased from 3,500 to over 45,000 because this method enabled the *de novo* assembly of the full *P. parvum* transcriptome. This represents a comprehensive characterization of global gene expression in this organism. Salinity stress

13

was selected as the treatment so that mechanisms of euryhaline adaptation could be evaluated along with those of acetate metabolism- and transport-related transcription.

Further insight into acetate metabolism in *P. parvum* is provided in Chapter 4, in which a fatty acid profile was established. This was achieved via the isolation of total lipids from *P. parvum* cells, which were subjected to fatty acid methyl ester (FAME) analyses using gas chromatography-mass spectrometry (GC-MS). Profiles of several extracts were also compared following growth in the same two salinity conditions that were evaluated in Chapter 3. This information further elaborates upon the transcriptomic data by providing a brief glimpse further downstream from transcription to clarify a subset of the metabolic products that are actually being produced.

Chapter 2: Differential gene expression corresponding with increased prymnesins in *Prymnesium parvum* cultures following nutrient limitation

2.1 INTRODUCTION

Bloom formation and toxin production in *P. parvum* are induced by abiotic and biotic stress conditions, including nutrient limitation, particularly that of nitrogen and phosphorus (Johansson and Graneli, 1999). Phosphorus limitation in particular has been well established as being associated with increased toxicity in *P. parvum*, both in the field and in laboratory-grown cultures (Shilo, 1967; Dafni *et al.*, 1972; Kaartvedt *et al.*, 1991; Larsen *et al.*, 1993; Meldahl *et al.*, 1994; Johansson and Graneli, 1999). This organism out-competes other algal species in such conditions, forming nearly monospecific blooms (Graneli and Johansson, 2003). An environment that is deficient in inorganic phosphate has been associated with a ten- to twentyfold increase in toxin production (Johansson and Graneli, 1999). Thus, phosphate limitation has been an established means of provoking *P. parvum* toxin production in a laboratory setting.

In an effort to understand the molecular basis of its ability to outcompete other algae under nutrient-limiting conditions, a cDNA library was previously constructed with mRNA from late-logarithmic growth phase *P. parvum* cultures, which resulted in the assembly of 3,415 tentative unigenes (TUGs) (La Claire, 2006). This study revealed high levels of transcripts encoding phosphate transporters, indicating that *P. parvum* may be very proficient in this regard. The more recent advent of high-throughput transcriptome assays, such as microarrays and RNA-Seq analyses, have facilitated the evaluation of gene expression in response to phosphate limitation in *P. parvum* and other algal species (Dyhrman *et al.*, 2006; Moseley *et al.*, 2006; Freitag *et al.*, 2011; Morey *et al.*, 2011; Yang *et al.*, 2011; Beszteri *et al.*, 2012; Dyhrman *et al.*, 2012; Harke and Gobler, 2013). Microarrays enable the assessment of the expression of many transcripts simultaneously

and also the comparison of different treatments to identify differentially expressed genes. Thus, in the present study, custom microarrays (constructed with oligonucleotides for the ~3,400 unigenes previously identified) were probed using amplified RNA (aRNA) that was prepared from cultures grown in phosphate-replete *versus* phosphate-limited seawater at a salinity level of 5 psu. This allowed for gene expression comparisons between conditions with potentially varying ichthyotoxicities. The elucidation of the transcriptomic changes that occur during *P*. *parvum* blooms and phosphate fluctuations may aid in their future management and/or prevention.

2.2 MATERIALS AND METHODS

2.2.1 Culture Conditions

One mL of a Texas strain of *P*. *parvum* (UTEX LB 2797) containing 1.05×10^6 cells was used to inoculate (8) 250 mL Erlenmeyer flasks containing 150 mL of 5 psu f/2 media (minus Si) (Guillard and Ryther, 1962). Five of the flasks contained 36.3 μM phosphate (NaH_2PO_4-H_2O) and 5 contained 5.67 μM phosphate, the latter representing the phosphate-limited cultures. Flasks were randomly assigned to positions on a gyrorotatory shaker (150 rpm) and incubated at a constant temperature of 23 °C under a 16:8 LD photoperiod with a photon flux of 20 μmole/m^2/s. They were grown until late-logarithmic phase (approximately 1.5 million cells/mL for phosphate-limited and 3 million cells/mL for phosphate-replete cultures) and then harvested by centrifugation at 5,000 rpm for 5 min at 22 °C. They were sampled 4 times throughout the experiment to verify growth phase status, which were assessed using previously constructed growth curves (Fig. 2.1).
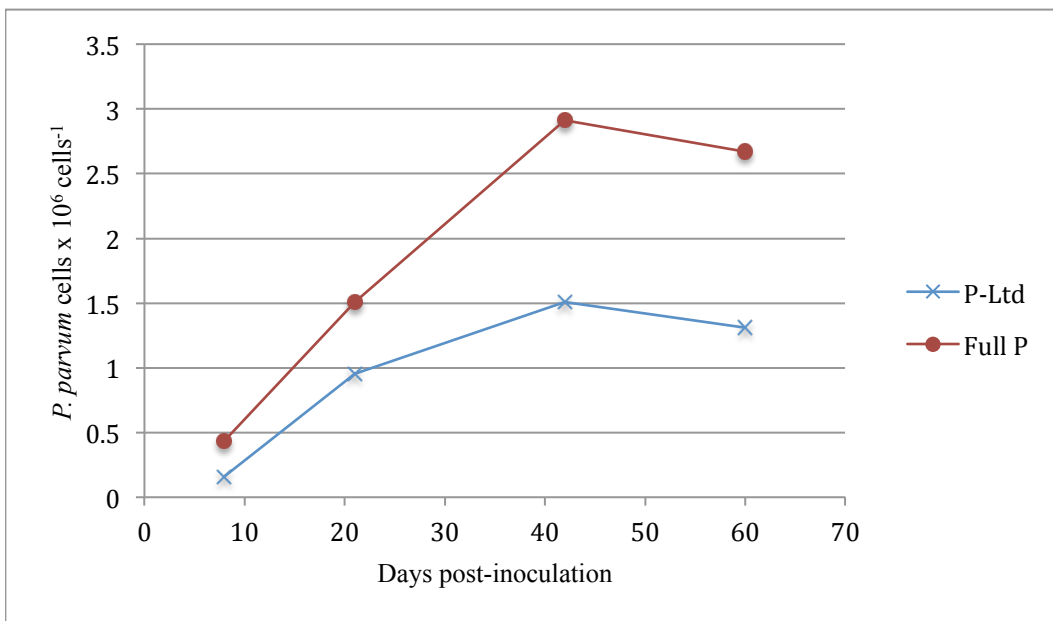
Figure 2.1   Growth curves of phosphate-limited (P-Ltd) versus full-phosphate (Full P) cultures.

2.2.2 Phosphate Analysis

Approximately 10 mL were removed from each of two phosphate-deficient and -replete cultures at days 14, 28, 38, and 48 post-inoculation (corresponding with the early-, mid-, late-, and post-logarithmic growth phases). Samples were centrifuged at 5,000 rpm for 10 min at 22 °C, and supernatants were harvested and frozen at -4 °C for further analyses. Additional supernatants were collected from the phosphate-replete cultures at day 0, 6, and 10.

A phosphorus (P) standard at a concentration of 1,000 parts per million (ppm = mg/L) (Cat. No. PP1KW-100, Ricca Chemical Co., Arlington, TX) was used to prepare a 125 ppm (mg/L) working stock solution using HPLC-grade water (OmniSolve, EMD Chemicals Inc., Gibbstown, NJ). This stock solution was then used to prepare 7 serial dilutions in total volumes of 10 mL to which 0.12 mL of nitric acid were added. The

dilutions contained the following concentrations: 50, 25, 10, 1.0, 0.5, 0.25, and 0 mg/L P. Next, 10 mL of the sample supernatants were combined with 0.12 mL of nitric acid. All dilutions were performed in 15 mL conical polypropylene centrifuge tubes.

The serial dilutions and sample supernatants were then loaded into a Varian 710-ES that was equipped with an autosampler (Agilent Technologies Inc., Santa Clara, CA), and P levels in mg/L were measured via inductively coupled plasma-optical emissions spectrometry (ICP-OES) using standard operating conditions and wavelengths of 177.434, 213.618, and 214.914 nm. Output was assessed using the ICP Expert II software (Agilent Technologies Inc.). For each sample supernatant, final P concentrations were determined by calculating the average of the 3 concentrations from each wavelength.

Phosphate concentrations were determined from those of P using a conversion factor of 3.06, which was obtained by dividing the molecular weight of phosphate (PO_4^{3-}) by that of P itself (95/31). This conversion factor was multiplied by the average P concentrations of the samples to determine the corresponding phosphate concentrations (mg/L) in the media.

2.2.3 RNA Extraction, Purification, and Amplification

RNA was isolated from cell pellets according to the Epicentre Biotechnologies Masterpure Complete DNA and RNA Purification Kit protocol with minor modifications (Epicentre Biotechnologies, Madison, WI). Following resuspension in 100 μl of diethylpyrocarbonate (DEPC)-treated water, 3 rounds of phenol-chloroform extraction were performed to further purify the samples (Sambrook and Russell, 2006). Next, ethanol precipitations were conducted, and dried pellets were resuspended in 20 μl of DEPC water containing 1 μl Scriptguard RNase Inhibitor (Epicentre Biotechnologies). The concentrations and qualities of the RNA samples were measured using a NanoDrop ND-100 Spectrophotometer (Thermo Fisher Scientific Inc., Wilmington, DE) and Agilent 2100 BioAnalyzer (Agilent Technologies Inc.), respectively. After quality was confirmed

(260/280 nm readings in the range of 1.8-2.0 and 260/230 nm readings > 1.8 on NanoDrop and no degradation apparent on BioAnalyzer), the samples were frozen at -80 °C for subsequent analyses.

2.2.4 Amplified RNA Preparation, Labeling, and Purification

Five hundred nanograms of total RNA from each sample were amplified using the Epicentre Biotechnologies TargetAmp-1-Round aRNA Amplification Kit protocol (Epicentre Biotechnologies) and purified using the Qiagen RNeasy Mini Kit or the Qiagen RNeasy MinElute Cleanup Kit with minor modifications depending on whether the expected yield of aminoallyl amplified RNA (aRNA) was > 40 μg or < 40 μg, respectively (Qiagen Inc., Valencia, CA). β-mercaptoethanol was added to the Epicentre RLT solution at a ratio of 1:1000 μl. Additionally, a phosphate wash buffer was used in place of the Epicentre RPE solution (100 mM KPO_4, pH = 8.0, 80% ethanol). The concentrations and qualities were again measured spectrophotometrically. The aRNA samples were then stored at -80 °C.

Five micrograms of aRNA were dried in a Savant SC-100 speed-vacuum concentrator (Thermo Fisher Scientific Inc.) prior to the subsequent fluorescent labeling steps. Dried aRNA was labeled using the Alexa Fluor 555 and Alexa Fluor 647 Reactive Dye Decapacks according to the manufacturer's protocol with modifications (Life Technologies, Grand Island, NY). The aRNA was resuspended in 8 μl of 2× coupling buffer (0.2 M sodium bicarbonate buffer, pH 8.6-9.0) and incubated at 37 °C for 15 min. It was then cooled to room temperature. Eleven μl of dimethyl sulfoxide was added to the tube of Alexa Fluor dye. This dye solution was combined with the aRNA sample and incubated in the dark in a desiccator at room temperature overnight (~18 h). To stop the reaction, 4.5 μl of 4 M hydroxylamine was added to the sample, incubated at room temperature for 15 min, and then purified using the Qiagen columns as previously described (for post-labeling purifications, β-mercaptoethanol was not used, and the kit-

supplied RPE solution was used instead of the phosphate wash buffer). Following purification, the sample concentration and quality were again measured spectrophotometrically, and the frequency of incorporation (FOI) value was assessed using the online Invitrogen Dye:Base Ratio Calculator (http://probes.invitrogen.com/resources/calc/dyebaseratio.html). An FOI value of at least 15 bases per 1000 nucleotides was indicative of adequate dye incorporation and suitability of the sample for microarray hybridization.

2.2.5 Microarray Preparation and Hybridization

Long (70-mer) oligonucleotide probes were designed and assembled by Operon Biotechnologies Inc. (Huntsville, AL) using the cDNA sequences identified by La Claire (2006). These probes included 3,500 oligonucleotides representing 3,415 unique genes. The dried probes (~600 pmol each) were resuspended in Pronto! Universal Spotting Solution (Corning Inc., Tewksbury, MA) to concentrations of 20 μM. They were then transferred to Corning 384-well microplates (Corning Inc.) in preparation for array printing. Plates were stored at 4 °C during printing runs and were stored long-term at -20 °C. Before each print run, they were centrifuged at 1,000 rpm for 3 min.

The oligonucleotide probes were printed onto UltraGAPS coated slides (Corning Inc.) using the Calligrapher Mini-Arrayer (Bio-Rad, Hercules, CA) and Telechem SMP3 pins (ArrayIt Corp., Sunnyvale, CA) according to the manufacturer's protocol with minor modifications. Printing was conducted at 55% humidity. Printed arrays were cross-linked at 600 mJ using a Stratagene UV Stratalinker 1800 (Agilent Technologies Inc.) and stored in a desiccator. They were probed within 6 months of fabrication.

Each array was hybridized with 2 dual-labeled samples (phosphate deficient *versus* replete) according to the scheme presented in Fig. 2.2. With the balanced loop experimental design, samples are hybridized to the arrays in a loop pattern, and each sample is labeled once with each dye. This reduces any technical variation that is due to

dye effects. Prior to hybridization, slides were pre-treated according to the Pronto! Universal Hybridization Kit protocol (Corning Inc.) and then dried by centrifugation in microarray slide dryers (Molecular Devices Inc., Sunnyvale, CA). A LifterSlip (Thermo Scientific Inc., Portsmouth, NH) that had been pre-soaked with pre-hybridization solution (Corning Inc.) was placed over the printed array.
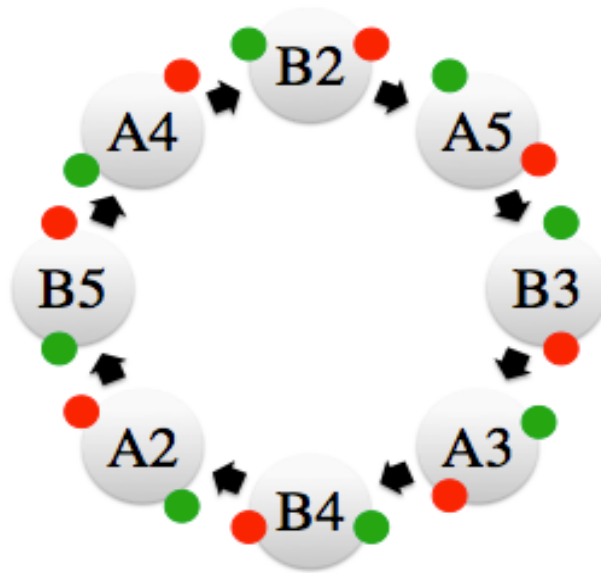
Figure 2.2   Balanced-loop design used for microarray hybridizations. A2-A5 represent phosphate-limited and B2-B5 represent phosphate-replete cultures. Arrows denote "hybridization with". Green and red colors indicate Alexa Fluor 555 and 647 dyes, respectively. (n = 4 biological replicates for each treatment).

To prepare the dye-labeled aRNA samples for hybridization, they were dried in a speed-vacuum concentrator in subdued light and then dissolved in the recommended volume of Long Oligo/cDNA hybridization solution (Corning Inc.) according to the manufacturer's protocol. They were then heated to 85 °C, centrifuged at 13,500 × g for 2 min, and cooled to room temperature. The labeled aRNA was injected under the

LifterSlip, and the array was placed into a hybridization chamber (Molecular Devices Inc.) and incubated at 42 °C for 12-16 h. Following hybridization, the arrays were washed successively in wash solutions 1, 2, and 3 according to the manufacturer's recommendations (Corning Inc.), briefly dipped in double-distilled water, and dried by centrifugation at 500 rcf for 4 min. Immediately after drying, the slides were scanned, and the images were quantitated and normalized with the locally weighted scatterplot smoothing (LOWESS) algorithm using the Perkin Elmer ScanArray Gx and associated software (Perkin Elmer Inc., Waltham, MA). Spots that were flagged by the software as "not found," "absent," and "bad" were discarded from further analyses, and those that were flagged as "good" and "found" were retained. These latter spots were visually verified for each array.

2.2.6 Microarray Data Evaluation

Normalized data were processed with the MultiExperiment Viewer (MeV) version 10.2, which is part of the TM4 software suite (Saeed *et al*., 2003). Log ratios (base 2) of signal intensities of low-phosphate versus full-phosphate grown samples were calculated for each spot on the arrays, and a Student's t-test was performed at $p \leq 0.01$. Those that registered as (statistically) significant different were subjected to BlastX alignments with the National Center for Biotechnology Information (NCBI) non-redundant (NR) database at expect values of $E < 10^{-3}$. Pathways were assessed using the Kyoto Encyclopedia of Genes and Genomes (KEGG) Orthology (KO) database (http://www.genome.jp/kegg/ko.htmL). Differences in KEGG pathways between conditions were assessed using Fisher's Exact Test ($p < 0.05$).

2.2.7 Reverse Transcription Polymerase Chain Reaction (RT-PCR) Validation

Confirmatory RT-PCR analyses were performed using RNA samples from the 2 treatments. PCR primers were synthesized by Integrated DNA Technologies (Coralville, IA) for 2 transcripts of known identity, one showing increased expression levels in phosphate-deficient conditions (60S ribosomal protein L24) and one showing decreased levels of expression (malate synthase). For the PCR, cDNA was created from the RNA samples as follows: 1 μg of RNA was added to a PCR tube containing 2 μl of anchored oligo(dT) primer (Life Technologies Inc.), and DEPC double-distilled water was added to a final volume of 18 μl. The tube was incubated at 70 °C for 5 min in a PTC-200 thermocycler (MJ Research, Inc., Quebec, Canada). Next, 6 μl of 5X first strand buffer, 1.5 μl of 0.1 M dithiothreitol (DTT), 1.5 μl of 10 mM dNTP Mix, 1 μl of RNase Out, and 2 μl of Superscript III reverse transcriptase (Life Technologies Inc.) at a 200 U/μl dilution were added to the tube, and cDNA synthesis was carried out in the PTC-200 thermocycler, in which the temperature was increased to 55 °C in increments of 0.1°/s and maintained at 55 °C for 1 h. Twenty-five nanograms of each sample was obtained for PCR using the Takara PCR Amplification Kit (Clontech Laboratories Inc., Mountainview, CA) according to the manufacturer's protocol with minor modifications. The PCR reactions were run using an initial denaturation at 95 °C for 5 min and then a denaturation step at 95 °C for 30 s, annealing at 57 °C for 45 s, and extension at 72 °C for 15 s for 25 cycles. A final extension step was performed at 72°C for 5 min. Images were semi-quantitated using ImageJ (Schneider *et al.*, 2012), and values were used to calculate $\log_2$ (phosphate-deficient versus –replete) values for each gene.

2.2.8 Solid-Phase Extraction (SPE) and Prymnesin Detection

Three each of phosphate-deficient and -replete cultures were grown as described above. Supernatants were obtained at 3 time points (corresponding with the early/mid-,

23

late-, and post-logarithmic growth phases) following the centrifugation of cultures at 5,000 rpm for 10 min at 22 °C. The volumes of each supernatant were halved to produce technical replicates. SPE were performed to isolate polyketide prymnesins according to Manning and La Claire (2013).

The semi-quantitative detection of the polyketide prymnesins was carried out according to La Claire *et al*. (in preparation). The statistical significance of results was evaluated using the Student's t-test at $p < 0.05$.

2.3 RESULTS

The phosphate-limited cultures exhibited slower and reduced growth compared to the phosphate-replete cultures as expected, peaking at approximately 1.5×10^6 cells/mL (compared with 3.0×10^6 cells/mL for the phosphate-replete cultures) (Fig. 2.1). Thus, the final concentrations of the phosphate-limited cultures only reached approximately half of those of the phosphate-replete cultures.

2.3.1 ICP-OES Analysis of Phosphate Levels

The ICP analysis of phosphorus/phosphate levels at the early-, mid-, late-, and post-logarithmic growth phases (corresponding with days 14, 28, 38, and 48) revealed a steep decline in phosphate concentrations (from 3.8 to 0.5 mg/L) in the replete cultures from the early- to late-logarithmic growth phases, respectively, while the deficient cultures remained at fairly even levels averaging 0.2 mg/L throughout the growth phases (Fig. 2.3). Additionally, from days 0 to 14, phosphate levels initially underwent a slow, steady decline in the phosphate-replete cultures from 4.3 to 3.8 mg/L, with the most rapid drop occurring from days 14 to 38, representing the early- to late-logarithmic growth phases, respectively.
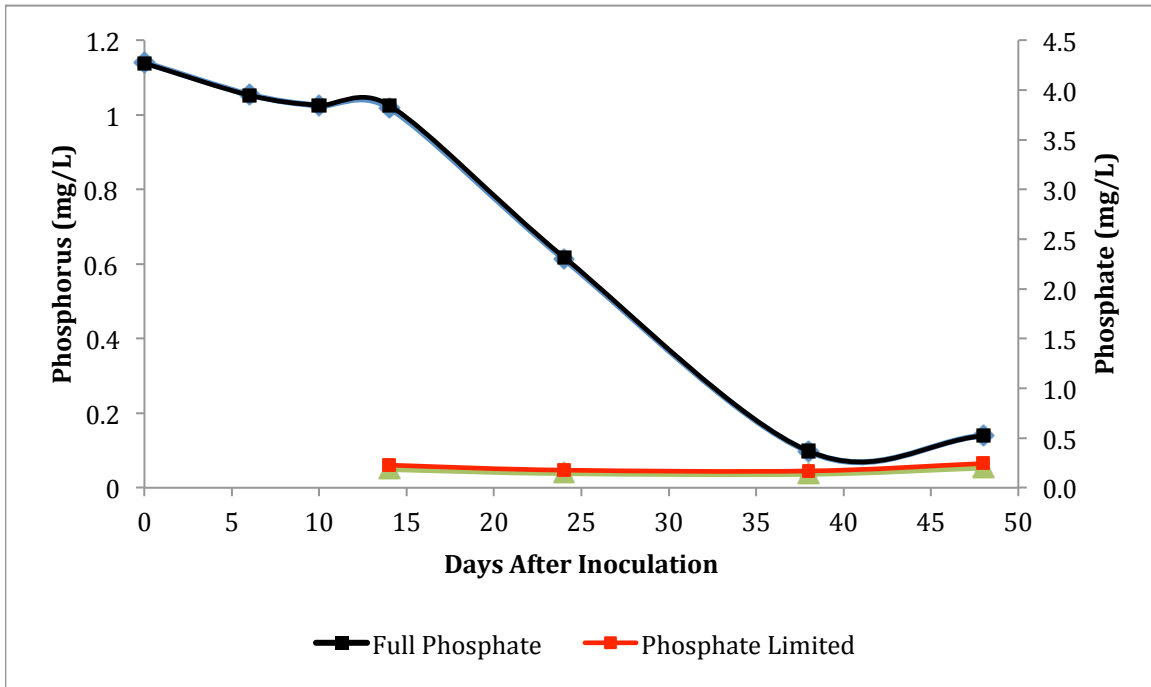
Figure 2.3 Phosphorus (left y-axis) and phosphate (right y-axis) concentrations in mg/L for the phosphate-replete cultures at days 0, 6, and 10, and both the phosphate-deficient and -replete cultures at day 14 (early-), 24 (mid-), 38 (late-), and 48 (post-logarithmic growth phases). (n = 2 for each treatment).

2.3.2 Microarray-based Gene Expression Analysis

Of the 3,500 oligonucleotides that were analyzed, 207 (6%) registered a fluorescent signal that was (statistically) significantly different across the 8 arrays. One hundred thirty-six (3.9%) displayed decreased transcription levels, and 71 (2.0%) displayed increased transcription levels in low-phosphate *versus* full-phosphate conditions, which are listed in Appendix A: Tables 1 and 2, respectively. Of these, 94 (45.4%) were identifiable by sequence homology. The remainder could not be recognized by sequence identity, and therefore some might encode potentially novel proteins. The fold change distributions are summarized in Table 2.1, which ranged from -3.19 to 3.07.

25

A heat map of the 207 statistically significant genes across the 8 arrays is depicted in Fig. 2.4, in which the downregulated and upregulated genes are each grouped together and clustered. Additionally, the volcano plot is shown in Fig. 2.5, which shows all of the genes on the array, highlighting those that are statistically significant in red.

Among the genes whose transcription was downregulated in phosphate-deficient conditions, there were a variety of cell metabolism-associated genes, including β-ketoacyl-ACP reductase, which is a domain of the modular Type I polyketide synthase (PKS) enzyme. Additionally, two homologs of carbonic anhydrase were downregulated, one of which was the top downregulated gene (log ratio = -3.19, p = 0.005177). The majority of photosynthesis-associated homologs were downregulated. Molecular transport-associated genes that were downregulated included one homolog of a chloroplast phosphate translocator (glucose-6-phosphate/phosphate and phosphoenolpyruvate/phosphate translocator) and several anion transporters. Particular KEGG pathways that were only present among the downregulated genes included inorganic ion transport, DNA replication, recombination, and repair, and inositol phosphate and lipid metabolism. The pathway representing energy production and conversion was significantly downregulated.

TUGs that were upregulated in low phosphate conditions included those involved with cellular stress responses. Additionally, a number of vesicular transport-associated genes were upregulated. Several cytoskeletal-associated genes were also upregulated. Twenty-three different 60S, 40S, and 30S ribosomal proteins were upregulated, and the top upregulated gene was homologous to 60S ribosomal protein L38 (log ratio = 3.07, p = 2.87E-05). The KEGG pathway representing intracellular traffic, secretion, and vesicular transport was only present among the upregulated transcripts. Additionally, the pathways representing the cytoskeleton and translation, ribosomal structure, and biogenesis were both significantly downregulated.

Table 2.1 Distributions of fold changes (FC) for both down- and upregulated TUGs representing $\log_2$ (phosphate-limited *versus* -replete) values that were obtained from microarrays.

Down: FC > 3	Down: FC > 2	Down: FC > 1	All down	Up: FC > 3	Up: FC > 2	Up: FC > 1	All up
1	8	64	136	1	3	24	71
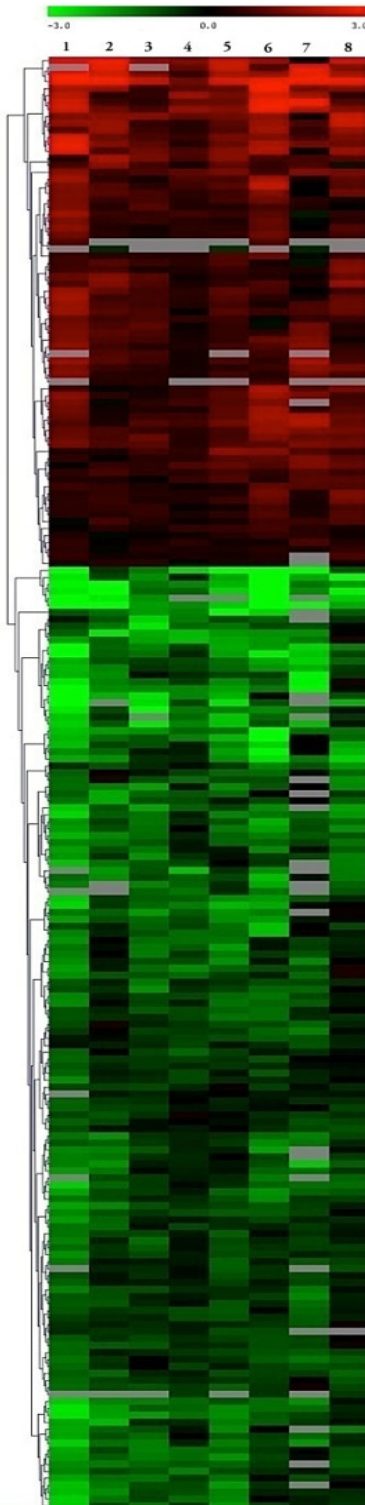
Figure 2.4 Heat map of log$_2$ (phosphate-deficient *versus* – replete) fold changes of 207 differentially expressed genes (p ≤ 0.01) across the 8 arrays; columns represent arrays, and rows contain individual genes. Green represents downregulated genes, and red depicts upregulated genes, which range from -3.0 to 3.0 as indicated by colored bar at top of figure. Arrays 1 through 8 represent the following hybridizations: A4 and B5 (1), A3 and B3 (2), A3 and B4 (3), A2 and B4 (4), A2 and B5 (5), A4 and B2 (6) A5 and B1 (7), and A5 and B3 (8).

28
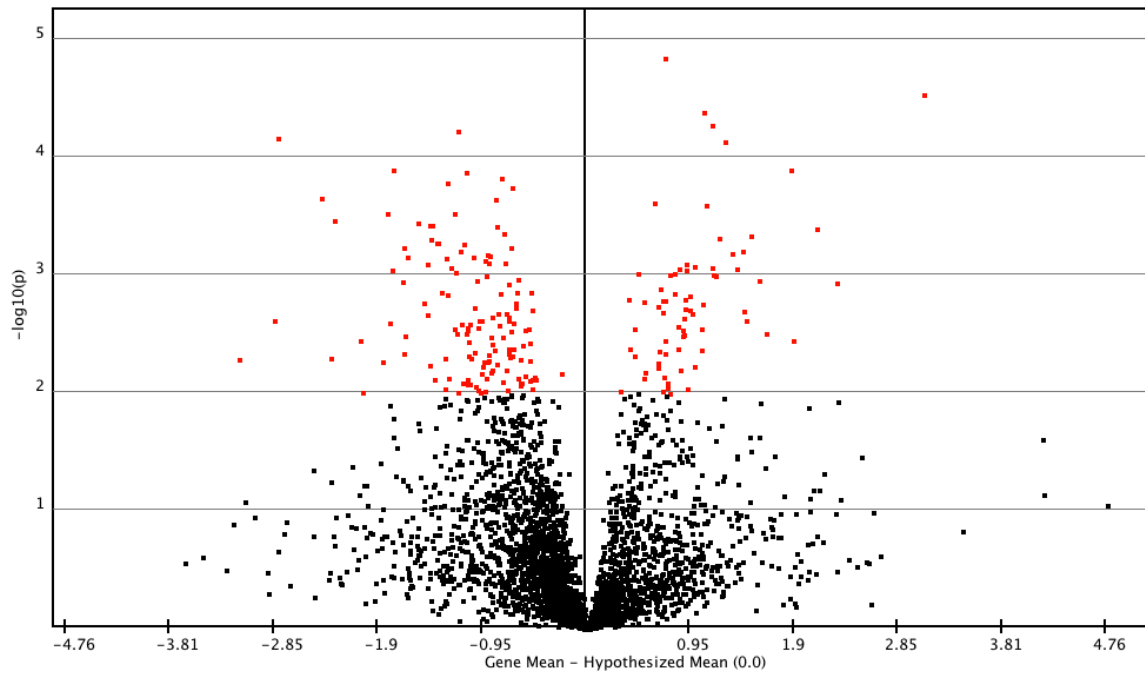
Figure 2.5 Volcano plot. Each point represents an individual gene. X-axis depicts $\log_2$ fold changes; y-axis indicates negative $\log_{10}$–transformed p-values from Student's t-test. Red data points represent genes that are significantly differentially expressed.

2.3.3 RT-PCR Validation

Confirmatory RT-PCR results correlated with those observed on the microarray for 60S ribosomal protein L24, which showed increased expression levels in phosphate-deficient conditions, and malate synthase, which showed decreased levels of expression (Fig. 2.6), although to lesser degrees than microarrays indicated (-0.8 fold change from RT-PCR *versus* -1.88 from microarray for malate synthase and 0.5 versus 1.86 for 60S ribosomal protein L24).

Malate Synthase   **Malate Synthase**   **60S RPL24**   **60S RPL24**
(-)P   (+)P   (-)P   (+)P
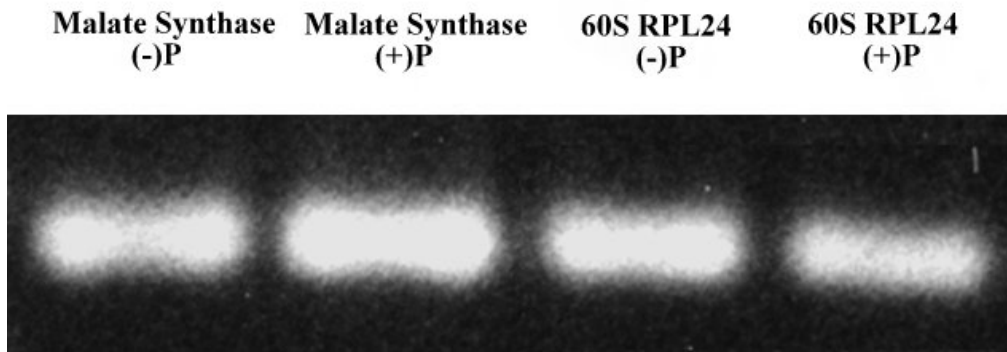
Figure 2.6   Electrophoresis of RT-PCR products. $\log_2$ of (-)P/(+)P for lanes 1/2 (malate synthase) = -0.8; $\log_2$ of (-)P/(+)P for lanes 3/4 (60S RPL24) = 0.5.

2.3.4 Prymnesin Detection and Quantitation

The fluorescence assay revealed that the prymnesins were more abundant in the phosphate-limited *versus* replete supernatants on a pg/cell basis throughout the growth phases (Fig. 2.7). They peaked in the early-/mid-logarithmic growth phase samples for both the phosphate-limited (3 pg/cell) and –replete (2.8 pg/cell) supernatants. However, while levels in the phosphate-limited samples dropped to approximately 2 pg/cell in the late-logarithmic growth phase and then to 1.9 pg/cell in the post-logarithmic growth phase, representing only a 5% decline, levels in the phosphate-replete cultures fell from 1.7 pg/cell to 0.5 pg/cell in late- and post-logarithmic growth phases, respectively, representing a decrease of 71% (significant at $p < 0.05$). Additionally, the greatest differences between prymnesin levels in the phosphate-limited versus –replete cultures occurred in the post-logarithmic growth phase, in which the phosphate-limited cultures had 74% greater levels of prymnesins ($p < 0.05$).
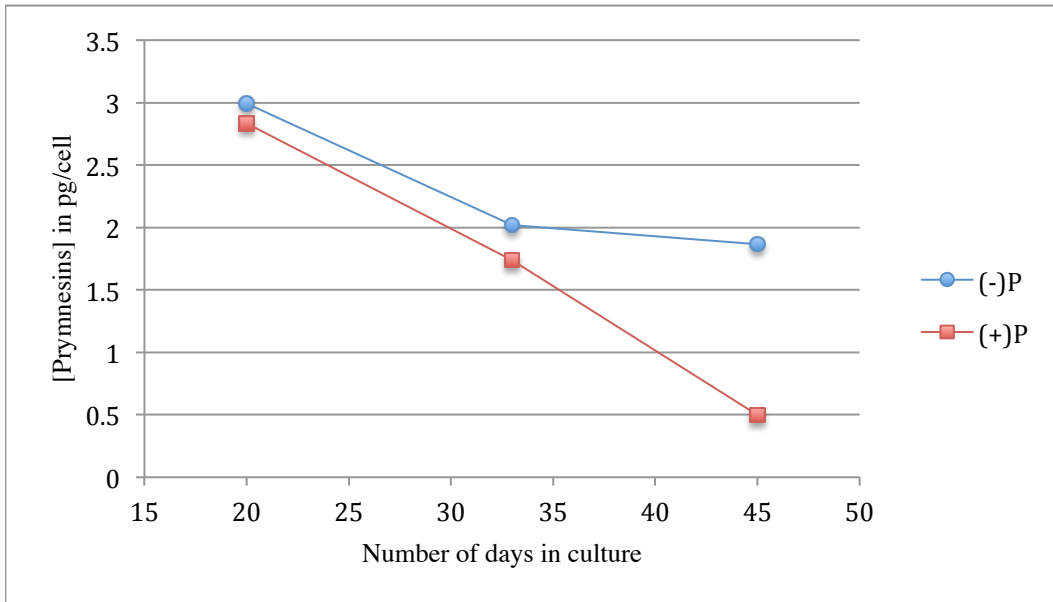
Figure 2.7   Fluorescence detection of prymnesins in supernatants from cultures that were grown in phosphate-limited and -replete media for the early-/mid- (day 20), late- (day 33), and post (day 45)-logarithmic growth phases. Prymnesin concentrations are reported in pg/cell. (n = 4 total measurements for each treatment).

2.4 DISCUSSION

As expected in full-phosphate media, declining levels of phosphate were indicated, with the most significant decrease occurring in mid-logarithmic phase cultures when cells were most actively dividing. Phosphate limitation clearly had an effect on prymnesin presence in the culture medium. The increased prymnesin content that was observed in the phosphate-limited supernatants validates the presence of increased extracellular prymnesins under phosphate-limiting conditions and thus supports a correlation of pertinent gene expression changes as markers of toxin synthesis/secretion. Further, the RT-PCR results substantiated some of the microarray findings, and the comparatively diminished magnitudes of the fold changes that were observed were likely

31

due to the semi-quantitative nature of PCR gel analysis. Although a substantial proportion (45.4%) of the 207 differentially expressed TUGs in the microarrays were recognized by sequence identity, over half were not and therefore potentially encode novel proteins. It is possible that some of these unidentified proteins are involved in the synthesis and excretion of toxins.

Several of the TUGs that were identified on the arrays are associated with acetate metabolism and thus are potentially linked to toxin synthesis. These include acetyl-CoA synthetase, biotin carboxylase (which is a component of acetyl-CoA carboxylase) (Huerlimann and Heimann, 2013), and phosphate acetyltransferase. All were expressed at decreased levels in phosphate-deficient conditions. Two other genes of interest in this context that were expressed at lower levels were β-ketoacyl-ACP reductase and methylmalonyl-CoA mutase, which are potential candidate enzymes for polyketide prymnesin synthesis. Two participants in the glyoxylate cycle, malate synthase and isocitrate lyase, were also less abundant. The main function of the glyoxylate cycle is to utilize lipids as alternative carbon sources for energy (Kunze *et al.*, 2006). However, by facilitating acetate assimilation, those enzymes could also potentially provide precursors for polyketide biosynthesis (Li *et al.*, 2004). The expression of these two genes in addition to the two potential candidates for prymnesin synthesis at decreased levels in low phosphate conditions, in which extracellular prymnesin content was higher, and the lack of significant differential expression of any other potential participants in prymnesin synthesis points to the presence of post-transcriptional regulation, which has been previously reported in the dinoflagellate *Karenia brevis* (Erdner and Anderson, 2006; Monroe *et al.*, 2010; Morey *et al.*, 2011).

The assessment of the expression of transport-associated gene products revealed the upregulation of homologs associated with vesicular trafficking in low phosphate conditions. These included *ARF1*, clathrin, *Ras*, and profilin, supporting the concept of increased toxin secretion in these cells. With regard to transmembrane transporters, an

32

ABC-type phosphate transporter was previously reported to be highly expressed in *P. parvum* in an EST study of phosphate-replete late-logarithmic phase cultures (La Claire, 2006). It was postulated that it may confer a competitive advantage to this alga under low-phosphate conditions. However, it was not significantly differentially expressed in the current analysis, suggesting that if it is involved, it is not regulated at the transcriptional level. One chloroplast phosphate translocator (glucose-6-phosphate/phosphate and phosphoenolpyruvate/phosphate translocator) was expressed at lower levels in the phosphate-limited compared with the phosphate-replete conditions. Notably, this translocator is localized to the chloroplast membrane, and it transports organic molecules in addition to phosphate (Kammerer *et al.*, 1998; Rausch and Bucher, 2002). Thus, its lower expression in phosphate-limited conditions may be associated with the decreased metabolism that is occurring because it is involved in glucose-6-phosphate import, which is used for the synthesis of starch and fatty acids (Flügge, 2001; Niewiadomski *et al.*, 2005). Additional transmembrane transport-associated homologs that decreased in abundance in low phosphate conditions included band 3 protein, which is a bicarbonate/chloride exchanger. The decreased expression of this gene in addition to carbonic anhydrase, which play roles in photosynthesis, correlates with the aforementioned decrease in photosynthetic gene expression (Cook *et al.*, 1986; Drechsler and Beer, 1991; Moroney *et al.*, 2001).

The collective downregulation of metabolic enzymes in addition to those that are associated with photosynthesis (as verified by the significant upregulation of the KEGG pathway for energy production and conversion) are typical in conditions of stress because cells slow these processes to conserve energy. In particular, the low phosphate levels of the phosphate-deficient cultures likely hindered ATP formation and thus the synthesis of photosynthetic assimilates, nucleic acids, and phospholipids (Plaxton and Carswell, 1999; de Groot *et al.*, 2003; Beardall *et al.*, 2005; Morey *et al.*, 2011). This would lead to reduced rates of growth and cell division in accordance with the downregulation of

centrin 3 and β-tubulin that was observed. The finding that homologs for gene products with direct involvement in the cellular stress response were upregulated in low phosphate conditions was not unexpected, and these products included several ubiquitins and both cold- and heat-shock proteins. Cell stress may have also led to the significant increase in ribosomal gene expression that was observed under phosphate limitation. Although ribosomal proteins are typically involved in translation, they also play a potential role in monitoring the physiological status of cells (Wamer and McIntosh, 2009). Thus, their high expression in low phosphate conditions in the current analysis may be due to the poorer health of the nutrient-deprived cells.

There are a number of studies in the algal literature assessing gene expression under phosphate-limiting conditions (for summary, see Table 2.2). For example, Beszteri *et al*. (2012) performed a microarray analysis using stationary-phase *P. parvum* cultures that were grown in varying nutrient conditions, including both nitrogen and phosphate (replete *vs*. depleted). In particular, potential biomarkers of nitrogen and phosphate deficiencies were evaluated. Their analysis revealed the differential expression of 1,742 (27%) TUGs, including the upregulation of a number that are related to transport and cell motility, including *ARF*, similar to the present study. In contrast, they also reported the upregulation of some phosphate-associated transcripts and the downregulation of ribosomal proteins in phosphate-limiting conditions. It is possible that the differing salinities of the growth media (26 psu *versus* 5 psu in present study) or other variable growth conditions, different microarray hybridization conditions, and/or dissimilar data normalization/analysis methods contributed to some of the variations between studies. For example, they found a larger proportion of differentially expressed genes, including the upregulation of a number of phosphate transporters, while only one phosphate transporter was found to be significantly differentially expressed in the current analysis, and it was downregulated under phosphate limitation. They suggested that phosphate transporters increase in numbers in phosphate-limiting conditions to facilitate increased

34

phosphate uptake in the nutrient-stressed cells. Notably, while we used phosphate-deficient growth media (5.67 μM concentration), they omitted it from the media entirely, so it is likely that the cells were more stressed in their study. Further, at the time of harvest (late-logarithmic phase) in the current study, both the phosphate-deficient and – replete cultures contained very low levels of phosphate (0.14 and 0.30 mg/L phosphate, respectively); thus, the expression of phosphate transporter genes may have been correspondingly similar in both conditions. Further transcriptional analyses of *P*. *parvum* under phosphate limitation may clarify the discrepancies in these findings.

Dyhrman *et al*. (2006), who studied the effects of phosphate depletion in the closely related alga *Emiliana huxleyi* using long serial analysis of gene expression (SAGE), reported the upregulation of several photosynthesis-related genes including light harvesting complex and fucoxanthin cholorphyll a/c binding protein in contrast with the present study. However, they attributed this to increased calcification rates in this coccolithophorid alga; *P*. *parvum* does not possess a calcified coccosphere (Paasche, 1998). They further reported the upregulation of ribosome-associated transcription similar to the present study, noting that the mechanisms behind this overabundance of rRNA transcription were unclear. However, they found *ARF* to be downregulated in contrast with the present findings. It is possible that there are differences in vesicular transport-associated transcription in these two algae due to the trafficking of components of the coccosphere in *E*. *huxleyi*, which does not form toxic blooms, so toxin transport and exudation from the cells are not relevant in that alga.

A long SAGE analysis of phosphorus limitation in *Aureococcus anophagefferens* revealed the upregulation of photosynthesis-related transcripts similar to Dhyrman *et al*. (2006). They noted that the response of this category of genes to nutrient stress in other algae has been variable and suggested that although many genes are typically downregulated in stress conditions to conserve energy, this process may not be as strong or rapid for genes such as the light harvesting complex in this particular algal species and

likely others (Wurch *et al.*, 2011). They found ubiquitin to be downregulated in contrast with our findings; however, they isolated cells in the mid-logarithmic growth phase that were undergoing exponential growth and they proposed that higher levels of ubiquitin were present in the nutrient-replete cultures due to the general cellular stress that was present in relation to the rapid protein turnover that was occurring in that growth phase. In accordance with the present findings, they found Clp protease to be downregulated, which is dependent upon ATP and thus would intuitively be less active in conditions of limiting phosphate.

A previous microarray study of *Chlamydomonas reinhardtii* exhibited many parallels with the current findings despite the fact that the cells were not isolated at similar time points in the growth phase (Moseley *et al.*, 2006). However, ribosomal proteins were largely downregulated in contrast with the current findings in addition to protein disulfide isomerase, β-tubulin, and centrin. It is quite possible that such unrelated algae as *Prymnesium* and *Chlamydomonas* respond differently to similar stresses, and it is likely that their contrasting harvesting schedules contributed to the differences that were observed.

Finally, Harke and Gobler (2013) examined phosphate limitation in the cyanobacterium *Microcystis aeruginosa* using RNA-Seq. Similar to what was observed by Moseley *et al.* (2006) in *C. reinhardtii* and the current results for *P. parvum*, this species also exhibited a downregulation of photosynthesis-related transcription. Additionally, GST was upregulated similar to *C. reinhardtii* and *P. parvum*. Some metabolism-related transcripts were also similarly downregulated, including β-ketoacyl reductase. Ribosomal genes were downregulated in contrast with our findings and those by Dyhrman *et al.* (2006) for *E. huxleyi*, and it was suggested that this was a growth rate-dependent regulatory response to cell stress.

The comparisons of the present findings with others in the literature pertaining to the transcriptional responses of algae to phosphate limitation are highly variable.

However, it must be noted that microarray studies in particular are prone to variation. Although great efforts have been made to standardize protocols and provide guidelines for best practice that have greatly reduced this variation, it is not possible to eliminate all of it. The more recent advent of RNA-Seq technologies have also greatly reduced variation (among other advantages), making results more comparable across studies and facilitating the comparison of the expression of larger numbers of genes over a broader range of expression levels. Future RNA-Seq analyses of phosphate limitation in *P. parvum* and other algae will provide more thorough information regarding gene expression in response to this abiotic stress. As more of these analyses are carried out, a clearer picture of the consequences of deficiencies in this critical nutrient will emerge. For bloom-forming algae such as *P. parvum,* gene expression patterns may also be further clarified that characterize HAB formation in response to not only nutrient limitation but additional toxicity-stimulating abiotic stresses, such as temperature and salinity.

Table 2.2 Similarities of current data with previous studies in literature assessing algal/cyanobacterial gene expression in response to phosphate limitation/depletion (decreased and increased gene expression in phosphate-deficient or -depleted conditions).

Organism	Culturing conditions	Growth stage	Analysis type	Decreased	Increased	Author
P. parvum	P-replete and -depleted	Stationery	Microarray	Photosynthesis, cell division	Transport, cell motility	Beszteri *et al.,* 2012
E. huxleyi	P-replete and -depleted	P-replete: mid-logarithmic; P-depleted: stationery	Long SAGE		Ribosomal, Ras GTP-binding protein	Dyhrman *et al.,*2006
A. anophagefferens	P-replete and -deficient (36.3 μM)	P replete: mid-logarithmic; P-deficient: stationery	Long SAGE	Clp protease, centrin, DNA ligase		Wurch *et al.,*2011
C. reinhartdii	P-replete and -deficient (cells transferred to P-depleted media in mid-log phase)	P replete: mid-logarithmic; P-depleted: 0, 4, 12, 24, and 48 h after transfer to P-depleted medium	Microarray	Photosynthesis, acetyl CoA synthetase, malate synthase	Cell stress	Moseley *et al.,*2006
M. aeruginosa	P-replete (1.26 x 10⁻³ P) and -depleted	P replete: mid-logarithmic; P-depleted: late to stationery	RNA-Seq	Photosynthesis, β-ketoacyl reductase, acetyltransferase, biotin carboxylase, short chain dehydrogenase/reductase, carbonic anhydrase	Glutathione -s- transferase	Harke and Gobler, 2013

Chapter 3: Transcriptome analysis of the euryhaline alga, *Prymnesium parvum* N. Carter: effects of salinity on differential gene expression

3.1 INTRODUCTION

Salinity is a crucial parameter defining the growth and distribution of microalgae, some of which can tolerate large fluctuations in salt concentrations in their environments. One such euryhaline alga is the unicellular haptophyte, *Prymnesium parvum*, which is a globally significant species that causes extensive blooms and costly fish kills in response to a variety of biotic and abiotic environmental stimuli, including fluctuations in salinity (Jeffrey and Wright, 1994; Baker *et al.*, 2007; Olli and Trunov, 2007; Manning and La Claire, 2010). The adaptive mechanisms of osmoregulation in *P. parvum* at the transcriptome level have not been investigated to date. Thus, this alga represents a model organism for studying the effects of salinity fluctuations on gene expression, which may lend further insight into the mechanisms that plants and algae use to tolerate this abiotic stress.

Studies investigating the effects of salinity variations on the toxicity of *P. parvum* show a collective trend toward decreased extracellular toxicity at higher levels of salinity (Ulitzur and Shiloh, 1964; Paster, 1973; Larsen *et al.*, 1993; Baker *et al.*, 2007 and 2009; Manning and La Claire, 2010; Freitag *et al.*, 2011; Weissbach and Legrand, 2012). It is currently unknown whether this organism actively secretes/excretes toxins or whether they are merely released when cells lyse. Therefore, those responses potentially underlying the formation of HABs as well as the production of toxins may also be revealed by a transcriptome analysis, due to the propensity of *P. parvum* to form HABs in low-salinity waters (Hallegraeff, 1993; Larsen *et al.*, 1993; Baker *et al.*, 2007; Brooks *et al.*, 2010; Manning and La Claire, 2010).

Salinity stress has been shown also to increase the synthesis of TAG in various algal species (Elenkov *et al.*, 1996; Hu *et al.*, 2008; Pal *et al.*, 2011; Zhila *et al.*, 2011),

39

which is significant to biofuel production. Microalgae in particular have the unique ability to produce abundant quantities of TAG following the manipulation of certain environmental conditions. PUFA are a co-product of TAG synthesis, which are economically valuable alternative sources of fish oil and other oils with abundant ω-3 fatty acids (Bruton *et al.,* 2009; Singh *et al.,* 2011). Thus, a closer inspection of acetate metabolism-related transcription in relation to osmotic stress in *P. parvum* may uncover patterns that are not only associated with alterations in the transcription of polyketides or other putative ichthyotoxins during HAB events but also provide valuable knowledge regarding the mechanisms of TAG and PUFA production in this and other organisms, as well as elucidating the potential roles of salinity in the optimization of their syntheses.

Microarrays and RNA-Seq are valuable tools for evaluating gene expression at the transcriptome level. The Genbank expressed sequence tag (EST) database currently contains 23,443 ESTs for *P. parvum* (http://www.ncbi.nlm.nih.gov/dbEST/index.html), and the literature to date includes EST analyses, microarrays, and qPCR (La Claire, 2006; Freitag *et al.,* 2011; Beszteri *et al.,* 2012); however, there are no reported RNA-Seq analyses of this organism. Therefore, a study of this magnitude would greatly expand upon the current knowledge of gene expression in *P. parvum*.

In the current study, RNA-Seq was used to assemble a *P. parvum* transcriptome and to compare gene expression in cultures that were grown at two salinity levels (5 and 30 psu). The salinity variations allowed for comparisons focusing on the mechanisms underlying long-term osmoregulatory adaptation and acetate metabolism-associated pathways in addition to those involving the intracellular and extracellular transport of various ions and molecules. This work should contribute to current knowledge regarding abiotic stress tolerance as well as toxin, glycerolipid, and PUFA syntheses and transport mechanisms in this and possibly other species of algae. The present study represents the first comprehensive transcriptomic analysis of *P. parvum* and is one of few RNA-Seq analyses investigating the osmoregulation of eukaryotic euryhaline algae.

3.2 MATERIALS AND METHODS

3.2.1 Culture Maintenance and Harvesting

A strain of *P. parvum* (UTEX LB 2797) that was isolated in Texas was used in this study. The f/2 media (minus Si) were prepared at both 5 and 30 psu using steamed seawater (Guillard and Ryther, 1962). From an inoculum containing 2.0 x 10^6 cells, 3.4 mL were added to (2) 250 mL Erlenmeyer flasks, each containing 150 mL of 5 psu medium. The same concentration of inoculum from a 30 psu culture that had been gradually pre-acclimated from 5 psu was also added to (2) 250 mL Erlenmeyer flasks containing 150 mL of 30 psu medium. Cultures were maintained on a gyrorotatory shaker (150 rpm) under a 16:8 LD photoperiod with a photon flux of 20 μmole/m^2/s at 23 °C. They were grown until mid-log phase (approximately 1 million cells/mL), after which the cells were harvested by centrifugation at 5,000 rpm for 5 minutes at 23 °C. A small aliquot of cells was also retained for morphological assessment using light microscopy.

3.2.2 RNA Extraction and Purification

Cell pellets were resuspended in Trizol reagent (Life Technologies, Grand Island, NY) and flash-frozen in liquid nitrogen. Total RNA was extracted from each culture using the Trizol RNA extraction protocol. Precipitated RNA was dissolved in 100 μl of diethylpyrocarbonate (DEPC) water, and 3 rounds of phenol-chloroform extraction were performed to further purify the samples (Sambrook and Russell, 2006). Next, the RNA was again precipitated and resuspended in 100 μl DEPC water. Finally, the samples were purified using the Qiagen RNeasy Mini Kit (Qiagen Inc., Valencia, CA), and 1 μl of ScriptGuard RNase Inhibitor was added to each (Epicentre Biotechnologies, Madison, WI). The concentration and quality of RNA samples were assessed using a NanoDrop ND-100 Spectrophotometer (Thermo Fisher Scientific Inc., Wilmington, DE), an Agilent 2100 BioAnalyzer (Agilent Technologies Inc., Santa Clara, CA), and RNA denaturing

gel electrophoresis, according to Grierson (1990), with minor modifications. After the quality of the RNA was confirmed (260/280 nm readings in the range of 1.8-2.0, $A_{260/230}$ nm readings > 1.8 on NanoDrop and no degradation apparent on BioAnalyzer or RNA gels), the 5 and 30 psu samples were frozen at -80 °C for subsequent RNA-Seq analyses.

3.2.3 RNA-Seq Transcriptome Analysis

RNA sequencing was carried out by the National Center for Genome Resources (NCGR, Santa Fe, NM). Upon receipt, the NGCR prepared paired-end Illumina RNA-Seq libraries for each condition (5 and 30 psu salinities), which were then sequenced using Illumina HiSeq 2000 technology (one sample per lane on the flow cell) (Illumina, Inc., San Diego, CA). The resulting raw reads from the 5 and 30 psu libraries were deposited in the NCBI Sequence Read Archive under accession numbers SRR931174 and SRR931877, respectively. These reads were dynamically trimmed to remove substandard bases and adaptor sequences, and then assembled *de novo* using the Trinity software (version r20120317) with a *k*-mer size of 25, minimum contig length of 200, and paired fragment length of 500 (Grabherr *et al.,* 2011). This software was run on the Texas Advanced Computing Center Lonestar Linux Cluster. Subsequently, BlastX alignments between the transcripts and the National Center for Biotechnology Information (NCBI) non-redundant (NR) and Swiss-Prot databases at $E < 10^{-6}$ were carried out, and gene ontology (GO) analyses were conducted using the Blast2GO software (Conesa and Gotz, 2008). Pathways were evaluated with the Kyoto Encyclopedia of Genes and Genomes (KEGG) Automatic Annotation Server (KAAS) (http://www.genome.jp/tools/kaas). The contiguity and completeness of the assembly were evaluated according to Zhang *et al*. (2013) with minor modifications. Contiguity was calculated according to a subset of approximately 1,000 of the top-ranked complete transcripts. For these calculations, the *E. huxleyi* "All Models" fasta file (Emihu1_all_proteins.fasta.gz) was used as the reference

assembly, which was produced by the U.S. Department of Energy Joint Genome Institute (http://www.jgi.doe.gov) in collaboration with the user community (Read *et al.*, 2013).

Likely coding sequences were extracted from the assembly using TransDecoder, which was included in the Trinity software package. Target peptides were assessed from coding sequences using the TargetP 1.1 Server (http://www.cbs.dtu.dk/services/TargetP/) (Emanuelsson *et al.*, 2000).

3.2.4 Identification of Differentially Expressed Genes

For the differential expression analyses, the recommended pipeline that is built into the Trinity software was used (http://trinityrnaseq.sourceforge.net). The reads from each salinity treatment were first aligned to the Trinity assembly output using the "alignReads.pl" script with the Bowtie option as previously described by Langmead *et al.* (2009). Separate alignments were performed for each salinity treatment (5 and 30 psu). The output (SAM) files were assessed for quality using the SAMtools flagstat function from the SAMtools software (http://davetang.org/wiki/tiki-index.php?page=SAMTools) and visualized using the Integrated Genomics Viewer software (IGV) (Thorvaldsdóttir *et al.*, 2013).

Following the Bowtie alignments, the "run_RSEM.pl" script that is built into the Trinity software was used to estimate transcript abundance for each treatment using the RSEM software (Li and Dewey, 2011). The two files were then joined into a matrix, and the "run_EdgeR.pl" script was used to direct the Bioconductor EdgeR software to perform trimmed means of M-values normalization and identify transcripts with two-fold or greater changes in expression with p-values < 0.01 [cut-off at 5% false discovery rate (FDR)] (Robinson *et al.*, 2009)**.** BlastX searches were conducted on the corresponding sequences using the NR and Swiss-Prot databases at E < 10^{-6}, which were then annotated using Blast2GO. An annotation enrichment analysis was performed on the GO categories

in each condition using the Blast2GO software, which applies the Fisher's Exact Test to obtain those with significant FDR-adjusted p-values (< 0.05) (Blüthgen *et al.*, 2005).

3.2.5 Solid-Phase Extraction and Prymnesin Detection

Supernatants from both sets of cultures were obtained at 3 time points (corresponding with the early/mid-, late-, and post-logarithmic growth phases) following the centrifugation of cultures at 5,000 rpm for 10 min at 22 °C. The volumes of each supernatant were halved to produce technical replicates. Solid-phase extractions (SPE) were performed to isolate polyketide prymnesins according to Manning and La Claire (2013).

The semi-quantitative detection of the polyketide prymnesins was carried out according to La Claire *et al*. (in preparation). The statistical significance of results was evaluated using the Student's t-test at $p < 0.05$.

3.3 RESULTS

3.3.1 Transcriptome Sequencing and Assembly

Approximately 19.4 and 22.8 million paired-end reads averaging 100 base pairs (bp) in length were obtained for the 5 and 30 psu libraries, respectively. Assemblies generated a total of 47,289 transcripts with an N50 of 1,271 (the value at which 50% of the transcripts are larger than or equal to the average size of 829.5 bp). Sizes ranged from 201 to over 5000 bp (Fig. 3.1). In total, 12,555 (approximately 26.5%) transcripts were larger than 1 kb. Out of the 47,289 transcripts, there were a total of 41,957 components, which are collections of closely related contigs that are grouped by the Trinity software. Table 3.1 describes various characteristics of the final output of the assembly. In addition to the N25, N50, and N75 values, the quality of the assembly was evaluated via

completeness and contiguity scores. Completeness refers to the percentage of sequences that are covered at greater than 80% of their lengths, while contiguity measures the percentage of sequences that are covered by a single contig to greater than 80% of their lengths; *i.e.* the likelihood that a full-length transcript is represented by a single contig (Martin and Wang, 2011).
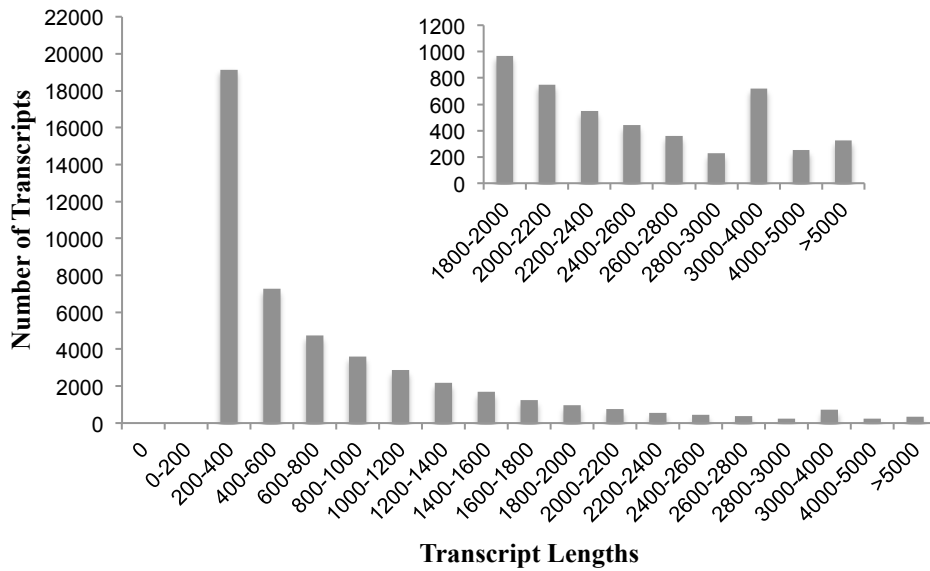
Figure 3.1 Length distribution of transcripts assembled by Trinity software. The inset shows a closer view of transcripts with lengths of 1800 to >5000 bp.

Table 3.1 Output of the RNA-Seq assembly.

Total length of sequence:	39225809 bp
Total number of sequences:	47289
N25:	2199 bp
N50:	1271 bp
N75:	657 bp
Total GC count:	23126729 bp
GC %	58.96%
Completeness	84%
Contiguity	82.6%

3.3.2 Sequence Identification and Functional Annotation

A total of 16,731 (35.4%) of the transcripts were putatively identified by BlastX, and 14,393 (30.4%) could be functionally annotated using Blast2GO. Out of the latter, 12,221 involved more than one GO term. In total, 37,749 annotations were assigned. The biological process, molecular function, and cellular component sub-ontologies consisted of 17,890 (47.4%), 10,722 (28.4%), and 8,488 (22.5%) annotations, respectively. Functional classifications at GO level 3 are depicted in Fig. 3.2, which are grouped by the 3 sub-ontologies. GO levels can generally be considered as annotation depths, with level 1 terms being the most broad and each subsequent level increasing in specificity. The classifications revealed that stimulus response and the development and organization of cellular structures were well represented within the biological process sub-ontology. Within molecular function, binding and enzymatic activity were prominent, primarily involving hydrolases and transferases. The cellular component sub-ontology shows that both membrane- and non-membrane-bound organelles in addition to the extracellular region were active in *P*. *parvum* under the tested conditions.
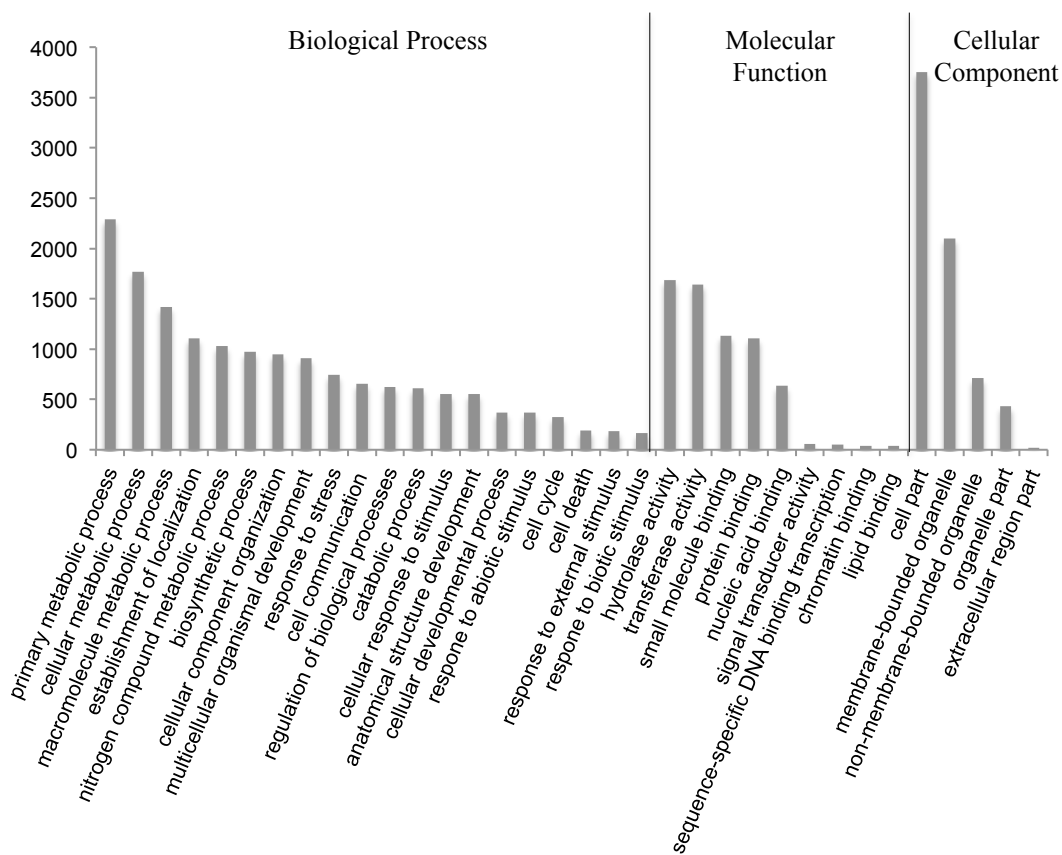
Figure 3.2 GO annotations by Blast2GO at level 3.

The distribution of KEGG pathways was also evaluated, which is an alternative method of categorizing gene functions based on biochemical pathways. This assessment revealed a total of 287 pathways involving 7,960 (47.6%) of the 16,725 transcripts that were identified by BlastX. The top predicted pathways included those associated with ribosomes (114 members), spliceosomes (97 members), purine metabolism (87 members), RNA transport (70 members), and protein processing in the endoplasmic reticulum (ER) (70 members). Other KEGG pathways of note included vesicular transport (13 members) and ABC transporters (28 members). Many acetate metabolism-related pathways were present, in addition to the glycerolipid metabolic pathway that is

involved in TAG synthesis (26 members). Furthermore, the pathways for the metabolism of the PUFA arachidonic (C20:4n-6), linoleic (C18:2n-6), and α-linolenic (C18:3n-3) acid were present (7, 5 and 3 members, respectively).

3.3.3 Genes Associated with Transmembrane and Vesicular Transport

At the sequence identity level, the analysis was partly focused on transport-associated transcription. The transcripts with the highest FPKM values (fragments per kilobase of transcript per million mapped reads - essentially measuring transcript abundance) were calculated by combining the values from each condition (5 and 30 psu) to demonstrate their total relative abundances (summarized in Table 3.2). Among the most prominent homologs specific to the transport of ions and/or solutes included a solute carrier 4 family transporter with a total FPKM value of over 3,000. Numerous additional ion channels and exchangers, symporters, antiporters, and other transporters were also revealed. In terms of vesicular transport, many pertinent homologs were identified, including those that are associated with ER and Golgi processing and trafficking, which amounted to 50/202 (25%) of those transcripts with FPKM values > 100. There are also approximately 40/202 (20%) homologs within this subset with roles in vesicle trafficking, membrane fusion, and secretion.

Table 3.2   Subset of top-expressed transcripts involved in transport-related metabolism ranked by total FPKM value.

Seq ID	Identity	FPKM*	E-value
Transmembrane transport			
comp21942_c0_seq4	Solute carrier 4 family	3126.7	8.0E-162
comp21973_c0_seq1	ABC transporter ATP-binding protein	3113.8	9.4E-15
comp21857_c0_seq1	Cyclic nucleotide binding protein	2897.2	3.0E-99
comp17813_c0_seq1	Phosphate ABC transporter substrate binding protein	2252.6	1.0E-68
comp8560_c0_seq1	V-type H(+)-translocating pyrophosphatase	2153.8	0
comp8590_c0_seq1	Porin	2027.3	9.4E-91
comp16040_c0_seq1	ABC transporter ATP-binding protein	1690.2	9.0E-157
comp8584_c0_seq1	Mitochondrial carrier family protein	1365.5	3.19E-93
Vesicular transport			
comp8489_c0_seq1	ADP-ribosylation factor 1	1994.5	3.3E-106
comp15884_c0_seq1	*RAB* family GTPase	1280.3	4.1E-107
comp14651_c0_seq1	Autophagy-related protein 8 precursor	1143.3	5.6E-58
comp22199_c0_seq1	*RAS*-related protein *RAB-5c*	758.3	3.0E-101
comp12660_c0_seq1	Clathrin heavy chain 1	618.02	0
comp19832_c1_seq1	β-adaptin-like protein c	598.73	0
comp9044_c0_seq1	*RAS*-related protein *RAB-7a*	513.48	1.3E-119
comp3514_c0_seq1	Clathrin assembly small subunit protein	472.65	6.8E-73

3.3.4 Genes Associated with Acetate Metabolism

With regard to acetate metabolism, a subset of transcripts with the highest total FPKM values are listed in Table 3.3. The full transcriptome included homologs to Type I and Type III PKS (26 and 2 members, respectively), which in some cases represented one or several PKS domains, including ketoreductase, ketosynthase, enoyl reductase, and phosphopantetheine binding, the latter of which serves as a prosthetic group of acyl-carrier protein (ACP) (Appendix B: Table 1). Acetyl-CoA carboxylase was the most highly expressed acetate metabolism-associated transcript. Isocitrate lyase and malate synthase also possessed high FPKM values (7070.0 and 1898.9, respectively). There were 55 acetate metabolism-related transcripts in total with FPKM values > 100.

Transcripts that are associated with TAG and PUFA synthesis are also depicted in Table 3.3 and in some cases overlap with several of those mentioned above.

Table 3.3   Subset of top-expressed transcripts involved in acetate-related metabolism ranked by total FPKM value.

Seq ID	Identity	FPKM	E-value
comp19265_c0_seq1	Acetyl-CoA carboxylase	1509.8	0
comp14084_co_seq1	Alcohol dehydrogenase	1036.7	6.27E-105
comp16429_c0_seq1	Δ9-oleate desaturase	922.0	5.0E-145
comp8897_c0_seq1	Glycerol-3-phosphate dehydrogenase	871.0	9.32E-117
comp15582_c0_seq1	Acyl carrier protein	827.3	2.5E-33
comp14555_c0_seq1	Acyl-CoA dehydrogenase	737.0	0
comp14856_c0_seq1	Glycerol-3-phosphate dehydrogenase	597.5	1.83E-110
comp9029_c0_seq1	Long-chain-fatty-acid-CoA ligase	499.2	1.5E-155
comp14895_c0_seq1	Glycolipid transfer protein *HET-C2*	487.5	1.87E-22
comp20237_c0_seq1	Carnitine O-acetyltransferase	470.8	8.03E-138
comp19967_c0_seq1	Acetyl-CoA synthetase	434.6	0
comp19555_c0_seq1	Glycerol-3-phosphate dehydrogenase	382.5	1.63E-136

3.3.5 Comparative Analysis of Cultures Grown at 5 and 30 psu

The microscopic evaluation revealed that cell morphologies were largely similar at the two salinities. There were 2,507 (6%) transcripts in total that were differentially expressed at a fold change of 2 or greater in 30 psu cultures when compared to those grown at 5 psu (p-value < 0.01, 5% FDR cut-off). The upregulated transcripts at 30 psu amounted to 1,507 (3.2%), and 1,000 (2.1%) transcripts were downregulated. Among the former, 600 (39.8%) were putatively identified by BlastX in addition to 478 (47.8%) of the 1,000 downregulated transcripts. There were 626 (41.5%) and 470 (47%) identifiable annotations among the up- and down-regulated transcripts, respectively, and a total of

1,984 and 1,601 GO terms were assigned to each. For the biological process sub-ontology, there were 858 (44.8%) and 683 (42.7%) GO terms represented in the up- and downregulated transcripts; for molecular function, there were 710 (37.1%) and 491 (29.2%); and for cellular component, there were 345 (18.0%) and 394 (23.4%), respectively. The annotation enrichment analysis confirmed the significance of differentially expressed GO categories at $p < 0.05$, a subset of which are listed in Table 3.4.

Table 3.4   Subset of differentially expressed GO categories determined to be significant by annotation enrichment analysis (P- biological process, F-molecular function, C- cellular component).

GO ID	GO Term	Category	P-value
Down at 30 psu			
GO:0071840	Cellular component organization or biogenesis	P	1.8E-05
GO:0070727	Cellular macromolecule localization	P	0.014543
GO:0034613	Cellular protein localization	P	0.014543
GO:0015995	Chlorophyll biosynthetic process	P	0.037864
GO:0045184	Establishment of protein localization	P	0.048091
GO:0034220	Ion transmembrane transport	P	0.024657
GO:0043231	Intracellular membrane-bounded organelle	C	4.5E-04
GO:0006886	Intracellular protein transport	P	0.030471
GO:0032991	Macromolecular complex	C	0.043608
GO:0009059	Macromolecule biosynthetic process	P	0.002178
GO:0016020	Membrane	C	0.009677
GO:0043227	Membrane-bounded organelle	C	4.5E-04
GO:0009536	Plastid	C	3.5E-06
GO:0004872	Receptor activity	F	0.002000
GO:0005840	Ribosome	C	1.2E-10
GO:0003723	RNA binding	F	0.014543
GO:0005198	Structural molecule activity	F	6.5E-07
GO:0006412	Translation	P	5.5E-07
Up at 30 psu			
GO:0005488	Binding	F	7.6E-04
GO:0009081	Branched chain family amino acid metabolic process	P	0.029703
GO:0019752	Carboxylic acid metabolic process	P	0.001289
GO:0006520	Cellular amino acid metabolic process	P	0.004135
GO:0042180	Cellular ketone metabolic process	P	0.002133
GO:0006952	Defense response	P	0.025378
GO:0003677	DNA binding	F	0.013611
GO:0043167	Ion binding	F	0.024115
GO:0005874	Microtubule	C	0.002794
GO:0001071	Nucleic acid-binding transcription factor activity	F	0.025378
GO:0006082	Organic acid metabolic process	P	6.9E-04
GO:0006796	Phosphorus-containing compound metabolic process	P	0.006633
GO:0004672	Protein kinase activity	F	2.8E-04
GO:0036211	Protein modification process	P	5.5E-04
GO:0006950	Response to stress	P	0.043622
GO:0044281	Small molecule metabolic process	P	0.045731
GO:0016740	Transferase activity	F	0.004042

3.3.6 Transmembrane Transport-Related Differential Expression

Inspections were performed of the differentially expressed transcripts' sequence identities with regard to transport, which were grouped by components; fold changes and p-values were averaged if multiple transcripts existed for the same component. These included general transmembrane transporters, which are listed in Table 3.5. Many homologs are evident involving both the unidirectional and bidirectional transport of ions across cellular membranes. Transcription involving general transmembrane transport included numerous ABC transporter homologs (14 members), and the top up- and downregulated transcripts were ABC transporters (sub-families B and F, respectively).

Table 3.5　Subset of differentially expressed components associated with general transmembrane transport.

Seq ID	Description	Fold Change	P-value
UPREGULATED			
comp15188_c0_seq6	ABC transporter sub-family B member 9	5.771	0.002864
comp21644_c0_seq2-8	Major facilitator superfamily transporter	4.213	0.000869
comp179972_c0_seq1	ABC transporter sub-family A member 1-like	4.013	0.001743
comp19592_c0_seq1, 4	Permease	3.537	0.000592
comp20284_c0_seq1	ABC transporter sub-family A member 3-like	3.189	1.3E-05
comp21858_c0_seq1-2	ABC transporter sub-family B	3.174	0.001334
comp20833_c0_seq2	ABC transporter sub-family C	2.956	0.000306
comp16671_c0_seq1	ABC transporter sub-family C member 1	2.538	0.000383
DOWNREGULATED			
comp11681_c0_seq1	ABC transporter sub-family F	-3.491	5.4E-05
comp21280_c0_seq1	Permease	-3.340	5.4E-06
comp7704_c0_seq1	ABC transporter sub-family F	-2.948	0.000189
comp134647_c0_seq1	ABC transporter sub-family A member 3	-2.793	0.002912
comp17791_c0_seq1	ABC transporter sub-family C member 2	-2.688	0.000397
comp10024_c0_seq1	ABC transporter sub-family G member 7	-2.559	0.000534
comp17606_c0_seq2	ABC transporter sub-family A member 3	-2.404	0.000759
comp2218_c0_seq1	ABC transporter ATP-binding protein	-2.377	0.001234
comp14568_c0_seq1	ABC transporter sub-family A member 2	-2.142	0.003283

3.3.7 Salinity Adaptation/Osmoregulation-Associated Transcription

The highest fold-change among the downregulated salinity-associated transcripts at 30 psu belonged to a voltage-gated ion channel homolog (Table 3.6). A hydrogen/chloride exchanger and chloride channel were the 2 top upregulated salinity-associated transcripts. A number of other pertinent transporters were also observed. Notably, salt stress response-related transcription was upregulated, including the tryptophan-rich sensory protein/peripheral-type benzodiazepine receptor (*TSPO/MBR*)-related protein (fold change = 7.520, p-value = 1.0E-06) and *AMMECR1* (fold change = 3.068, p-value = 0.000102). Also, several homologs with potential involvement in osmolyte synthesis were upregulated at 30 psu, including S-adenosylmethionine S-methyltransferase and sulfotransferase.

Table 3.6   Subset of differentially expressed salinity-specific transport-related
components.

Seq ID	Description	Fold Change	P-value
UPREGULATED			
comp21899_c0_seq2	Hydrogen/chloride exchange transporter 7-like	8.245	1.8E-08
comp21894_c0_seq2	Chloride channel protein 2	7.752	3.0E-07
comp17830_c0_seq2	Sulfotransferase	7.100	9.5E-06
comp17608_c0_seq2	S-adenosylmethionine S-methyltransferase	7.092	9.5E-06
comp13420_c0_seq2	Potassium channel protein	6.665	7.4E-05
comp21203_c0_seq2	Transient receptor potential cation channel subfamily M member 2	6.022	0.001006
comp19353_c0_seq1	Transient receptor potential cation channel subfamily M member 3	5.816	0.001997
comp17214_c0_seq2	Sodium myo-inositol co-transporter	5.026	1.6E-10
comp19216_c0_seq1	Calcium-activated outward-rectifying potassium channel	3.544	2.0E-06
comp19801_c0_seq1	Bestrophin-like protein	3.529	0.000977
comp13488_c0_seq1,2	S-adenosylmethionine S-methyltransferase	3.422	0.000101
comp18877_c0_seq1	S-adenosylmethionine S-methyltransferase	3.164	8.6E-06
comp21617_c0_seq2	Vanilloid receptor-related osmotically activated channel	3.055	0.000774
comp21107_c0_seq1	Sodium/calcium exchanger 3	2.816	7.1E-05
comp20702_c0_seq1	Cation-chloride co-transporter	2.672	0.000145
comp21620_c0_seq1	Sodium/calcium exchanger 1-like	2.653	0.000152
comp20699_c0_seq1	Potassium voltage-gated channel H member 5	2.217	0.002832
DOWNREGULATED			
comp21855_c0_seq1	Voltage-gated ion channel superfamily	-10.895	8.3E-16
comp9358_c0_seq2	Potassium voltage-gated sub-family H member 7	-8.259	1.8E-08
comp21377_c0_seq2	Sodium/hydrogen exchanger 8	-7.466	1.4E-06
comp9953_c0_seq1	Potassium channel *KOR1*	-3.304	3.4E-05
comp15314_c0_seq1	Potassium voltage-gated channel H member 2	-3.276	1.4E-05
comp216851_c0_seq1	Sodium/calcium exchanger 3	-2.803	0.000617
comp7033_c0_seq1	Sodium/potassium/calcium exchanger 3	-2.689	0.000521
comp18085_c0_seq1	Sodium/potassium/calcium exchanger 4	-2.398	0.000898
comp12500_c0_seq1	Outward rectifying potassium channel	-2.374	0.002996
comp15349_c0_seq1	Sodium/hydrogen exchanger 8	-2.209	0.001220
comp21026_c0_seq2	Potassium voltage-gated channel H member 6	-2.196	0.003031

3.3.8 Vesicular Transport-Related Differential Expression

A subset of differentially expressed vesicular transport-associated transcripts are listed in Table 3.7. The top upregulated transcript was *SEC61* and the top downregulated one was trafficking protein particle complex subunit 2 (*TRAPPC2*).

Table 3.7 Subset of differentially expressed components associated with vesicular transport.

Seq ID	Description	Fold Change	P-value
UPREGULATED			
comp19925_c0_seq2	Protein transporter *SEC61* subunit	6.233	0.000391
comp7586_c0_seq1	*RAS*-related protein *RAB-1a*	4.255	1.3E-05
comp15563_c0_seq1	Double C2 domain-containing protein alpha	4.055	4.2E-06
comp15562_c0_seq2	Multiple C2 and transmembrane domain-containing protein 1	3.447	9.7E-05
comp20380_c0_seq1-2	*ARF-GAP*	3.217	1.3E-05
comp19739_c0_seq1	Multiple C2 and transmembrane domain-containing protein 1	2.967	4.8E-05
DOWNREGULATED			
comp17350_c0_seq2	Trafficking protein particle complex subunit 2	-7.077	1.2E-05
comp4935_c0_seq1	*SEC14p*-like protein *TAP3*	-3.400	0.000815
comp20469_c0_seq1	*RAB1*-family small GTPase	-2.938	4.3E-05
comp18879_c0_seq1	Signal peptidase I-1	-2.658	0.000219
comp15204_c0_seq2	Lipoprotein signal peptidase	-2.524	0.002122
comp11203_c0_seq1	*ARF-GAP: ZAC*	-2.501	0.001108
comp78103_c0_seq1	Trafficking protein particle complex subunit 12	-2.440	0.000732
comp3190_c0_seq1	*RAS*-related protein *ORAB-1*	-2.491	0.000359
comp16927_c0_seq1	ADP-ribosylation factor 6	-2.488	0.000467
comp15610_c0_seq1	ADP-ribosylation factor 3	-2.306	0.001514
comp18024_c0_seq1	*RAB1*-family small GTPase	-2.155	0.003162

3.3.9 Acetate Metabolism-Related Expression

The differentially expressed transcripts that were associated with acetate metabolism were also assessed and are listed in Table 3.8. One homolog for β-ketoacyl-acyl carrier protein (ACP) synthase and one for malonyl-CoA ACP transacylase were downregulated. Notably, acetate kinase was the top upregulated transcript within this subset, and a G-D-S-L family lipolytic protein experienced the highest downregulation. Isocitrate lyase (fold change = 2.425, p-value = 0.000423) and malate synthase (fold change = 3.569, p-value = 7.69E-07) were also upregulated. With regard to TAG synthesis, one wax ester synthase/acyl-CoA:diacylglyceride acyltransferase/acyl-CoA:monoacylglyceride acyltransferase (*WS/DGAT/MGAT*) homolog was found to be downregulated in 30 psu cultures. Additionally, one *de novo* PUFA synthase was upregulated.

Table 3.8   Subset of differentially expressed components associated with acetate metabolism.

Seq ID	Description	Fold Change	P-value
UPREGULATED			
comp19954_c0_seq2	Acetate kinase	10.298	4.4E-14
comp19101_c0_seq1	1-phosphatidylinositol-4,5-bisphosphate phosphodiesterase	7.084	9.48E-06
comp21893_c0_seq3, 8	*De novo* PUFA synthase	6.999	0.000503
comp19433_c0_seq2	Acyltransferase-domain-containing protein	6.299	0.000391
comp17328_c0_seq1	Short-chain dehydrogenase reductase	5.598	8.71E-05
comp18144_c0_seq1	Acetyltransferase	5.137	9.4E-11
comp21947_c0_seq3, 4, 6	1-phosphatidylinositol-4,5-bisphosphate phosphodiesterase	4.283	0.000524
comp10678_c0_seq1	Acyl-CoA binding protein	3.709	1.6E-06
comp6347_c0_seq1	Fatty acid synthase	3.299	6.2E-05
comp620_c0_seq1	Lipase esterase	3.165	0.002088
comp15199_c0_seq1	Coenzyme A transferase	2.985	0.000200
comp16397_c0_seq1	Acyl-CoA oxidase	2.918	3.3E-05
comp3307_c0_seq1	Phosphate acetyltransferase	2.854	4.6E-05
comp21756_c0_seq1	Fatty acid synthase	2.837	5.7E-05
comp20442_c0_seq1	Galactolipid galactosyltransferase	2.759	0.000263
comp19374_c0_seq1	Methylmalonate-semialdehyde dehydrogenase	2.541	0.000237
comp14725_c0_seq1, 2	Acyl-CoA dehydrogenase	2.376	0.001078
comp14555_c0_seq1	Acyl-CoA dehydrogenase	2.257	0.000968
comp19967_c0_seq1	Acetyl-CoA synthetase	2.204	0.001252
comp20802_c0_seq2	Glycosyltransferase family protein	2.166	0.001830
comp20903_c0_seq1	Sterol-3-β-glucosyltransferase	2.166	0.001704
DOWNREGULATED			
comp20314_c0_seq5	Lipolytic protein GDSL family	-6.148	0.000291
comp17516_c0_seq2	Acyl-CoA binding protein	-4.138	5.6E-07
comp2616_c0_seq1	Sphingosine-1-phosphate lyase	-3.614	4.31E-05
comp177464_c0_seq1	β-ketoacyl-ACP synthase	-3.569	0.000169
comp7167_c0_seq1	Phytol kinase 2	-3.324	4.01E-05
comp18562_c0_seq1, 2	Methyltransferase-like protein	-3.077	0.000316
comp176632_c0_seq1	Acyltransferase, *WS/DGAT/MGAT*	-3.027	0.000253
comp21140_c0_seq1	Cyclopropane-fatty-acyl-phospholipid synthase	-2.871	6.68E-05
comp7926_c0_seq1	Δ4-desaturase	-2.173	0.002509
comp20217_c0_seq1	Monogalactosyldiacylglycerol synthase	-2.104	0.002529
comp20058_c0_seq1	Malonyl-CoA acyl carrier protein transacylase	-2.005	0.003268

3.3.10 Prymnesin Detection and Quantitation

The fluorescence assay revealed that the prymnesins were 53% less abundant in the 30 psu *versus* 5 psu supernatants on a pg/cell basis ($p < 0.05$) (Fig. 3.3).
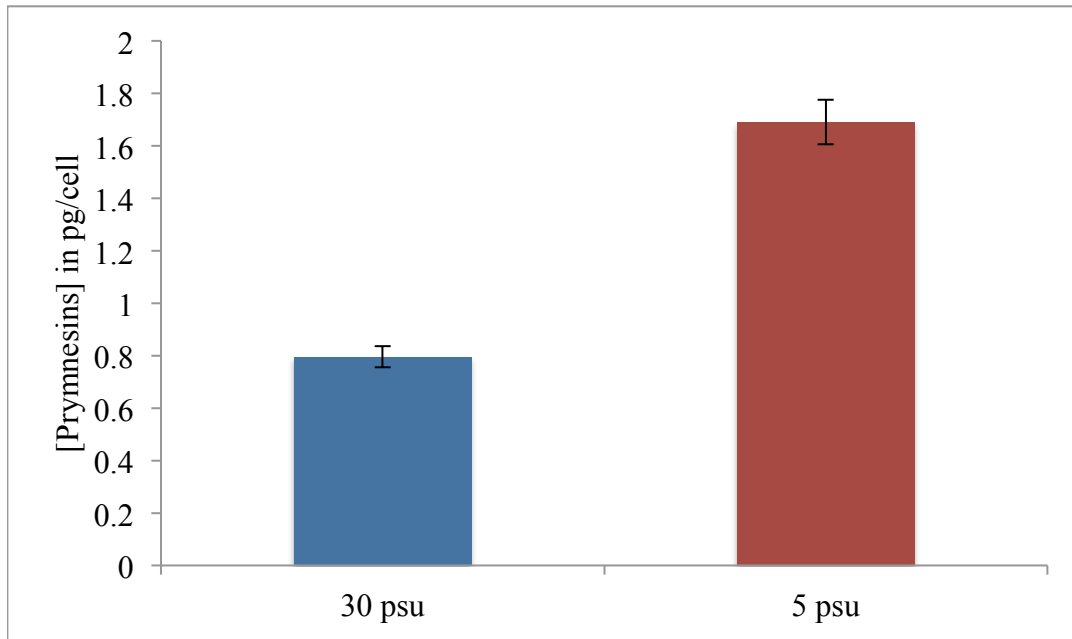
Figure 3.3 Fluorescence detection of prymnesins in supernatants from cultures that were grown in 5 and 30 psu media. Prymnesin concentrations are reported as average pg/cell values (n = 12 total measurements for each treatment).

3.4 DISCUSSION

This study presents the first extensive transcriptome analysis of *P. parvum*. The goal of this examination was to characterize the transcriptome of this organism and determine changes in gene expression that occur in response to altered salinity levels. This would allow for the delineation of molecular patterns that are associated with salinity adaptation in this euryhaline alga. Additionally, the focus was on acetate

metabolism- and general transport-related gene expression to gain insight into the synthesis and transport of pertinent metabolites and cellular constituents including toxins, glycerolipids, and PUFA.

There are currently very few published studies examining the transcriptomic responses of *P. parvum* to fluctuations in salinity. Freitag *et al.* (2011) used qPCR to examine the expression of 3 PKS ESTs in *P. parvum* following exposure to several physiological shock treatments, finding inconclusive evidence of differential expression following a two-hour salinity shock. The effects of salinity alterations on gene expression have also been evaluated in a variety of other eukaryotic algal species, including the heterokont *Ectocarpus siliculosis*, the dinoflagellates *Karenia brevis* and *Oxyrrhis marina,* and several red algae (Collen *et al.,* 2007; Dittami *et al.,* 2009; Teo *et al.,* 2009; Ichihara *et al.,* 2011; Liu *et al.,* 2011; Lowe *et al.,* 2011; Dittami *et al.,* 2012). These studies have looked at both short- and long-term responses to changes in salinity using EST analyses, microarrays, and qPCR; few RNA-Seq analyses have been reported. Thus, the present data represent an important contribution to research involving salinity-based high-throughput gene expression analyses of eukaryotic, euryhaline algae.

3.4.1 Transcriptome Characterization

The general ouput of the present sequence assembly correlates well with a previous, less extensive EST study that reported an overall GC content of 58% (La Claire, 2006), and the completeness and contiguity scores verify its quality. The GO annotation and KEGG pathway analyses that were obtained provide categorical overviews of the functioning of *P. parvum* at the transcriptome level. The abundance of transcripts that are associated with structural activities, including those involving membrane- and non-membrane-bound organelles as revealed by the GO annotations, include components of the secretory pathway. This suggests the relevance of their structural integrity in *P. parvum*. Additionally, the prominence of the stimulus response

GO category correlates well with the ability of this organism to adapt to salinity stress conditions.

The individual assessment of transcripts revealed many specific homologs that are involved in salinity adaptation. For example, a solute carrier family 4 (*SLC4*) homolog was the most prominent in this subgroup, which functions as a chloride/bicarbonate exchanger (Alper, 2009). Further, the presence of cyclic nucleotide binding protein transcripts involving sulfate transport may play a role in sulfur assimilation for the synthesis of the osmolyte dimethylsulfoniopropionate (DMSP) and thus be involved in osmoregulation. Significantly, V-type H($^+$)-translocating pyrophosphatases and sodium/hydrogen antiporters have been implicated in increased salt tolerance in plants, and their abundance within the transcriptome of *P. parvum* may well contribute to its euryhaline capabilities (Silva and Geros, 2009).

Regarding secretion, transcripts encoding components of the conventional secretory pathway were well represented, pointing to their importance in this organism. Additionally, autophagy-related protein has been implicated in the unconventional secretion of a variety of compounds in yeasts (Manjithaya and Subramani, 2011), suggesting that this organism may utilize similar mechanisms for some of its secretory activities. The presence of other transcripts that have been observed to be involved in this type of secretion, including autophagy-related proteins (*ATG4, 5, 8,* and *13*), *SEC18*, *TLG2*, and vacuolar protein sorting (*VPS4* and *23*) homologs, support this notion (Reggiori *et al*., 2004; Yorimitsu and Klionsky, 2005; Xie and Klionsky, 2007; Duran *et al.,* 2010; Manjithaya and Subramani, 2011). Unconventional secretion includes both non-vesicular and vesicular routes that deviate from the conventional pathway (Nickel, 2010). Non-vesicular proteins that have been reported to be involved include ABC transporters and lipid transfer proteins, homologs of which were both present at high levels in the present assembly (McGrath and Varshavsky, 1989; Duden *et al.,* 1991; Kader, 1996; Lev, 2010).

Acetate metabolism-related transcripts included 32 PKS homologs in total. The majority showed homology to PKS Type I transcripts from the closely related haptophyte *E. huxleyi* in addition to several bacterial species. All of the PKS transcripts were present as unique components, suggesting the absence of isoforms, which would have indicated possible splice variants. However, some of these transcripts only coded for one or two particular PKS domains. Typically, full-length PKS Type I transcripts code for the complete set of corresponding enzymatic domains (Zhu *et al*., 2002). Similar single domain transcripts have been observed in the dinoflagellate *K. brevis*, which possesses a trans-splicing mechanism of transcriptional regulation (Zhang *et al*., 2007; Monroe and Van Dolah, 2008). Although my study provided a comprehensive overview of genome-wide transcription in *P. parvum*, it led to difficulty in obtaining full-length transcripts because it was a *de novo* assembly. Thus, it may be interesting to assess these PKS transcripts using a technique which generates full length sequences, such as rapid amplification of cDNA ends (RACE), to assess the possible presence of such single domain transcripts and spliced leader sequences in *P. parvum*.

Other transcripts that are associated with acetate metabolism included two encoding PKS Type III, which belong to the chalcone synthase superfamily and are involved in the synthesis of a variety of secondary metabolites in plants (Austin and Noel, 2003; Abe and Morita, 2010). β-ketoacyl synthase transcripts showed similar homology distributions as were observed with PKS. The *sxtA* homologs were similar to those from the dinoflagellate *Alexandrium fundyense* and the cyanobacterium *Aphanizomenon*. Its gene product is involved in the first step in saxitoxin synthesis as part of an integral PKS module (Al-Tebrineh *et al*., 2010). *P. parvum* is not known to produce saxitoxin. But, because *stxA* homologs have been observed in other non-saxitoxin producing organisms, they are likely derived from a common ancestral gene to those in the dinoflagellates and cyanobacteria (Hackett *et al*., 2013).

Some transcripts were also identified that play roles in fatty acid and polyketide biosynthesis. Acetyl-CoA, which was the most prominent transcript in this subset, converts acetyl-CoA to malonyl-CoA to provide substrates for fatty acid biosynthesis (Oliver *et al.*, 2009). This particular transcript was predicted to be localized to the chloroplast by TargetP with relatively high likelihood [reliability class (RC) = 2], which supports its functioning within the chloroplast as the main site of fatty acid synthesis. However, it remains unclear whether all or part of the synthesis of prymnesins also occurs in the chloroplast.

PUFA-related homologs included Δ-9 elongase and Δ-8 desaturase, indicating that like its close relative *E*. *huxleyi*, *P*. *parvum* may not synthesize ω-3 long-chain PUFA via the conventional Δ-6 pathway. Instead, these findings suggest that it uses an alternative pathway that involves the elongation of α-linolenic acid (C18:3n-3) to eicosatrienoic acid (C20:3n-3) followed by two subsequent desaturation events (Sayanova *et al.*, 2011; Read *et al.*, 2013). This pathway has also been observed in freshwater dinoflagellates, the prymnesiophytes *Isochrysis galbana* and *Pavlova salina*, and the euglenoid *Euglena gracilis* (Wallis and Browse, 1999; Qi *et al.*, 2002; Zhou *et al.*, 2007; Robert *et al.*, 2009; Sayanova *et al.*, 2011). Its evolutionary significance is unknown, but sequence similarities of the various desaturases (Δ-5, Δ-6, and Δ-8) suggest that they all diverged from a common ancestor (Sayanova *et al.*, 2011). Interestingly, stearidonic acid (SDA; C18:4n-3) has been reported to be a prominent PUFA in *P*. *parvum* that potentially contributes to its ichthyotoxicity during HABs (Henrikson *et al.*, 2010). This fatty acid is synthesized by the conventional Δ-6 pathway, suggesting the utility of both the alternative and conventional pathways in this organism (Bell and Pond, 1996). It is possible that this strategy enables the selective increase in the production of certain long-chain PUFA, such as SDA, during HAB formation.

Additional PUFA-related findings included homologs to a *de novo* PUFA synthase in *Schizochytrium* sp. This organism accumulates abundant quantities of both

docosahexaenoic acid (DHA; C22:6n-3) and docosapentaenoic acid (DPA, C22:5n-6) by a pathway involving this PUFA synthase, which is separate from the fatty acid synthase that produces the C14:0 and C16:0 fatty acids that are predominately found in its TAG (Metz *et al.*, 2001; Hauvermale *et al.*, 2006; Johnson and Wen, 2009). Thus, it is possible that *P. parvum* uses a similar mechanism for PUFA production, which may act as an additional long-chain PUFA synthesis pathway. This information further clarifies the findings from the GO and KEGG analyses and characterizes the most prominently expressed transcripts in *P. parvum*. As a whole, the identification of candidate transcripts involving salinity adaptation, transport, and acetate metabolism confers in-depth insight into the particular molecular mechanisms that are utilized by *P. parvum*. For example, the abundance of ion transporter homologs of various types within the transcriptome in addition to those involving the salt stress response and osmolyte biosynthesis indicate that this organism is well suited for survival in divergent salinities. The prominence of transcripts encoding components of both conventional and unconventional secretory pathways bring about questions regarding the manner of release of prymnesins from this organism. The collective assessment of these transcripts by a differential expression analysis in varying salinities provided further insight into these activities at the transcriptional level.

3.4.2 Differential Expression Analysis - Comparisons to Previous Studies

Due to the relatively small number of transcriptomic studies that have been performed on algae involving osmotic stress and the variable experimental treatments (salinity levels and exposure times) that have been applied, accurate comparisons between the present findings and those of previous studies are difficult. However, a few general similarities were noted. For example, Dittami *et al.* (2009) studied short-term (6 h) responses to hyper- and hyposalinity shock in *Ectocarpus siliculosis* (a filamentous brown alga) using microarrays, reporting the upregulation of valine, leucine and

64

isoleucine metabolism and the downregulation of RNA binding and translation factor activity during hyperosmotic stress, which is similar to what we found for *P. parvum*. They also found isocitrate lyase to be strongly upregulated in response to stress conditions, suggesting that the activation of the glyoxylate cycle acts to re-allocate nutrients to crucial biological processes. However, amino acid metabolism was found to be downregulated by this group, while it was upregulated in the present study. Further, they described the downregulation of GST during hypersaline stress conditions; this was also observed with *P. parvum* in addition to the macroalgal rhodophyte *Gracilaria changii*, in which GST was downregulated following a 7-day exposure to hyposaline stress (Teo *et al.*, 2009). The expression of the following additional genes that were induced following osmotic stress in *P. parvum* have been previously described in the literature: serine acetyl transferase (Dittami *et al.*, 2009; Teo *et al.*, 2009), fructose bisphosphate aldolase (Collen *et al.*, 2007; Teo *et al.*, 2009), heat shock protein 90 (HSP90) (Collen *et al.*, 2007; Dittami *et al.*, 2009; Teo *et al.*, 2009; Lowe *et al.*, 2011), and hemolysin (Teo *et al.*, 2009). Additionally, osmotic stress was found to reduce the expression of light harvesting protein in *Gracilaria changii* and *Chondrus crispus* (Collen *et al.*, 2007; Teo *et al.*, 2009), which is in agreement with the present study. Further, Dittami *et al.* (2009) described the inhibition of photosynthesis-related transcripts (chlorophyll a/c-binding proteins) in osmotic stress conditions in *Ectocarpus*. In fact, photosynthesis may be less active in hypersaline conditions due to the inhibition of electron transfer and activation of repair pathways (Kirst, 1989). Finally, several of the aforementioned studies, including the current one, detected the downregulation of many ribosomal genes in stress conditions, which indicate that protein synthesis is repressed at high salinity levels, likely due to the osmotic stress (Collen *et al.*, 2007; Dittami *et al.*, 2009). Thus, this cross comparison of *P. parvum* with other osmoregulatory studies from the literature reveals a number of similarities, which sheds light on common responses to salinity stress across different strains of algae. However, additional high-throughput

65

studies involving the osmoregulation of these and other species might clarify such correlations.

3.4.3 Differential Expression Analysis - Highlights

My differential expression analysis sheds light on potential osmoregulatory mechanisms that are utilized in this organism. The annotation enrichment analysis indicated that in this strain and likely others, hyperosmotic conditions may trigger pertinent stress responses. Because *P. parvum* is widespread in the oceans and seas, this finding poses questions as to the origin of the alga. Perhaps it first evolved in hyposaline environments and subsequently migrated into oceans. Alternatively, our strain may have required a longer time period to adjust to higher salinity levels because it was isolated from freshwater, cultured at 5 psu initially and subsequently acclimatized to 30 psu. Thus, it may be interesting to compare the present gene expression data with those from an isolate that is naturally growing in open seawater.

The decreased abundance of the cellular trafficking and membrane activity GO categories at 30 psu along with macromolecular biosynthesis and organization support the notion of depressed toxin synthesis and secretion at the higher salinity level. Additionally, the decrease in transcripts belonging to the transmembrane ion transport GO category was surprising from an osmoregulation standpoint because the increase in environmental ion concentrations would presumably require increased transporters. However, the 30 psu culture was acclimated long-term over the course of many months. It is possible that there was an initial increase in the transcription of transporters at 30 psu that was not detectable in my study. The annotation enrichment analysis also indicated suppressed photosynthetic activity at 30 psu, which would necessitate fewer transmembrane transporters at that salinity level. Further, the decreases in the ribosome and translation GO categories at 30 psu indicate that translation is being repressed at the higher salinity level, which may be a stress response allowing for energy conservation.

This is in accordance with the heightened stress response at 30 psu. The elevated levels of transcripts that belong to the GO categories involving transcription factors, protein kinases, and protein modification may also play roles in the stress response and enzymatic regulation.

At the sequence level, the pattern of differential expression of particular ion transporter homologs was assessed. The elevated abundance of chloride transporter transcripts at 30 psu may indicate the increased sequestration of this ion as an osmoregulatory response or the extrusion of excess chloride that may have leaked into the cells. Additionally, the variable expression of sodium and potassium transporters can be explained by the fact that many are bidirectional. The high expression of the vanilloid receptor-related osmotically activated channel suggests that it plays a significant role in osmoregulation in *P. parvum*. The expression patterns of transcripts encoding enzymes that may be involved in DMSP synthesis (known to function in osmoregulation), including S-adenosylmethionine S-methyltransferase, were in accordance with the increased cellular need for this solute at the higher salinity level (Summers *et al.,* 1998). *PTC1* transcription decreased, which is a type 2C serine/threonine phosphatase that has been reported to be a negative regulator of osmotic stress in *Saccharomyces cerevisiae* (Warmka *et al.,* 2001). Accordingly, *TSPO/MBR*-related protein and *AMMECR1* transcription increased, which have been reported to be induced in response to salt stress in *Arabidopsis thaliana* (Jiang *et al.,* 2007; Guillaumot *et al.,* 2009). These findings also support those from the GO analysis regarding an increased stress response at 30 psu. ABC transporters showed variable expression patterns in line with their diverse biological functions. ABCB in particular may be potentially more functional in conditions of higher salinity because multiple transcripts from this sub-family were present solely at 30 psu. In contrast, ABCF may be less active at 30 psu. Collectively, these results indicate the pattern of ion transport-associated gene expression, the involvement of particular salt stress response genes, and evidence of increased osmolyte

synthesis that may all contribute to salinity adaptation and osmoregulation in *P. parvum*. They also suggest the possibility that chloride toxicity, rather than sodium toxicity, is the underlying factor controlling the molecular responses of *P. parvum* to long-term hypersalinity stress. Future analyses could assess short-term transcriptional changes at the two salinities for comparative purposes, which is typically when ion trafficking is most active to regulate the intracellular osmotic balance (Kirst, 1989; Kobayashi *et al*., 2007). Thus, a greater number and/or different types of ion transporters may be differentially expressed in the short-term. Gene expression analyses could also be performed over a wider variety of salinities to detect any incremental alterations that may be occurring. Further, a comparative assessment of the plasma membrane proteome of *P. parvum* at the two salinities may shed light on adaptive mechanisms that are occurring in this alga that are specific to this subcellular location. Analyses at the transcriptomic level revealed many potential plasma membrane-associated homologs, including those encoding numerous transmembrane transporters in addition to flagellar proteins, structural proteins, signaling molecules, antioxidative stress and lipid-metabolizing enzymes, and those involved in protein synthesis, stability, and degradation. However, their precise subcellular localization could not be determined in the majority of cases. Thus, an assessment of proteome-level responses would allow for a clearer picture of plasma membrane alterations that occur during salinity adaptation. This may also provide useful information regarding membrane protein restructuring in HAB-forming conditions.

Transcripts whose gene products are associated with secretion were generally reduced at the higher salinity level and thus more abundant at the lower salinity level, the latter being associated with the formation of HAB of this organism. This correlates with the comparative prymnesin assay that was performed at the two salinities. Pertinent transcripts that decreased in quantity at 30 psu included *ARF*, which are GTP-binding proteins that are localized to a variety of organellar membranes in addition to the plasma membrane and are involved in the regulation of membrane traffic and organelle structure

(D'Souza-Schorey and Chavrier, 2006; Donaldson and Jackson, 2011). Additionally, the reduced expression of signal peptidase homologs at 30 psu, which are responsible for converting secretory proteins and certain membrane proteins to their mature forms (Tuteja, 2005), and *TRAPP* complex subunits, which participate in ER to Golgi trafficking and are activators of RAB proteins (Barrowman *et al.*, 2010), further indicate the possibility of decreased cellular trafficking at the higher salinity. Some transport-related transcripts did not show a specific expression pattern and thus may undergo post-transcriptional regulation. The transcription of *SEC61*, which is involved in ER translocation in eukaryotes, and multiple C2 transmembrane domain-containing proteins increased at 30 psu. The latter are typically involved in both signaling and membrane trafficking (Wilkinson *et al.*, 1996; Shin *et al.*, 2005). Because the GO category involving protein kinase signaling also increased at 30 psu, this particular result may be indicative of the heightened activity of signaling-associated mechanisms and not be representative of those associated with transport *per se*. The fact that no transcripts that are involved with unconventional secretion were differentially expressed while a number of those that play roles in the conventional pathway were present at decreased levels at 30 psu suggests that vesicular transport may be occurring via the conventional pathway at the lower salinity. The presence of greater concentrations of extracellular prymnesins at the lower salinity indicates the likelihood that they are being extruded at a more rapid rate in those conditions, which are associated with HAB formation. Thus, I suspect that prymnesins are likely secreted via vesicles in such conditions. However, it must be noted that a number of ABC transporters were also downregulated as mentioned above, which could potentially be involved in non-vesicular prymnesin transport. However, this route is less likely due to the large size and molecular structure of these toxins. A future comparative analysis of signal peptides may provide valuable information regarding the proportions of proteins that are targeted for secretion in differing environmental conditions in addition to the subcellular localizations of proteins of interest. For these

analyses, it is crucial to obtain full-length transcripts from which coding sequences can be predicted because signal peptides are located at the N-terminus of proteins (Emanuelsson *et al.*, 2000). Thus, the RACE technique would enable a more thorough evaluation of signal peptides than was possible with this assembly (Zhang and Frohman, 1997).

The assessment of acetate metabolism-related transcription revealed the increased prominence of many pertinent transcripts at 30 psu. This is likely indicative of the heightened energy needs of the cells during hypersalinity stress. For example, acetate kinase was the most abundant homolog, which promotes acetyl-CoA production and works in conjunction with phosphate acetyltransferase, which was also present at increased levels (Bock *et al.*, 1999). The transcription of isocitrate lyase and malate synthase was also elevated, which ultimately condense glyoxylate with acetyl-CoA to form malate, thus facilitating acetate assimilation as an energy source via the tricarboxylic acid (TCA) cycle from fatty acids and other pertinent sources (Theodoulou and Eastmond, 2012). This might indicate an increased breakdown of fatty acids and other pertinent substrates needed for energy. Additionally, methylmalonate semialdehyde dehydrogenase produces acetyl-CoA in the mitochondrion (Sokatch *et al.*, 1968; Popov *et al.*, 1992), and acetyl-CoA synthetase may be also contributing to mitochondrial acetyl-CoA pools (Schwer *et al.*, 2006). Sterol-3-glucosyltransferase and the signaling molecule 1-phosphatidylinositol-4,5-bisphosphate phosphodiesterase have been previously associated with the stress response in other organisms, and they increased in abundance at 30 psu (Murakami-Murofushi *et al.*, 1997; Kunimoto *et al.*, 2002; Pokotylo *et al.*, 2013). A number of organisms have been reported to alter their distributions of membrane cyclopropane fatty acids in response to salinity fluctuations and other abiotic stresses, and the current analysis provides evidence of their decrease in abundance at 30 psu (Grogan and Cronen, 1997; Guillot *et al.*, 2000; Dominguez-Ferreras *et al.*, 2006). Several homologs that are involved in glycerolipid metabolism that were differentially expressed included galactolipid galactosyltransferase and glycosyltransferase (upregulated) and

70

monogalactosyldiacylglycerol (MGDG) synthase (downregulated). This is potentially interesting given the proposed ichthyotoxic properties of MGDG (Henrikson et al., 2010). Consequently, the increased ichthyotoxicity at lower salinities may result from increased production/secretion of MGDG as well as the prymnesins, making the alga doubly hazardous to fish. The decrease in MGDG synthase transcription at 30 psu also correlates with the decreased photosynthesis that is likely occurring at that salinity level due to cell stress because it constitutes a prominent part of the chloroplast thylakoid membrane (Block *et al.,* 1983; Masuda *et al.,* 2011). Interestingly, galactolipid galactosyltransferase has been shown to be involved with galactolipid remodeling in response to abiotic stress in *Arabidopsis* (Moellering *et al.,* 2010) and thus may play a role in adaptive membrane restructuring in *P. parvum*.

Several transcripts that are involved in fatty acid breakdown were differentially expressed, including acyl-CoA dehydrogenase, which increased in transcription at 30 psu and is involved in fatty acid β-oxidation (Thorpe and Kim, 1995). The decreased expression of phytol kinase may relate to its role in phytol recycling following chlorophyll degradation, including its incorporation into lipid esters and tocopherols (Ischebeck *et al.,* 2005; Valentin *et al.,* 2006). Thus, it correlates with the reduced photosynthetic activity that is occurring at that salinity. Sphingosine-1-phosphate lyase plays a degradative role in the sphingolipid metabolic pathway. Sphingolipids are predominately found in the plasma membrane and play roles in the cellular stress response, so its decrease in transcription at 30 psu supports the increased cell stress at the higher salinity level (Quist *et al.,* 2009; Zhang *et al.,* 2012).

Because fatty acid and polyketide biosynthesis follow similar pathways, and none of the PKS homologs were differentially expressed, no steadfast conclusions about gene expression at the transcriptional level can be drawn regarding toxin synthesis in *P. parvum* at differing salinities. However, homologs to β-ketoacyl ACP synthase and malonyl-CoA ACP transacylase, which are domains of the modular PKS synthase

71

enzyme, were present at decreased levels at 30 psu. Similar to our findings, Freitag *et al*. (2011) studied the expression of 3 PKS ESTs in *P. parvum* following physiological shock treatments (including salinity shock) and did not find conclusive evidence of differential PKS expression either. The current findings substantiate the presence of a post-transcriptional control mechanism for polyketide prymnesin production, such as that which has been reported in brevetoxin PKS expression in dinoflagellates (Van Dolah *et al*., 2009). The assessment of full-length transcripts using splice prediction tools for splice site consensus sequences is warranted as evidence of this type of post-transcriptional regulation. Notably, the spliceosome KEGG pathway was prominent in this transcriptome, suggesting that splicing is an important means of expression regulation in *P. parvum*.

One homolog to hemolysin III also decreased in abundance, which is a pore-forming hemolysin (Baida and Kuzmin, 1996). These molecules have been previously described as contributing to the toxicity of *P. parvum*. Here again, these compounds may further contribute to the alga's toxicity beyond the synergistic effects of the prymnesins and MGDG. The hemolysins had been characterized as galactolipids, but studies have produced variable results likely depending on the chemical isolation methods that were used. One such study reported that the highest abundance of hemolysin I (out of 6) was present in *P. parvum*; however, another described 6 structurally different molecules (Ulitzur and Shilo, 1970; Kozakai *et al*., 1982; Yasumoto *et al*., 1990; Manning and La Claire, 2010). The decrease in hemolysin III transcription at 30 psu (and thus its increased abundance at 5 psu), and the lack of hemolysin I homologs in the present study, may indicate that different growing conditions stimulate the production of different hemolysins.

My analysis of TAG and PUFA expression indicated that the expression of a *de novo* PUFA synthase increased 30 psu, suggesting the potential for higher levels of ω-3 PUFA synthesis at higher salinities. Interestingly, one Δ-4 desaturase was present at

decreased levels, which also synthesizes DHA, pointing to the preferential utilization of particular long-chain PUFA pathways in varying salinities. FAME profiles have been previously carried out for *P. parvum* (Lee and Loeblich, 1971; Lang *et al.*, 2011). However, none of these analyses compared the fatty acids that are produced by this organism at varying salinities. Comparative FAME analyses at different growth phases and salinity levels may shed light on the potential utility of *P. parvum* for the production of high quantities of PUFA, such as DHA. Such work is covered in the next chapter. The transcriptomic data laid the foundation for further investigation into the utility of *P. parvum* in this realm.

Chapter 4: Characterization and analysis of fatty acids of *Prymnesium parvum* N. Carter (UTEX 2797)

4.1 INTRODUCTION

Lipids are crucial to organisms for supplying metabolic energy, the formation of cellular membranes, and cellular communication and signaling (Berge and Barnathan, 2005; Subramaniam *et al.*, 2011). The ability of algae in particular to thrive in a wide variety of environmental conditions is in part due to the variable lipid compositions of the different genera and species that confer adaptive capabilities; often, unique fatty acid profiles are even observed between different strains of the same species (Kayama *et al.*, 1989; Rezanka, 1989; Christie, 2003; Dalsgaard *et al.*, 2003; Lang *et al.*, 2011). Thus, fatty acid profiling is an excellent tool to characterize species and for identifying strain-specific fatty acid compositions, particularly in response to environmental fluctuations.

In non-stress conditions inside of the cell, the majority of lipids are esterified to form glycerol-based membrane lipids (Ohlrogge and Browse, 1995). Typical algal lipid content during optimal growth conditions has been reported to be approximately 5-20% of culture dry cell weight (DCW). Particular environmental stressors that often lead to the modification of lipid content include temperature, light, nutrient availability, and salinity (Teshima *et al.*, 1983; Ben-Amotz *et al.*, 1985; Cohen *et al.*, 1988; Lee *et al.*, 1989; Al-Hasan *et al.*, 1990; Roessler, 1990; Thompson, 1996). In some cases, lipid yields may double or even triple and be directed toward the formation of TAG under stress conditions, in part due to the reorganization and degradation of intracellular membrane systems, such as the photosynthetic membranes (Guckert and Cooksey, 1990; Hu *et al.*, 2008; Singh *et al.*, 2011). TAG consist of 3 fatty acids that are covalently bound to a glycerol backbone; they act as energy reserves and carbon storage units (Hu *et al.*, 2008). These neutral lipids are similar to fossil oils, and thus, much research has been performed investigating their capacities as biofuels (Dyer and Mullen, 2008; Cagliari *et al.*, 2011). In addition to TAG, many algae show promise for the production of PUFA, which are

pharmaceutically and nutritionally valuable molecules. Chromist species in particular, including cryptomonads, heterokonts, and haptophytes, tend to produce abundant quantities of long-chain PUFA, including the ω-3 PUFAs, eicosapentaenoic acid (EPA; C20:5n-3) and docosahexaenoic acid (DHA; C22:6n-3), although compositions vary from species to species (Cavalier-Smith, 2010; Mulroth *et al*., 2013).

Fatty acids may be synthesized with variable chain lengths, double-bond positions, and/or functional groups. It is likely that many have not yet been discovered, highlighting the importance of investigations into the fatty acid profiles of various unstudied algae. There have been several investigations into lipid production and fatty acid profiling in the haptophyte algae, including *Prymnesium parvum* (Renaud and Parry, 2004; Hu *et al*., 2008; Lang *et al*., 2011; Makri *et al*., 2011; Sayanova *et al*., 2011; Custodio *et al*., 2014). Investigations into its lipid composition and that of its close relative, *Emiliana huxleyi*, have revealed unique features, such as an abundance of C14:0 and DHA in addition to the PUFA octodecapentaeonic acid (OPA; C18:5n-3), which has also been associated with ichthyotoxicity in other algal species (Lee and Loeblich, 1971; Volkman *et al*., 1981; Viso and Marty, 1993; Lang *et al*., 2011; Makri *et al*., 2011; Sayanova *et al*., 2011). However, because fatty acid profiles of microalgae have been observed to differ by strain, isolate and/or habitat, it is difficult to make generalizations.

To date, the effects of salinity alterations on the fatty acid composition of *P. parvum* have not been evaluated nor has the lipid profile of *P. parvum* N. Carter (UTEX strain LB 2797) been fully elucidated. Thus, in this study, the methyl esters of fatty acids from total lipid extracts of *P. parvum* cells that were isolated in stationary phase at both 5 and 30 practical salinity units (psu) were evaluated by gas chromatography-mass spectrometry (GC-MS) to determine the general fatty acid profile of this strain in addition to the effects of salinity manipulations on fatty acid composition.

4.2 MATERIAL AND METHODS

4.2.1 Culture Maintenance and Harvesting

A strain of *P. parvum* (UTEX 2797) that was isolated in Texas was used in this study. The f/2 media (minus Si) were prepared containing steamed seawater at final salinities of 5 and 30 psu (Guillard and Ryther, 1962). From an inoculum containing approximately 2 x 10^6 pre-acclimated cells, 5 mL were added to each of four 250 mL Erlenmeyer flasks, two containing 150 mL each of 5 psu medium and two containing 150 mL each of 30 psu medium. Cultures were grown as described in Chapter 2. Cultures were sampled at regular intervals throughout growth for spectrophotometric quantification at 680 nm using the following extinction coefficient:

$$\varepsilon = 2.0\text{E-07 cm}^2 \text{ cell}^{-1}.$$

Cultures were grown until post-log phase (approximately 2.5 and 2.2 million cells/mL for 5 and 30 psu cultures, respectively), after which they were harvested by centrifugation at 5,000 rpm for 5 min at 23 °C.

4.2.2 Lipid Extractions

Lipid extractions were performed according to Jones *et al.* (2012) with minor modifications for small-scale isolations. Cell particulates were removed using vacuum filtration, and extracts were dried by rotary evaporation. The following day, extract weights were determined. They were then resuspended in 1 mL 2:2:1:1 hexane:toluene:acetone:MeOH (v/v/v/v), transferred to 14.8 mL borosilicate vials (ThermoFisher Scientific Inc., Wilmington, DE), and stored at 4 °C until further analyses.

4.2.3 Thin-Layer Chromatography (TLC)

TLC analyses were performed according to Jones *et al*. (2012) with minor modifications. First, 10 µl of each lipid extract was spotted onto a silica gel 60 F_{254} aluminum-backed TLC plate (10 cm x 10 cm; EMD Chemicals Inc., Gibbstown, NJ) using Wiretrol™ capillary micropipettes (Drummond Scientific Co., Broomall, PA). Two sequential solvent systems were used; first, the plate was developed to the halfway point in 65:10:20:10:3 chloroform:MeOH:acetone:acetic acid:H_2O (v/v/v/v). The plate was then dried and developed to completion in 80:20:1 hexane:diethyl ether:acetic acid (v/v/v). The plate was again dried, and spots were stained and visualized by exposure to iodine vapors.

4.2.4 Preparation of Fatty Acid Methyl Ester (FAME) Derivatives

FAME derivatives were prepared by transesterification according to O'Fallon *et al*. (2007) with as follows: first, lipid extracts were dried overnight in the fume hood and resuspended in 5.3 mL MeOH. Next, 500 µl of 10 N potassium hydroxide was added, and the solutions were incubated at 60 °C for 1 h. The solutions were then brought to room temperature, and 500 µl of 18 M sulfuric acid was slowly added to each. The vials were then rinsed with MeOH, vortexed, and incubated at 60 °C for 1 h. The solutions were cooled to room temperature and 5 mL of hexane was added to each vial and vortexed. Finally, the top hexane layers were transferred to new pre-weighed borosilicate vials and dried overnight in the fume hood, after which dry weights were obtained. Samples were resuspended in 1 mL of hexane and transferred to 1.5 mL amber vials (Alltech Associates Inc., Deerfield, IL) for further analyses. Full conversion of fatty acids to their methyl ester derivatives was assessed using the same TLC solvent system described above.

4.2.5 Gas Chromatography-Mass Spectrometry (GC-MS)

GC-MS analyses were carried out using an Agilent 5973-6890 system (Agilent Technologies, Cedar Creek, TX). One microliter each of the FAME samples was injected via a 5 μl, 23-gauge syringe (cone tip, needle length = 50 mm; SGE Analytical Science Inc., Austin, TX) into a Restek Rxi®-5SilMS column (30 m, 0.25 mm ID, 0.25 μm df; Bellefonte, PA). The initial temperature was 40 °C, which was held for 1 min, after which the temperature was raised to 200 °C at a rate of 30 °C/min, increased to 230 °C at a rate of 5 °C/min, and finally, heated to 250 °C at a rate of 30 °C/min, where it was held for 3 min. The GLC-30 FAME standards mix (Sigma Aldrich Co. LLC, St. Louis, MO) (containing C8, C10, C12, C14, and C16) was injected to establish retention times . Quantitative and qualitative analyses were conducted using the Xcalibur software, version 1.4 (Thermo Fisher Scientific Inc.). Unknown mass spectral data were compared with spectra from the American Oil Chemists' Society Lipid Library (http://lipidlibrary.aocs.org/ms/masspec.html), and their relative abundances were calculated based on the known C14:0 standard.

4.3 RESULTS AND DISCUSSION

Cells that were grown at 5 and 30 psu demonstrated similar densities for approximately the first 6 weeks of culturing as determined spectrophotometrically. However, the 30 psu cultures entered post-log phase approximately 2 weeks earlier than the 5 psu cultures (Fig. 4.1).
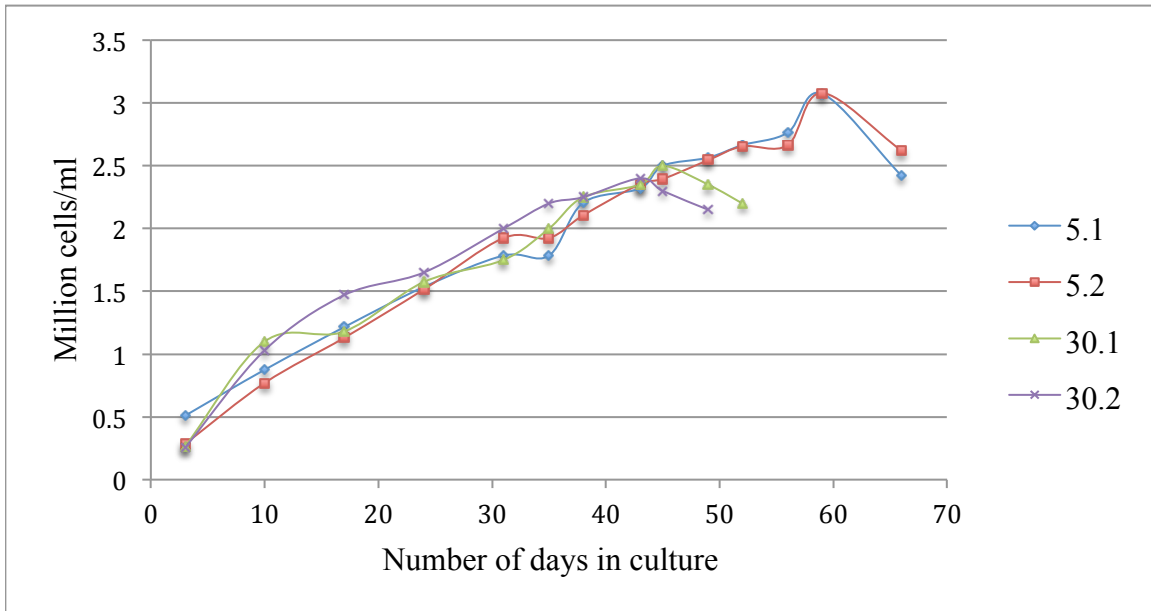
Figure 4.1   Growth curves for 5 and 30 psu cultures over 70 days (n = 2 for each treatment).

There was a 29% lower average relative abundance of lipids (based on DCW) in the 30 psu cultures when compared with the 5 psu cultures. This contrasts with reports in the literature that describe increased total cellular lipids following increases in salinity in a number of algal species, including the prymnesiophyte, *Isochrysis galbana* (Renaud and Parry, 1994; Guschina and Harwood, 2006; Kirrolia *et al*., 2011; Jayanta *et al*., 2012; Sharma *et al*., 2012). However, similar trends of decreasing lipid content with increasing salinity have been reported in several organisms, including the freshwater diatom *Fragilaria capucina,* a marine species of the diatom *Nitzchia frustulum*, and the marine heterokont *Schizochytrium limacinum* (Renaud and Parry, 1994; Zhu *et al*., 2007; Chaffin *et al*., 2011).

The TLC revealed that the total lipids were distributed into 6 main fractions, including β-carotene, TAG, free fatty acids, pigments (chlorophylls and xanthophylls), galactolipids, and phospholipids. Similar distributions of both polar and non-polar lipids

were observed for each replicate lipid extract at both 5 and 30 psu (Fig. 4.2). The polar lipids, pigments, and TAG represented the major fractions, while free fatty acids were the least prominent. Thus, although salt stress-induced TAG accumulation has been observed in other algal species, it did not appear to occur in this strain of *P. parvum* (Hu *et al.*, 2008; Muhlroth *et al.*, 2013). The fatty acids that were bound to the lipids were converted to FAME, which were also assessed by TLC, indicating full conversion of available fatty acids to their methyl ester derivatives (Appendix C: Figure 1).
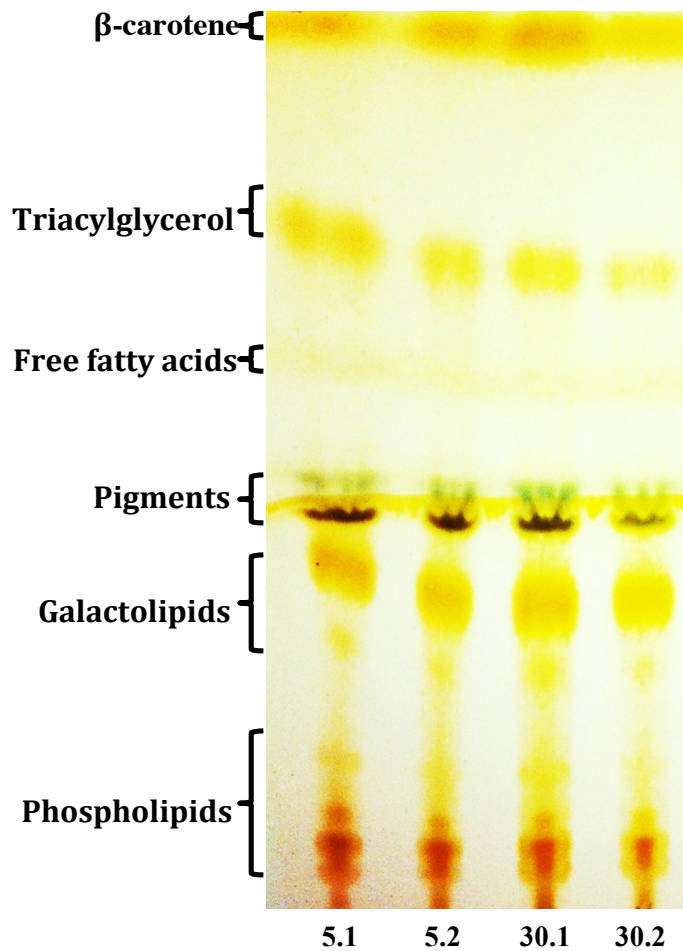
Figure 4.2   TLC plate of 4 lipid extracts for cultures grown at 5 and 30 psu (n = 2 for each treatment).

GC-MS analyses of the 4 samples resulted in similar chromatographs, demonstrating comparable fatty acid profiles between the two salinities, with the most abundant species being myristic acid (C14:0) followed by palmitic acid (C16:0), respectively (Appendix C: Figure 2). Overall, the relative abundance of C14:0 was 20% greater on average in the 30 psu cultures. The relative abundance of C16:0 was not significantly different (Fig. 4.3). Additionally, low levels of lauric acid (C12:0) were detected in the 5 psu (averaging 3.5%) but not in the 30 psu samples. Figure 4.4 depicts a

closer view of the chromatograph for sample 5.2, in which the 10 identified peaks are labeled. Those that were identified by their respective mass spectra included stearidonic acid (SDA, C18:4n-3), linoleic acid (LA, C18:2n-6), oleic acid (C18:1), stearic acid (C18:0), and DHA. Palmitoleic acid (C16:1) and eicosadienoic acid (C20:2) were also present at very low levels.
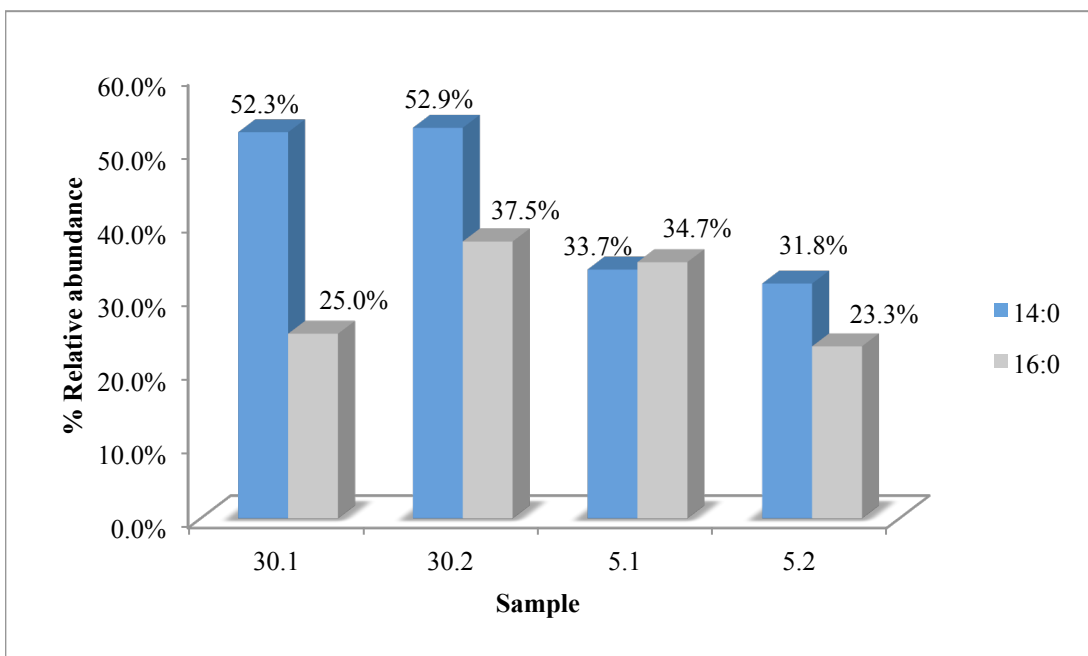
Figure 4.3   Percent relative abundance of the 2 major fatty acids (C14:0 and C16:0) in each sample (based on ng of sample injected into GC column) (n=2 for each treatment).
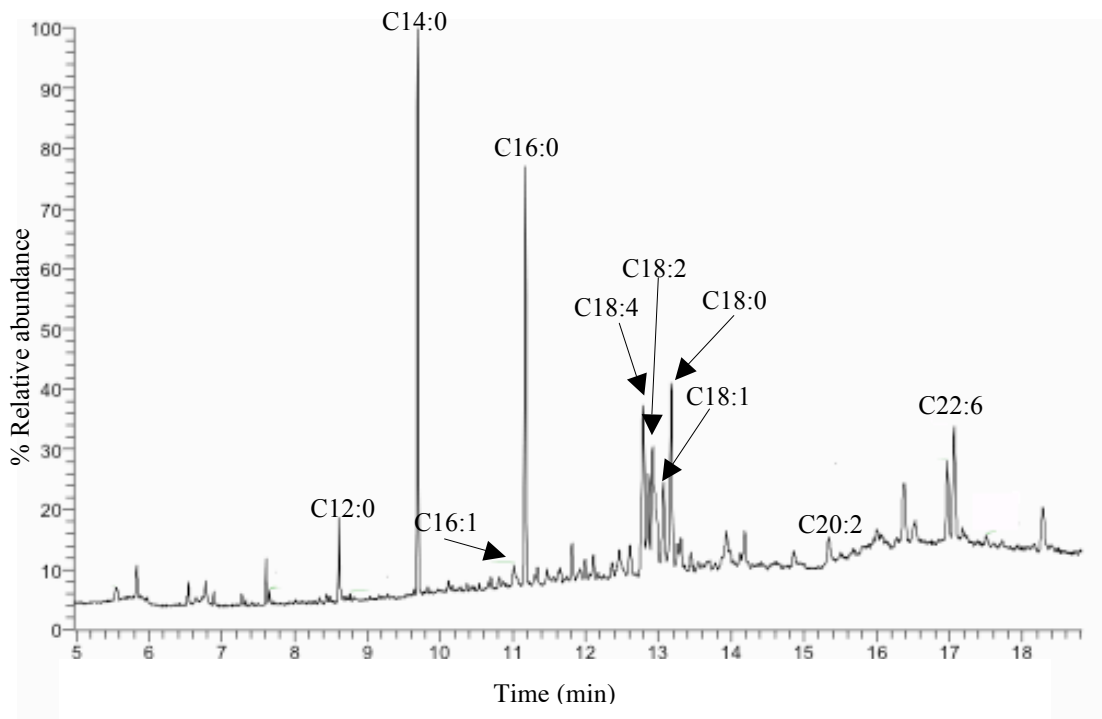
Figure 4.4 Chromatograph of total FAME with labels designating identified peaks.

There have been several reports in the literature describing the fatty acid profiles of a variety of *P. parvum* strains in addition to those of its close relative, *E. huxleyi*, including strains from Texas (TX), Scotland, England, and Greece (Volkman *et al*., 1981; Lee and Loeblich, 1971; Henrikson *et al*., 2010; Lang *et al*., 2011; Makri *et al*., 2011). A summary of previously reported results compared with those of the current study is shown in Table 4.1. Although C14:0 was the major fatty acid in the isolate from Scotland, representing nearly 70% of the total fatty acid constituents (Lee and Loeblich, 1971) and was present in the current analysis of the TX strain at levels of approximately 30% and 50% at 5 and 30 psu, respectively, it constituted less than 10% of the total fatty acids in the isolates from England and Greece (Lang *et al*., 2011; Makri *et al*., 2011). C14:0 also appears to be a prominent fatty acid in *E. huxleyi* (Volkman *et al*., 1981). Additionally, a previous analysis of fatty acids from the same strain as the current study

83

(UTEX 2797) using 20-day-old cultures that were grown in brackish media revealed similar results, with cells containing the highest levels of C14:0 (relative abundances (%) were not reported) (Henrikson *et al*., 2010).

Table 4.1 Comparison of the fatty acid profile for the isolate from TX (*P. parvum*$_1$) with 4 different isolates of *P. parvum* and *E. huxleyi*. All values indicate relative abundances (%). [*P. parvum*$_1$ – UTEX 2797 (TX); *P. parvum*$_2$- SMBA 65, Scotland (Lee and Loeblich, 1971); *P. parvum*$_3$- UTEX LB 995, England (Lang *et al*., 2011); *P. parvum*$_4$- Greece (Makri *et al*., 2011); *E. huxleyi*$_1$- England (Volkman *et al*., 1981)].

Fatty acids	*P. parvum*$_1$	*P. parvum*$_2$	*P. parvum*$_3$	*P. parvum*$_4$	*E. huxleyi*$_1$
C14:0	**31.8%**	68.9%	8.3%	<4.5%	35.1%
C16:0	**23.3%**	8.8%	3%	37.9%	3.1%
C16:1	**<1%**	0.6%	<1%	2.6%	
C16:2					
C18:0	**9.5%**			8.6%	1%
C18:1	**4.5%**	10.1%	1.5%	21.7%	15.3%
C18:2	**6%**	0.9%	1%	8.7%	2.1%
C18:3			4%	2.4%	7%
C18:4	**9%**		17%	4.5%	8%
C18:5			10.5%		10%
C20:1		1.7%		0.3%	
C20:2	**1.5%**	2.6%	1%		
C20:4		0.4%			
C20:5		0.3%	<1%	0.4%	
C22:5					1%
C22:6	**6.5%**	1.4%	12%	8.6%	11%

In addition to C14:0, a number of other fatty acids figured prominently in these strains, which in some cases varied. The minor fatty acids in the currently reported TX *P. parvum* samples (C16:1 and C20:2) were present in correspondingly low proportions in the other strains and were not detected in *E. huxleyi*. These findings verify the effects of

habitat location on fatty acid composition and provide insight into the particular alterations that underlie the exceptional ability of *P*. *parvum* and other euryhaline algae to adapt to a variety of environmental conditions. The fact that fatty acid profiles were generally similar across salinities in the current study indicates that salinity alterations by themselves do not appear to induce gross changes in fatty acid composition in this (and potentially all) strain(s). However, the disparate degrees of desaturation among some of the reported strains potentially point to the restructuring of membranes as an adaptive mechanism in response to variable environmental conditions. For example, increased membrane desaturation (and thus decreased membrane fluidity) has been reported in association with environmental stress, including temperature and osmotic stress, in a number of organisms (Lee *et al*.*,* 1989; Chintalapati *et al*.*,* 2004; Romantsov *et al*.*,* 2009). Although only one (Δ-4) desaturase was downregulated at 30 psu in the *P*. *parvum* transcriptome, a number of transcripts involving membrane remodeling increased in expression, such as those associated with galactolipids and sphingolipids. Additionally, the relative abundance of C14:0 was observed to be 20% greater at 30 psu, potentially indicating that a restructuring of the plasma membrane was occurring. Thus, it may be interesting to assess fatty acids that are present in the plasma membrane in comparison with those in the microsomes and thylakoids in altering salinities to attain more specific insight into adaptive changes that may be occurring in this context.

In terms of PUFA, EPA was not detected in the TX *P*. *parvum* or *E*. *huxleyi* strains and was present at low levels (<1%) in the other reported *P*. *parvum* strains. Thus, it is likely that these algal species are not abundant EPA producers. However, DHA represented one of the major fatty acids in the English strain (12%) and was fairly prominent in all evaluated isolates with the exception of that from Scotland (1.4%). DHA-producing organisms that are of commercial interest are able to produce upwards of 50% total fatty acids as DHA under optimal conditions (Iida *et al*., 1996; Nakahara *et al*., 1996; Yaguchi *et al*., 1997; De Swaaf *et al*., 1999). Therefore, *P*. *parvum* likely does not

have capabilities for commercial DHA production, but it does appear to produce it at moderate quantities. The PUFA OPA was not detected in the TX strain nor in most others that were evaluated with the exception of the English *P. parvum* and *E. huxleyi* strain, the latter of which was also English in origin. Interestingly, in the previous evaluation of the TX strain, SDA was found to be a relatively prominent constituent of the fatty acid profile of both laboratory-grown cultures and active blooms and was revealed to have ichthyotoxic properties (Henrikson *et al.*, 2010). Although this fatty acid was present at toxic levels in their laboratory cultures, it did not reach adequate levels to induce lethality to fish in the natural bloom samples (Henrikson *et al.*, 2010). The role of SDA in the ichthyotoxicity of *P. parvum* blooms and the identity of other as yet unknown toxins remain to be elucidated, but the presence of SDA at moderate levels in the current study verifies its prominence in this strain.

In addition to comparing the fatty acid profile of the current study with those of other *P. parvum* and *E. huxleyi* strains, comparisons with *Schizochytrium* may also be of interest because of the similar PUFA synthases that these two organisms possess, in addition to the similar responses of decreased lipid production following salinity stress. For example, several parallels may be drawn between the current study and that of *Schizochytrium limacinum*, which was evaluated for fatty acid content following growth at 5 different salinities (Zhu *et al.*, 2007). Like *P. parvum*, this heterotrophic heterokont inhabits marine waters and produces substantial quantities of C14:0 and C16:0 in addition to DHA, which it synthesizes using the *de novo* PUFA synthase that is distinct from the fatty acid synthases that generate its saturated fatty acids (Hauvermale *et al.*, 2006). Because this enzyme was also detected in the *P. parvum* transcriptome, long-chain PUFA synthesis could be carried out using similar mechanisms in both *Schizochytrium* and *P. parvum*. However, related organisms, such as *E. huxleyi,* which also share similar fatty acid profiles, utilize the alternative Δ-8 desaturation and conventional Δ-6 pathways for long-chain PUFA synthesis. The *P. parvum* transcriptome displayed evidence of both.

Thus, this organism may utilize any or all of these pathways depending on the environmental conditions and pertinent cellular needs that enable adaptation to occur. Future studies may confirm and evaluate the role of the PUFA synthase in *P. parvum* in addition to assessing the activities of the different enzymes of the Δ-6 and Δ-8 pathways to verify which pathway(s) is(are) being utilized in *P. parvum*.

Chapter 5: Concluding remarks

This dissertation describes differential gene expression in *P. parvum* N. Carter (UTEX 2797) cultures in response to abiotic factors, including phosphate limitation and salinity variations, in addition to providing a comprehensive transcriptome assembly for this organism. These studies impart insights into euryhaline adaptation, acetate-related metabolism, and transport. Additionally, fatty acid profiling was performed for cultures growing at two different salinities and although the profiles were largely similar, information was obtained regarding the impacts of salinity and habitat location (via a comparative analysis) on fatty acid composition.

The RNA-Seq analysis allowed for the assessment of long-term osmoregulation and salinity adaptation, providing novel insight into the mechanisms underlying the euryhaline capabilities of *P. parvum*. Pertinent gene homologs for ion transport, salt-stress response, and osmolyte biosynthesis within the transcriptome, a number of which were differentially expressed, likely play roles in the ability of this organism to inhabit a wide variety of salinities. This strain exhibited an increased salt-stress response at the higher salinity, bringing to question its origin because it is typically a marine alga. The slow acclimation of this strain from 5 psu, in which it was originally cultured, to 30 psu may have also activated the stress response. This analysis particularly revealed evidence of heightened chloride sequestration/extrusion, pointing to its potential role in adaptation to long-term salinity stress in *P. parvum*. Fatty acid profiling also indicated increased fatty acid desaturation and the potential restructuring of membranes as a means of salinity adaptation. This was supported by transcriptomic data.

Correlations between the microarray (P-limited *vs*. P-replete) and RNA-Seq (30 psu *vs*. 5 psu) analyses provided a number of potential biomarkers of HAB formation in addition to producing evidence for the post-transcriptional regulation of polyketide prymnesin synthesis. The RNA-Seq analysis revealed that the increased expression of

MGDG and hemolysin at low salinities may confer synergistic effects towards ichthyotoxicity. Fatty acid profiling demonstrated that appreciable levels of the PUFA SDA are present in this organism as well, which may produce further ichthyotoxic effects in this organism. Several long-chain PUFA synthesis pathways were identified, including the *de novo*, conventional Δ-6, and alternative Δ-8 pathways, among which *P. parvum* may preferentially utilize to selectively increase the production of particular PUFA during HAB formation.

This work additionally provided evidence of the involvement of vesicular transport in the active secretion of algal toxins in *P. parvum*, both transcriptionally and through the detection of extracellular prymnesins. These transport-related findings bring to light a question of the evolutionary origin of this increased transport activity. It is possible that *P. parvum* evolved to increase secretion under particular environmental conditions that correspond with increased secondary metabolism, in order to extrude toxic metabolites as part of competitor inhibition. On the other hand, secreting toxins might improve its phagotrophic ingestion of other organisms. Alternatively, it may have developed increased secretion in these conditions as a means of waste product elimination with prymnesin transport being increased by proxy because increased HAB formation typically occurs late in the growth cycle, coinciding with their accumulation (Graneli and Johansson, 2003). Further research into the mechanisms of allelopathy, toxicity, and transport in this organism may clarify these questions.

Collectively, important findings were revealed regarding the mechanisms underlying HAB formation in *P. parvum*, in addition to potential biomarkers of salinity adaptation and indicators for bloom development, including those involved in toxin synthesis and transport. Increased knowledge of the mechanisms of HAB formation in this alga, which causes devastating impacts on aquaculture globally, are crucial for the future development of detection and mitigation strategies.

APPENDIX A

Table 1.   Subset of downregulated TUGs that were identified at $p \leq 0.01$ [$\log_2$ (-) phosphate/(+) phosphate ranging from -0.5 to -3.19].

Description	$\log_2$ fold change	E-value	P-value
Carbonic anhydrase	-3.19	2E-08	0.005177
Band 3 protein	-2.43	5E-05	2.19E-04
Centrin 3	-2.07	3E-07	0.003511
Light harvesting complex protein I	-2.06	2E-17	0.009777
Malate synthase	-1.88	7E-147	0.005371
Fucoxanthin chlorophyll a/c-binding protein	-1.83	1E-57	2.93E-04
Cell surface protein	-1.81	5E-35	0.002509
Glucose-6-phosphate & phosphoenol pyruvate/ phosphate translocator	-1.68	5E-13	5.72E-04
NLI-interacting factor-like phosphatase	-1.46	5E-31	0.002122
Band 3 protein	-1.42	1E-10	3.68E-04
Putative lipoprotein	-1.30	7E-19	0.005059
Zinc finger protein 135	-1.28	5E-08	1.60E-04
DNA ligase	-1.28	1E-05	0.001440
Band 3 protein	-1.15	1E-24	0.002586
Biotin carboxylase	-1.13	2E-32	5.42E-04
Isocitrate lyase	-1.11	1E-51	0.003053
Biotin carboxylase	-1.10	2E-32	0.002869
Dolichyl phosphate mannosyltransferase polypeptide 2	-1.09	7E-05	0.004826
Cytochrome b6-F complex iron sulfur subunit	-1.08	4E-72	0.003620
Low CO_2-inducible protein	-1.07	8E-13	0.002570
β-ketoacyl-ACP reductase	-1.06	3E-105	0.005051
Elongation factor EF-TS, mitochondrial	-1.04	2E-51	6.89E-04
Aldehyde reductase	-1.04	4E-65	0.004478
Zinc finger protein (C_2H_2-type)	-1.04	5E-20	0.001874
Histidine-rich protein	-0.98	2E-22	0.002388
Light harvesting protein 3	-0.94	1E-59	0.009577
β-tubulin	-0.93	2E-18	7.38E-04
Acetyl-CoA synthetase	-0.92	6E-16	6.62E-04
Phosphate acetyltransferase	-0.90	5E-70	0.004692
Translation initiation inhibitor, ijgF family	-0.89	1E-14	0.003327
Exonuclease I	-0.87	3E-22	0.003790
40S ribosomal protein S25-1	-0.84	1E-07	2.24E-04

Table 1 cont.

Description	Log$_2$ fold change	E-value	P-value
Dioxygenase, alpha chain	-0.83	8E-49	0.005624
Proteasome (26S), regulatory subunit RPN5	-0.72	2E-19	0.002421
Methyltransferase type 11	-0.72	3E-06	0.004116
Glutamine amidotransferase of anthranilate synthetase	-0.72	2E-05	0.002239
Flavoprotein (flavin) oxygenase/reductase (FMN-binding)	-0.68	1E-27	0.002489
FtsH, AAA-metalloprotease; cell division protein	-0.67	2E-51	0.004146
NADH dehydrogenase	-0.66	9E-08	0.001844
Dehydrogenase/reductase (SDR, short chain)	-0.64	2E-36	0.001079
Methylmalonyl-CoA mutase	-0.59	4E-58	0.003872
ATP-dependent Clp protease, proteolytic subunit	-0.57	3E-74	0.007098
Transcriptional regulator, araC family	-0.50	2E-17	0.001942
Carboxyl esterase	-0.50	6E-33	0.007515

Table 2.   Subset of upregulated TUGs that were identified at $p \leq 0.01$ [$\log_2$ (-) phosphate/(+) phosphate ranging from 0.37 to 1.88].

Description	Log$_2$ fold change	E- value	P-value
40S ribosomal protein S13	1.88	3E-61	0.003547
60S ribosomal protein L24	1.86	5E-23	1.25E-04
60S ribosomal protein P1 (acidic)	1.64	4E-15	0.003056
Heat shock protein 90	1.57	0	0.001083
60S ribosomal protein P0 (acidic)	1.50	2E-38	4.53E-04
60S ribosomal protein L44	1.45	1E-34	0.002396
60S ribosomal protein L6	1.44	2E-43	0.001983
40S ribosomal protein S21	1.32	1E-23	6.45E-04
60S ribosomal protein L22	1.25	1E-44	7.27E-05
60S ribosomal protein L8	1.20	6E-93	4.79E-04
PsbA (Photosystem II Q (b) protein D1; YCF35 protein), chloroplast	1.14	5E-152	8.46E-04
40S ribosomal protein S4	1.14	8E-52	5.20E-05
Actin depolymerizing factor (ADF)	1.09	3E-25	2.48E-04
Actin depolymerizing factor (ADF)	1.07	3E-25	4.10E-05
Glycine-rich protein (cold shock protein)	1.06	1E-18	0.001739
Ubiquitin C	1.05	3E-29	0.002822
Ubiquitin (ubiquitin-60S ribosomal protein fusion; ubiquitin extension protein)	1.04	1E-36	0.004247
40S ribosomal protein S5	0.98	2E-82	0.005898
40S ribosomal protein S23	0.97	4E-25	8.27E-04
40S ribosomal protein S19	0.94	7E-32	0.001948
Protein disulfide isomerase	0.91	4E-26	0.009135
60S ribosomal protein L38	0.90	3E-16	8.87E-04
Profilin	0.89	5E-14	0.001579
Glutathione-S-transferase	0.89	2E-15	0.001897
40S ribosomal protein S10	0.88	4E-29	0.003517
60S ribosomal protein L27	0.88	2E-41	0.002261
Ubiquitin C	0.87	3E-29	0.002913
40S ribosomal protein S3	0.85	5E-89	0.006316
60S ribosomal protein L35a	0.83	9E-31	0.002688
30S ribosomal protein S3E	0.80	3E-115	0.001417
Profilin	0.79	2E-13	9.54E-04
40S ribosomal protein S26	0.76	4E-21	0.009928
60S ribosomal protein L19	0.75	9E-45	9.81E-04

Table 2 cont.

Description	Log$_2$ fold change	E-value	P-value
Glycerol kinase	0.73	3E-42	0.008141
Heat shock protein HsIV, ATP-dependent protease	0.71	1E-56	0.003517
Zinc finger protein (C4-type)	0.71	9E-36	0.001630
Glvcosvl transferase	0.71	4E-12	1.41E-05
Checkpoint with forkhead and ring finger domains	0.69	7E-05	0.009606
Ras, GTP-binding protein	0.67	3E-52	0.001283
60S ribosomal protein L17	0.65	7E-45	0.001827
ADP-ribosylation factor 1	0.64	3E-83	0.005456
GDP dissociation inhibitor	0.52	4E-17	0.001638
60S ribosomal protein L15	0.47	5E-75	9.54E-04
Cytochrome C	0.43	3E-29	0.002834
Annexin A13	0.43	1E-04	0.004825
Ni-binding urease accessory protein	0.39	1E-72	0.004131
Clathrin-adaptor complex protein AP-1	0.37	5E-53	0.001576

APPENDIX B

Table 1. Analysis of PKS and PKS-associated homologs from *P. parvum* transcriptome.

Sequence ID	Description	Species	E-value	Conserved Domains/Comments
comp298233_c0_seq1	polyketide synthase	*E. huxleyi*	5.00E-15	none
comp180298_c0_seq1	polyketide synthase	*E. huxleyi*	6.00E-78	none
comp386299_c0_seq1	polyketide synthase	*E. huxleyi*	3.00E-23	none
comp725357_c0_seq1	polyketide synthase	*E. huxleyi*	6.00E-18	none
comp704780_c0_seq1	polyketide synthase	*E. huxleyi*	1.00E-13	none
comp528_c0_seq1	polyketide synthase, partial	*E. huxleyi*	2.00E-22	none
comp686861_c0_seq1	polyketide synthase	*E. huxleyi*	2.00E-17	none
comp328676_c0_seq1	polyketide synthase, partial	*E. huxleyi*	3.00E-28	none
comp695227_c0_seq1	polyketide synthase	*E. huxleyi*	4.00E-28	none
comp16_c0_seq1	polyketide synthase	*E. huxleyi*	8.00E-25	none
comp936250_c0_seq1	polyketide synthase	*E. huxleyi*	2.00E-30	none
comp508564_c0_seq1	polyketide synthase	*E. huxleyi*	2.00E-46	none
comp7125_c0_seq1	polyketide synthase	*E. huxleyi*	2.00E-13	Phosphopantetheine (PP)-binding superfamily
comp685553_c0_seq1	polyketide synthase	*E. huxleyi*	4.00E-11	PP-binding superfamily
comp550676_c0_seq1	polyketide synthase	*E. huxleyi*	2.00E-17	PP-binding superfamily
comp10250_c0_seq1	polyketide synthase	*E. huxleyi*	6.00E-79	Ketoacyl synthase (KAS)/ PP-binding/ ketoreductase (KR)
comp5345_c0_seq1	polyketide synthase	*E. huxleyi*	1.00E-11	KR / PP-binding
comp955576_c0_seq1	polyketide synthase	*E. huxleyi*	2.00E-28	KR
comp10346_c0_seq1	polyketide synthase family protein	*Cylindrospermum stagnale*	2.00E-30	KR
comp227706_c0_seq1	polyketide synthase module	*Streptoalloteichus* sp.	7.00E-20	KAS

comp5978_c0_seq1	polyketide synthase subunit	*Bacillus pumilus*	2.00E-43	KAS
comp42_c0_seq1	polyketide synthase, partial	*Actinoplanes* sp.	3.00E-08	KAS
comp536793_c0_seq1	polyketide synthase	*E. huxleyi*	3.00E-25	Medium chain dehydrogenase/reductase (MDR) superfamily enoyl reductase
comp18297_c0_seq1	polyketide synthase	*Norocardia brasiliensis*	2.00E-45	enoyl reductase
comp220599_c0_seq1	polyketide synthase	*E. huxleyi*	2.00E-36	ω-3 PfaA
comp8306_c0_seq1	polyunsaturated fatty acid synthase subunit A	*Schizochytrium* sp.	2.00E-37	ω-3 PfaA
comp6776_c0_seq1	polyketide synthase	*E. huxleyi*	0	ω-3 PfaA
comp21893_c0_seq1-9	polyketide synthase	*E. huxleyi*	0	ω-3 PfaD
comp7646_c0_seq1	putative non-ribosomal polyketide synthase, partial	*Clostridium botulinum*	1.00E-59	Nonribosomal peptide synthase (NRPS) adenylation domain
comp406498_c0_seq1	chalcone synthase 1	*E. huxleyi*	1.00E-76	PKS type III
comp366249_c0_seq1	chalcone synthase 1	*E. huxleyi*	7.00E-48	PKS type III
comp447301_c0_seq1	β-ketoacyl synthase, partial	*Nannochloropsis gaditana*	4.00E-20	KAS
comp539607_c0_seq1	β-ketoacyl synthase	*Clostridium papyrosolvens*	2.00E-14	KAS
comp565215_c0_seq1	β-ketoacyl synthase: acyl transferase region	*Crocosphaera watsonii*	3.00E-11	KAS
comp278119_c0_seq1	β-ketoacyl-ACP synthase	*E. huxleyi*	2.00E-24	3-oxoacyl-(acyl carrier protein) synthase II
comp5271_c0_seq1	β-ketoacyl synthase	*Candidatus Solibacter usitatus Ellin6076*	2.00E-51	KAS
comp8064_c0_seq1	β-ketoacyl-ACP synthase	*E. huxleyi*	6.00E-49	KAS
comp20233_c0_seq1-2	β-ketoacyl synthase	*Ectocarpus siliculosus*	2.00E-143	KAS
comp89774_c0_seq1	β-ketoacyl-ACP synthase II, putative	*Acanthamoeba castellanii str. Neff*	2.00E-129	KAS
comp20988_c0_seq1	3-oxoacyl synthase	*E. huxleyi*	4.00E-173	KAS
comp16920_c0_seq1	3-oxoacyl synthase	*E. huxleyi*	0	KAS
comp333291_	sxtA long isoform	*Alexandrium*	9.00E-05	none

c0_seq1	precursor	*fundyense*		
comp21499_c0_seq1	sxtA	*Aphanizomenon sp.*	2.00E-104	keratin high-sulfur B2 protein
comp199664_c0_seq1	StxA short form precursor	*Alexandrium fundyense*	9.00E-15	adenosylmethionine-dependent methyltransferase superfamily
comp177464_c0_seq1	fatty acid elongase, partial	*E. huxleyi*	2.00E-76	elongase superfamily
comp20842_c0_seq1-2	ketoyl reductase domain protein	*Amphidiunium carterae*	5.00E-76	KR

96

APPENDIX C

Fig. 1.   TLC plate showing successful trans-esterification of fatty acids for cultures
               grown at 5 (5.1 and 5.2) and 30 (30.1 and 30.2) psu as indicated by the
               presence of only 2 major spots representing the FAME and β-carotene
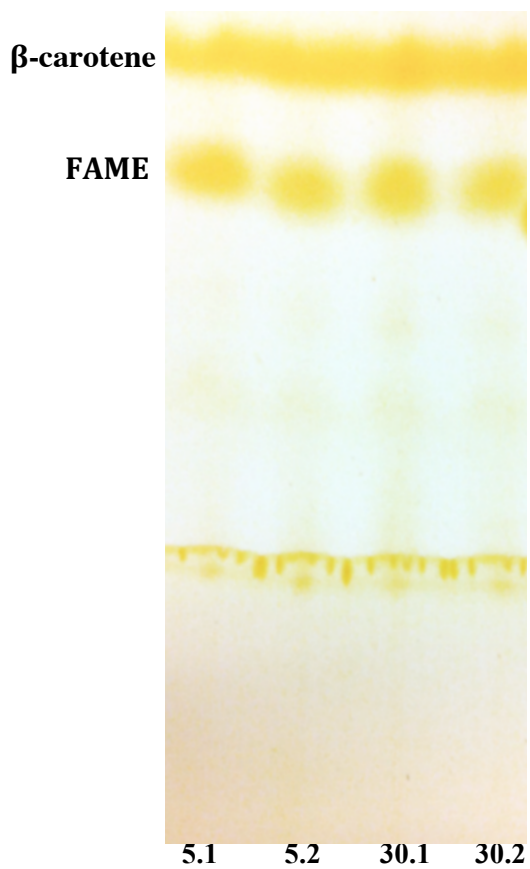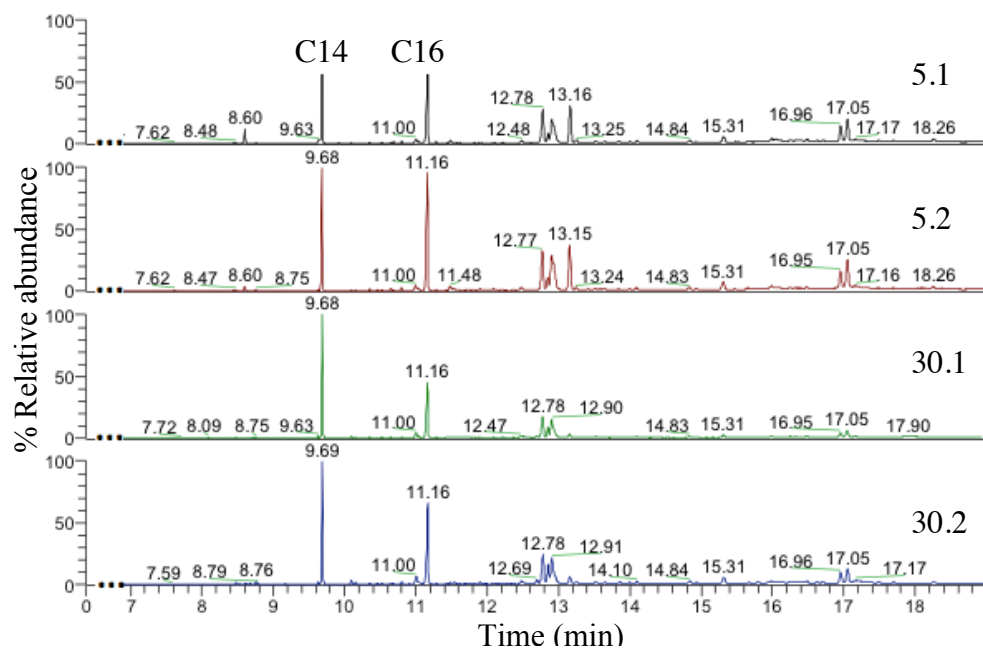   fractions. Spots are labeled on left.

Fig. 2.   Chromatographs of the 4 samples that were grown at 5 (5.1 and 5.2) and 30 (30.1 and 30.2) psu. Samples are labeled on right. The 2 most prominent fatty acids, C14:0 and C16:0 (with retention times of 9.68 and 11.16, respectively) are labeled at top

References

Al-Hasan R, Ali A, Ka'wash H, Radwan S (1990) Effect of salinity on the lipid and fatty acid composition of the halophyte *Navicula* sp: potential for mariculture. *J Appl Phycol* 2:215-222

Abe I, Morita H (2010) Structure and function of the chalcone synthase superfamily of plant type III polyketide synthases. *Nat Prod Rep* 27:809-838

Alper SL (2009) Molecular physiology and genetics of Na+-independent SLC4 anion exchangers. *J Exp Biol* 212:1672-1683

Al-Tebrineh J, Mihali TK, Pomati F, Neilan BA (2010) Detection of saxitoxin-producing cyanobacteria and Anabena circinalis in environmental water blooms by quantitative PCR. *Appl Environ Microbiol* 76(23):7836-7842

Arakawa K (2012) Diversity between PKS and FAS. *Nat Chem Biol* 8:604-605

Ashraf M (2009) Biotechnological approach of improving plant salt tolerance using antioxidants as markers. *Biotechnol Adv* 27:84-93

Austin MB, Noel JP (2003) The chalcone synthase superfamily of type III polyketide synthases. *Nat Prod Rep* 20(1):79-110

Baida GE, Kuzmin NP (1996) Mechanism of action of hemolysin III from *Bacillus cereus*. *Biochim Biophys Acta Biomembranes* 1284(2):122-124

Baker JW, Grover JP, Brooks BW, Urena-Boeck F, Roelke DL, Errera R, Kiesling RL (2007) Growth and toxicity of *Prymnesium parvum* (Haptophyta) as a function of salinity, light, and temperature. *J Phycol* 43:219-227

Baker JW, Grover JP, Ramachandrannair R, Black C, Valenti TW, Brooks BW, Roelke DL (2009) Growth at the edge of a niche: An experimental study of the harmful algae *Prymnesium parvum*. *Limnol Oceanogr* 54(5):1679-1687

Barkoh A, Paret JM, Lyon DD, Begley DC, Smith DG, Schlechte JW (2008) Evaluation of barley straw and a commercial probiotic for controlling *Prymnesium parvum* in fish production ponds. *N Am J Aquacult* 70:80-91

Barrowman J, Bhandari D, Reinisch K, Ferro-Novick S (2010) TRAPP complexes in membrane traffic: convergence through a common Rab. *Nat Rev Molec Cell Biol* 11:759-763

Bartholomew DM, Van Dyk DE, Lau SC, O'Keefe DP, Rea PA, Viitanen PV (2002) Alternate energy-dependent pathways for the vacuolar uptake of glucose and glutathione conjugates. *Plant Physiol* 130:1562-1572

Batoko H, Zheng HQ, Hawes C, Moore I (2000) A Rab1 GTPase is required for transport between the endoplasmic reticulum and Golgi apparatus and for normal Golgi movement in plants. *Plant Cell* 12:2201-2218

Beardall J, Roberts S, Raven JA (2005) Regulation of inorganic carbon acquisition by phosphorus limitation in the green alga *Chlorella emersonii*. *Can J Bot* 83:859-864

Bell MV, Pond D (1996) Lipid composition during growth of motile and coccolith forms of *Emiliania huxleyi*. *Phytochemistry* 41:465–471

100

Ben-Amotz A, Tornabene TG, Thomas WH (1985) Chemical profile of selected species of microalgae with emphasis on lipids. *J Phycol* 2:2-81

Berge JP, Barnathan G (2005) Fatty acids from lipids of marine organisms: molecular biodiversity, roles as biomarkers, biologically active compounds, and economical aspects. *Adv Biochem Engin/Biotechnol* 96:49-125

Bertin MJ, Zimba PV, Beauchesne KR, Huncik KM, Moeller PDR (2012) Identification of toxic fatty acid amides isolated from the harmful alga *Prymnesium parvum* Carter. *Harmful Algae* 20:111-116

Beszteri S, Yang I, Jaeckisch N, Tillmann U, Frickenhaus S, Glockner G, Cembella A, John U (2012) Transcriptomic response of the toxic prymnesiophyte *Prymnesium parvum* (N. Carter) to phosphorus and nitrogen starvation. *Harmful Algae* 18:1-15

Bhargava P, Srivastava AK (2013) Salt toxicity and survival strategies of cyanobacteria. In: Srivastava AK, Rai AN, Neilan BA (eds) Stress Biology of Cyanobacteria. CRC Press, Boca Raton, FL, p 171-188

Binzel ML, Hess FD, Bressan RA, Hasegawa PM (1988) Intracellular compartmentalization of ions in salt-adapted tobacco cells. *Plant Physiol* 86:607-614

Block MA, Dorne AJ, Joyard J, Douce R (1983) Preparation and characterization of membrane fractions enriched in outer and inner envelope membranes from spinach chloroplasts. II. Biochemical characterization. *J Biol Chem* 258:13281–13286

Blumwald E, Poole RJ (1985) Na$^+$/H$^+$ antiport in isolated tonoplast vesicles from storage tissue of *Beta vulgaris*. *Plant Physiol* 78:163-167

Blüthgen N, Brand K, Čajavec K, Swat M, Herzel, Beule K (2005) Biological profiling of gene groups utilizing gene ontology. *Genome Inform* 16(1):106-115

Bock AK, Glasemacher J, Schmidt R, Schonheit P (1999) Purification and characterization of two extremely thermostable enzymes, phosphate acetyltransferase and acetate kinase, from the hyperthermophilic eubacterium *Thermotoga maritima*. *J Bacteriol* 181(6):1861-1867

Booth WA, Beardall J (1991) Effects of salinity on inorganic carbon utilization and carbonic anhydrase activity in the halotolerant alga *Dunaliella salina* (Chlorophyta). *Phycologia* 30:220-225

Bowers HA, Brutemark A, Carvalho WF, Graneli E (2010) Combining flow cytometry and real-time PCR methodology to demonstrate consumption by *Prymnesium parvum*. *J Am Water Res Assoc* 46:133-143

Brooks BW, James SV, Valenti TW, Urena-Boeck F, Serrano C, Berninger JP, Schwierzke L, Mydlarz LD, Grover JP, Roelke DL (2010) Comparative toxicity of *Prymnesium parvum* in inland waters. *J Am Water Res Assoc* 46(1):45-62

Brown AD, Simpson JR (1972) Water relations of sugar-tolerant yeasts: the role of intracellular polyols. *J Gen Microbiol* 72:589-591

Bruton TH, Lyons H, Lerat Y, Stanley M, Rasmussen MB (2009) A review of the potential of marine algae as a source of biofuel in Ireland. *Sustainable Energy Ireland*

Burkholder JA, Gilbert PM, Skelton HM (2008) Mixotrophy, a major mode of nutrition for harmful algal species in eutrophic waters. *Harmful Algae* 8:77-93

Burridge K, Phillips JH (1975) Association of actin and myosin with secretory granule membranes. *Nature*, *London* 254:256-258

Cagliari A, Margis R, Maraschin FdS, Turchetto-Zolet AC, Loss G, Margis-Pinheiro M (2011) Biosynthesis of triacylglycerols (TAGs) in plants and algae. *Int J Plant Biol* 2:e10

Callahan TM, Rose MS, Meade MJ, Ehrenshaft M, Upchurch RG (1999) CFP, the putative cercosporin transporter of *Cercospora kikuchii*, is required for wild type cercosporin production, resistance, and virulence on soybean. *Mol Plant Microbe Interact* 12:901-910

Cane DE, Walsh CT (1999) The parallel and convergent universes of polyketide synthases and non-ribosomal peptide synthases. *Chem Biol* 6:R319-325

Cavalier-Smith T (2010) Kingdoms protozoa and chromista and the eozoan root of the eukaryotic tree. *Biol Lett* 6:342-345

Chaffin JD, Mishra S, Kuhaneck RM, Heckathorn SA, Bridgeman TB (2011) Environmental controls on growth and lipid content for the freshwater diatom, *Fragilaria capucina*: A candidate for biofuel production. *J Appl Phycol* 24:1045-1051

Chan YA, Podevels AM, Kevany BM, Thomas MG (2009) Biosynthesis of polyketide synthase extender units. *Nat Prod Rep* 26(1):90-114

Chanda A, Roze LV, Kang S, Artymovich KA, Hicks GR, Raikhel NV, Calvo AM, Linz
JE (2009) A key role for vesicles in fungal secondary metabolism. *Proc Natl Acad Sci USA* 106(46):19533-19538

Chen L, Yue Q, Zhang X, Xiang M, Wang C, Li S, Che Y, Ortiz-Lopez FJ, Bills GF, Liu
X, An Z (2013) Genomics-driven discovery of the pneumocandin biosynthetic gene cluster in the fungus *Glarea lozoyensis*. *BMC Genomics* 14:339

Chintalapati S, Kiran MD, Shivaji S (2004) Role of membrane lipid fatty acids in cold
adaptation. *Cell Mol Biol* 50:631–642.

Chiou CH, Lee LW, Owens SA, Whallon JH, Klomparens KL, Townsend CA, Linz JE
(2004) Distribution and sub-cellular localization of the aflatoxin enzyme versicolorin B synthase in time-fractionated colonies of *Aspergillus parasiticus*. *Arch Microbiol* 182:67-79

Chrispeels MJ (1991) Sorting of proteins in the secretory system. *Annu Rev Plant Physiol
Plant Mol Biol* 42:21-53

Christie WW (2003) In: Christie WW (ed) Lipid Analysis. Isolation, Separation,
Identification, and Structural Analysis of Lipids, 3rd edn. The Oily Press, Bridgewater, UK

Cohen Z, Vonshak A, Richmond A (1988) Effect of environmental conditions on the
fatty acid composition of the red alga *Porphyridium cruentum:* correlation to growth rate. *J Phycol* 24:328-332

Cole RA, Fowler JE (2006) Polarized growth: maintaining focus on the tip. *Curr Opin
Plant Biol* 9:579-588

Coleman A (1988). The autofluorescent flagellum: a new phylogenetic enigma. *J Phycol* 24(1):118-120

Collen J, Guisle-Marsollier I, Leger JJ, Boyen C (2007) Response of the transcriptome of the intertidal red seaweed *Chondrus crispus* to controlled and natural stresses. *New Phytol* 176:45-55

Conesa A, Götz S (2008) Blast2GO: a comprehensive suite for functional analysis in plant genomics. *Int J Plant Genomics* 2008:1–13

Cook HW (1996) Fatty acid desaturation and chain elongation in eukaryotes. *New Compr Biochem* 31:129-152

Cook CM, Lanaras T, Colman B (1986) Evidence for bicarbonate transport in species of red and brown macrophytic marine algae. *J Exp Bot* 37:977-984

Custodio L, Soares F, Pereira H, Barreira L, Vizetto-Duarte C, Rodrigues MJ, Rauter AP, Albericio F, Varela J (2014) Fatty acid composition and biological activities of *Isochrysis galbana* T-ISO, *Tetraselmis* sp. And *Scenedesmus* sp.: possible application in the pharmaceutical and functional food industries. *J Appl Phycol* 26:151-161

D'Souza-Schorey C, Chavrier P (2006) ARF proteins: roles in membrane traffic and beyond. *Nat Rev Mol Cell Biol* 7:347-358

Dafni Z, Shilo M (1966) The cytotoxic principle of the phytoflagellate *Prymnesium parvum*. *J Cell Biol* 28:461-471

Dafni Z, Ulitzur S, Shilo M (1972) Influence of light and phosphate on toxin production

and growth of *Prymnesium parvum*. *J Gen Microbiol* 70:199–207

Dalsgaard J, St. John M, Kattner G, Muller-Navarra D, Hagen W (2003) Fatty acid trophic markers in the pelagic marine environment. *Adv Mar Biol* 46:225-340

Daßler T, Maier T, Winterhalter C, Bock A (2000) Identification of a major facilitator protein from *Escherichia coli* involved in efflux of metabolites of the cysteine pathway. *Mol Microbiol* 36:1101-1112

De Groot CC, van den Boogaard R, Marcells LFM, Harbinson J, Lambers H (2003) Contrasting effects of N and P deprivation on the regulation of photosynthesis in tomato plants in relation to feedback limitation. *J Expt Bot* 54(389):1957-1967

De Swaaf ME, de Rijk TC, Eggink G, Sijtsma L (1999) Optimisation of docosahexaenoic acid production in batch cultivation by *Crypthecodinium cohnii*. *J Biotechnol* 70:185-192

Deneka M, Neeft M, van der Sluis P (2003) Regulation of membrane transport by rab GTPases. *Crit Rev Biochem Mol Biol* 38:121-142

Dickinson DMJ, Kirst GO (1986) The role of dimethylsulphoniopropionate, glycine betaine and homarine in the osmoacclimation of *Platymonas subcordiformis*. *Planta* 167:536-543

Dickinson DMJ, Kirst GO (1987) Osmotic adjustment in marine eukaryotic algae: the role of inorganic ions, quaternary ammonium, tertiary sulphonium and carbohydrate solutes II. Prasinophytes and haptophytes. *New Phytol* 106:657-666

Dittami SM, Gravot A, Goulitquer S, Rousvoal S, Peters AF, Bouchereau A, Boyen C, Tonon T (2012) Towards deciphering dynamic changes and evolutionary mechanisms involved in the adaptation to low salinities in *Ectocarpus* (brown algae). *Plant J* 71:366-377

Dittami SM, Scornet D, Petit JL, Segurens B, Da Silva C, Corre E, Dondrup M, Glatting KH, Konig R, Sterck L, Rouze P, Van de Peer Y, Cock JM, Boyen C, Tonon T (2009) Global expression analysis of the brown alga *Ectocarpus siliculosus* (Phaeophyceae) reveals large-scale reprogramming of the transcriptome in response to abiotic stress. *Genome Biol* 10:R66

Domínguez-Ferreras A, Pérez-Arnedo R, Becker A, Olivares J, Soto MJ, Sanjuán J (2006) Transcriptome profiling reveals the importance of plasmid pSymB for osmoadaptation of *Sinorhizobium meliloti*. *J Bacteriol* 188:7617–7625

Donaldson JG, Jackson CL (2011) ARF family G proteins and their regulators: roles in membrane transport, development and disease. *Nat Rev Mol Cell Biol* 12:533

Drechsler Z, Beer S (1991) Utilization of inorganic carbon by *Ulva lactuca*. *Plant Physiol* 97:1439-1444

Driscoll WW, Espinosa NJ, Eldakar OT, Hackett JD (2013) Allelopathy as an emergent, exploitable public good in the bloom-forming microalga *Prymnesium parvum*. *Evolution* 67(6):1582-1590

Duden R, Griffiths G, Frank R, Argos P, Kreis TE (1991). BCOP, a 110 kd protein associated with non-clathrin-coated vesicles and the Golgi complex, shows homology to fl-adaptin. *Cell* 64:649- 665

Duran JM, Anjard C, Stefan C, Loomis WF, Malhotra V (2010) Unconventional secretion of Acb1 is mediated by autophagosomes. *J Cell Biol* 188(4):527-536

Dyer JM, Mullen RT (2008) Engineering plant oils as high-value industrial feedstocks for biorefining: the need for underpinning cell biology research. *Physiol Plant* 132:11-22

Dyhrman ST, Haley ST, Birkeland SR, Wurch LL, Cipriano MJ, McArthur AG (2006) Long serial analysis of gene expression for gene discovery and transcriptome profiling in the widespread marine coccolithophore *Emiliania huxleyi*. *Appl Environ Microbiol* 72:252-260

Dyhrman ST, Jenkins BD, Rynearson TA, Saito MA, Mercier ML, Alexander H, Whitney LP, Drzewianowski A, Bulygin VV, Bertrand EM, Wu Z, Benitez-Nelson C, Heithoff A (2012) The transcriptome and proteome of the diatom *Thalassiosira pseudonana* reveal a diverse phosphorus stress response. *PLOS One* 7(3):e33768

Edwards DM, Reed RH, Stewart WDP (1988) Osmoacclimation in *Enteromorpha intestinalis*: long-term effects of osmotic stress on organic solute accumulation. *Mar Biol* 98:467-476

Elenkov I, Stefanov K, Dimitrova-Konaklieva S, Popov S (1996) Effect of salinity on lipid composition of *Cladophora vagabunda*. *Phytochemistry* 42(1):39-44

Emanuelsson O, Nielsen H, Brunak S, von Heijne G (2000) Predicting subcellular localization of proteins based on their N-terminal amino acid sequence. *J Mol Biol* 300:1005-1016

Erdner DL, Anderson DM (2006) Global transcriptomic profiling of the toxic
dinoflagellate *Alexandrium fundyense* using Massively Parallel Signature
Sequencing. *BMC Genomics* 8:88

Fatland BL, Ke J, Anderson MD, Mentzen WI, Cui LW, Allred CC, Johnston JL,
Nikolau BJ, Wurtele ES (2002) Molecular characterization of a heterotrimeric
ATP-citrate lyase that generates cytosolic acetyl-coenzyme A in Arabidposis.
Plant Cell 17:740-756

Fistarol GO, Legrand C, Graneli E (2003) Allelopathic effect of *Prymnesium parvum* on
a natural plankton community. *Mar Ecol-Prog Ser* 255:115-125

Flügge UI (2001) Plant chloroplasts and other plastids. Encyclopedia of Life Science.
Macmillan Publishers, Nature Publishing Group, London, England.

Ford CW (1984) Accumulation of low molecular weight solutes in water stress tropical
Legumes. *Phytochem* 23:1007-1015

Freitag M, Beszteri S, Vogel H, Uwe J (2011) Effects of physiological shock treatments
on toxicity and polyketide synthase gene expression in *Prymnesium parvum*
(Prymnesiophyceae). *Eur J Phycol* 46(3):193-201

Gage DA, Rhodes D, Nolte KD, Hicks WA, Leustek T, Cooper AJL, Hanson AD (1997)
A new route for synthesis of dimethylsulphonioproprionate in marine algae.
Nature 387(26):891-894

Gillingham AK, Munro S (2007) The small G proteins of the Arf family and their
Regulators. *Annu Rev Cell Dev Biol* 23:579-611

Grabherr MG, Haas BJ, Yassour M, Levin JZ, Thompson DA, Amit I, Adiconis X, Fan L, Raychowdhury R, Zeng Q, Chen Z, Mauceli E, Hacohen N, Gnirke A, Rhind N, di Palma F, Birren BW, Nusbaum C, Lindblad-Toh K, Friedman N, Regev A (2011) Full-length transcriptome assembly from RNA-seq data without a reference genome. *Nat Biotechnol* 29(7):644-52

Graneli E, Carlsson P (1998) The ecological significance of phagotrophy in photosynthetic flagellates. In: Anderson DM, Cembella AD, Hallegraeff GM (eds) Physiological Ecology of Harmful Algal Blooms. Springer-Verlag, Heidelberg, p 539-557

Graneli E, Edvardsen B, Roelke DL, Hagstrom JA (2012) The ecophysiology and bloom dynamics of *Prymnesium* spp. *Harmful Algae* 14:260-270

Graneli E, Johansson N (2003) Increase in the production of allelopathic substances by *Prymnesium parvum* cells grown underN- or P-deficient conditions. *Harmful Algae* 2:135-145

Grogan DW, Cronan JE Jr. (1997) Cyclopropane ring formation in membrane lipids of bacteria. *Microbiol Mol Biol Rev* 61(4):429-441

Guckert JB, Cooksey KE (1990) Triacylglyceride accumulation and fatty acid profile changes in *Chlorella* (Chlorophyta) during high-pH induced cell cycle inhibition. *J Phycol* 26:72-79

Guillamot D, Guillon S, Deplanque T, Vanhee C, Gumy C, Masquelier D, Morsomme P, Batoko H (2009) The Arabidopsis TSPO-related protein is a stress and abscisic acid-regulated, endoplasmic reticulum-Golgi-localized membrane protein. *Plant J* 60:242-256

Guillard RRL, Ryther JH (1962) Studies of marine planktonic diatoms I. *Cyclotella nana* Hustedt and *Detonula confervacea* (Cleve) Gran. *Can J Microbiol* 8:229–239

Guillot A, Obis D, Mistou MY (2000) Fatty acid membrane composition and activation of glycine-betaine transport in *Lactococcus lactis* subjected to osmotic stress. *Int J Food Microbiol* 55:47–51

Guo M, Harrison PJ, Taylor FJR (1996) Fish kills related to *Prymnesium parvum* N. Carter (Haptophyta) in the People's Republic of China. *J Appl Phycol* 8:111-117

Guschina IA, Harwood JL (2006) Lipids and lipid metabolism in eukaryotic algae. *Prog Lipid Res* 45:160-186

Hackett JD, Wisecaver JH, Brosnahan ML, Kulis DM, Anderson DM, Bhattacharya D, Plumley FG, Erdner DL (2013) Evolution of saxitoxin synthesis in cyanobacteria and dinoflagellates. *Mol Biol Evol* 30:70–78

Hallegraeff GM (1993) A review of harmful algal blooms and their apparent global increase. *Phycologia* 32:79–99

Harke MJ, Gobler CJ (2013) Global transcriptional responses of the toxic cyanobacterium, *Microcystis aeruginosa*, to nitrogen stress, phosphorus stress, and growth on organic matter. *PLOS One* 8(7):e69834

Hauvermale A, Kuner J, Rosenzweig B, Guerra D, Diltz S, Metz JG (2006) Fatty acid production in *Schizochytrium* sp.: Involvement of a polyunsaturated fatty acid synthase and a type I fatty acid synthase. *Lipids* 41(8):739-747

Hawes C, Satiat-Jeunemaitre B (2005) The plant Golgi apparatus - going with the flow. *Biochim Biophys Acta* 1744:93-107

Henrikson JC, Gharfeh MS, Easton AC, Easton JD, Glenn KL, Shadfan M, Mooberry SL, Hambright KD, Cichewicz RH (2010) Reassessing the ichthyotoxin profile of cultured *Prymnesium parvum* (golden algae) and comparing it to samples collected from recent freshwater bloom and fish kill events in North America. *Toxicon* 55:1396-1404

Holmquist E, Willen T (1993) Fish mortality caused by *Prymnesium parvum*. *Vatten* 49:110-115

Hong SY, Linz JE (2009) Functional expression and sub-cellular localization of the early aflatoxin pathway enzyme Nor-1 in *Aspergillus parasiticus*. *Mycol Res* 113:591-601

Hopwood DA, Sherman DH (1990) Molecular genetics of polyketides and its comparison to fatty acid biosynthesis. *Annu Rev Genet* 24:37-66

Hu Q, Sommerfeld M, Jarvis E, Ghirardi M, Posewitz M, Seibert M, Darzins A (2008) Microalgal triacylglycerols as feedstocks for biofuel production: perspectives and advances. *Plant J* 54:621-639

Huerlimann R, Heimann K (2013) Comprehensive guide to acetyl-carboxylases in algae. *Crit Rev Biotechnol* 33(1):49-65

Ichihara K, Mineur F, Shimada S (2011) Isolation and temporal expression analysis of freshwater-induced genes in *Ulva limnetica* (Uvales, Chlorophyta). *J Phycol* 47:584-590

Igarashi T, Satake M, Yasumoto T (1996) Prymnesin-2: A potent ichthyotoxic and hemolytic glycoside isolated from the red alga *Prymnesium parvum*. *J Am Chem Soc* 118:479-480

Igarashi T, Satake M, Yasumoto T (1999) Structures and partial stereochemical assignments for prymnesin-1 and prymnesin-2: potent hemolytic and ichthyotoxic glycosides isolated from the red tide alga *Prymnesium parvum*. *J Am Chem Soc* 121:8499-8511

Iida J, Nakahara T, Yokochi T, Kamisaka Y, Yagi H, Yamaoka M, Suzuki O (1996) Improvement of docosahexaenoic acid production in a culture of *Thrausochytrium aureum* by medium optimization. *J Ferment Bioeng* 81:76-78

Inaba M, Sakamoto A, Murata N (2001) Functional expression in *Escherichia coli* of low-affinity and high-affinity $Na^+(Li^+)/H^+$ antiporters of *Synechocystis*. *J Bacteriol* 183:1376-1384

Incharoensakdi A, Waditee-Sirisattha R (2013) Regulatory mechanisms of cyanobacteria in response to osmotic stress. In: Srivastava AK, Rai AN, Neilan BA (eds) Stress Biology of Cyanobacteria. CRC Press, Boca Raton, FL, p 203-230

Ischebeck T, Zbierzak AM, Kanwischer M, Dörmann P (2006) A salvage pathway for phytol metabolism in *Arabidopsis*. *J Biol Chem* 281:2470–2477

Ishikawa T, Li ZS, Lu YP, Rea PA (1997) The GS-X pump in plant, yeast, and animal cells: structure, function, and gene expression. *Biosci Rep* 17:189-207

Jayanta T, Chandra KM, Chandra GB (2012) Growth, total lipid content and fatty acid profile of a native strain of the freshwater oleaginous microalgae *Ankistrodesmus falcatus* (Ralf) grown under salt stress condition. *Int Res J Biol Sci* 1(8):27-35

Jeffrey SW, Wright SW (1994) Photosynthetic pigments in the Haptophyta. In: Green JC, Leadbeater BSC (eds) The Haptophyte Algae, The Systematics Association, Special Vol. 51. Oxford University Press, New York, NY, p 111-132

Jiang Y, Yang B, Harris NS, Deyholos MK (2007) Comparative proteomic analysis of NaCl stress-responsive proteins in Arabidopsis roots. *J Exp Bot* 58:3591-3607

Johansson N, Graneli E (1999) Influence of different nutrient conditions on cell density, chemical composition and toxicity of *Prymnesium parvum* (Haptophyta) in semi-continuous cultures. *J Exp Mar Biol Ecol* 239:243-258

John U, Beszteri B, Derelle E, Van de Peer Y, Read B, Moreau H, Cembella A (2008) Novel insights into evolution of protistan polyketide synthases through phylogenomic analyses. *Protist* 159:21-30

Johnson M, Wen Z (2009) Preparation of biodiesel fuel from the microalga *Schizochytrium limacinum* by direct transesterification of algal biomass. *Energy Fuels* 23:5179-5183

Jones J, Manning S, Montoya M, Keller K, Poenie M (2012) Extraction of algal lipids and their analysis by HPLC and mass spectrometry. *J Am Oil Chem Soc* 89:1371-1381

Joyard J, Ferro M, Masselon C, Seigneurin-Berny D, Salvi D, Garin J, Rolland N (2010) Chloroplast proteomics highlights the subcellular compartmentation of lipid metabolism. *Prog Lipid Res* 49:128-158

Kaartvedt S, Johnsen TM, Aksnes DL, Lie U, Svendsen H (1991) Occurrence of the toxic phytoflagellate *Prymnesium parvum* and associated fish mortality in a Norwegian fjord system. *Can J Fish Aquat Sci* 48(12):2316-2323

Kader JC (1996) Lipid-transfer proteins in plants. *Ann Rev Plant Physiol Plant Mol Biol* 47:627-654

Kammerer B, Fischer K, Hilpert B, Schubert S, Gutensohn M, Weber A, Flügge UI (1998) Molecular characterization of a carbon transporter in plastids from heterotrophic tissues: the glucose 6-phosphate/phosphate antiporter. *Plant Cell* 10:105-117

Katz A, Waridel P, Shevchenko A, Pick U (2007) Salt-induced changes in the plasma membrane proteome of the halotolerant alga *Dunaliella salina* as revealed by blue native gel electrophoresis and nano-LC-MS/MS analysis. *Mol Cell Proteomics* 6:1459-1472

Kayama M, Araki S, Sato S (1989) Lipids of marine plants. In: Ackman RG (ed) Marine Biogenic Lipids, Fats, and Oils, Vol. II. CRC Press, Boca Raton, FL, p 3-48

Ke J, Behal RH, Back SL, Nikolau BJ, Wurtele ES, Oliver DJ (2000) The role of pyruvate dehydrogenase and acetyl-coenzyme A synthetase in fatty acid synthesis in developing Arabidopsis seeds. *Plant Physiol* 123:497-508

Khozin-Goldberg I, Cohen Z (2011) Unraveling algal lipid metabolism: Recent advances in gene identification. *Biochimie* 93:91-100

115

Kirrolia A, Bishnoi NR, Singh N (2011) Salinity as a factor affecting the physiological and biochemical traits of *Scenedesmus quadricauda*. *J Algal Biomass Ultn* 2(4):28-34

Kirst GO (1989) Salinity tolerance of eukaryotic marine algae. *Annu Rev Plant Physiol Plant Mol Biol* 40:21-53

Knight H, Trewavas AJ, Knight MR (1997) Calcium signaling in *Arabidopsis thaliana* responding to drought and salinity. *Plant J* 12:1067-1078

Kobayashi Y, Torii A, Kato M, Adachi K (2007) Accumulation of cyclitols functioning as compatible solutes in the haptophyte alga *Pavlova* sp. *Phycol Res* 55:81-90

Kolukisaoglu HU, Bovet L, Klein M, Eggmann T, Geisler M, Wanke D, Martinoia E, Schulz B (2002) Family business: the multidrug-resistance related protein, (MRP) ABC transporter genes in *Arabidopsis thaliana*. *Planta* 216:107-119

Korman TP, Ames B, Tsai SC (2010) Structural enzymology of polyketide synthase: the structure-sequence-function correlation. In: Mander L, Liu HW (eds) Comprehensive Natural Products, Vol 1: Natural Products Structural Diversity- I Secondary Metabolites: Organization and Biosynthesis. Elsevier Ltd., Kidlington, UK, p 305-345

Kosova K, Vitamvas P, Prasil IT, Renaut J (2011) Plant proteome changes under abiotic stress- contribution of proteomics studies to understanding plant stress response. *J Proteomics* 74:1301-1322

Kozakai H, Oshima Y, Yasumoto T (1982) Isolation and structural elucidation of hemolysin from the phytoflagellate *Prymnesium parvum*. *Agric Biol Chem* 46(1):233-236

Kunimoto S, Murofushi W, Kai H, Ishida Y, Uchiyama A, Kobayashi T, Kobayashi S, Murofushi H, Murakami-Murofushi K (2002) Steryl glucoside is a lipid mediator in stress-responsive signal transduction. *Cell Struct Funct* 27(3):157-162

Kunst L, Samuels AL (2003) Biosynthesis and secretion of plant cuticular wax. *Prog Lipid Res* 42:51-80

Kunze M, Pracharoenwattana I, Smith SM, Hartig A (2006) A central role for the peroxisomal membrane in glyoxylate cycle function. *BBA- Mol Cell Res* 1763(12):1441-1452

Kwan DH, Schulz F (2011) The stereochemistry of complex polyketide biosynthesis by modular polyketide synthases. *Molecules* 16:6092-6115

La Claire JW II (2006) Analysis of expressed sequence tags from the harmful alga, *Prymnesium parvum* (Prymnesiophyceae, Haptophyta). *Mar Biotech* 8:534–546

La Claire JW II, Manning SR, Talarski AE (2015) Quantifying polyketide prymnesins in *Prymnesium parvum* Carter culture (in preparation)

Lang I, Hodac L, Friedl T, Feussner I (2011) Fatty acid profiles and their distribution patterns in microalgae: a comprehensive analysis of more than 2000 strains from the SAG culture collection. *BMC Plant Biol* 11:124

Langmead B, Trapnell C, Pop M, Salzberg SL (2009) Ultrafast and memory-efficient alignment of short DNA sequences to the human genome. *Genome Biol* 10:R25

Larsen A, Bryant S (1998) Growth rate and toxicity of *Prymnesium parvum* and *Prymnesium patelliferum* (Haptophyta) in response to changes in salinity, light and temperature. *Sarsia* 83:409–418

Larsen A, Elkrem W, Paasche E (1993) Growth and toxicity in *Prymnesium patelliferum* (Prymnesiophyceae) isolated from Norwegian waters. *Can J Bot* 71:1357-1362

Latjinhouwers M, Hawes C, Carvalho C (2005) Holding it all together? Candidate proteins for the plant Golgi matrix. *Curr Opin Plant Biol* 8:632-639

Lee LW, Chiou CH, Klomparens KL, Cary JW, Linz JE (2004) Subcellular localization of aflatoxin biosynthetic enzymes Nor-1, Ver-1, and OmtA in time-dependent fractionated colonies of *Aspergillus parasiticus*. *Arch Microbiol* 181:204-214

Lee RF, Loeblich AR III (1971) Distribution of 21:6 hydrocarbon and its relationship to 22:6 fatty acid in algae. *Phytochemistry* 10:593-602

Lee Y, Tan H, Low C (1989) Effect of salinity of medium on cellular fatty acid composition of marina alga *Porphyridium cruentum* (Rhodophyceae). *J Appl Phycol* 1:19-23

Lev S (2010) Non-vesicular lipid transport by lipid-transfer proteins and beyond. *Nat Rev Mol Cell Biol* 11(10):739-750

Li B, Dewey CN (2011) RSEM: accurate transcript quantification from RNA-Seq data with or without a reference genome. *BMC Bioinformatics* 12:323

Li C, Florova G, Akopiants K, Reynolds KA (2004) Crotonyl-coenzyme A reductase provides methylmalonyl-CoA precursors for monensin biosynthesis by *Streptomyces cinnamonensis* in an oil-based extended fermentation. *Microbiology* 150:3463-3472

Lin Y, Irani NG, Grotewold E (2003) Sub-cellular trafficking of phytochemicals explored using auto-fluorescent compounds in maize cells. *BMC Plant Biol* 3:10

Lindehoff E, Graneli E, Graneli W (2009) Effect of tertiary sewage effluent additions on *Prymnesium parvum* cell toxicity and stable isotope ratios. *Harmful Algae* 8:247-253

Liska AJ, Shevchenko A, Pick U, Katz A (2004) Enhanced photosynthesis and redox energy production contribute to salinity tolerance in *Dunaliella* as revealed by homology-based proteomics. *Plant Physiol* 136:2806-2817

Liu C, Wang X, Huang X, Liu J (2011) Identification of hypo-osmotically induced genesin *Kappaphycus alvarezii* (Solieriaceae, Rhodophyta) through expressed sequence tag analysis. *Bot Mar* 54:557-562

Lowe CD, Mello LV, Samatar N, Martin LE, Montagnes DJS, Watts PC (2011) The transcriptome of the novel dinoflagellate *Oxyrrhis marina* (Alveolata: Dinophyceae): response to salinity examined by 454 sequencing. *BMC Genomics* 12:519

Lupashin V, Sztul E (2005) Golgi tethering factors. *Biochim Biophys Acta* 1744:325-339

Maggio-Hall LA, Wilson RA, Keller NP (2005) Fundamental contribution of beta-oxidation to polyketide mycotoxin production in planta. *Mol Plant Microbe Interact* 18:783-793

Makri A, Bellou S, Birkou M, Papatrehas K, Dolapsakis NP, Bokas D, Papanikolaou S, Aggelis G (2011) Lipid synthesized by micro-algae grown in laboratory- and industrial-scale bioreactors. *Eng Life Sci* 11(1):52-58

Manjithaya R, Subramani S (2011) Autophagy: a broad role in unconventional protein secretion? *Trends Cell Biol* 21(2):67-73

Mann J (2001) In: Atkins PW, Holker JSE, Holliday AK (eds) Secondary Metabolism, 2nd Edn. Oxford University Press, New York, NY

Manning SR, La Claire JW II (2013) Isolation of polyketides from *Prymnesium parvum* (Haptophyta) and their detection by liquid chromatography/mass spectrometry metabolic fingerprint analysis. *Anal Biochem* 442:189-195

Manning SR, La Claire JW II (2010) Prymnesins: toxic metabolites of the golden alga, *Prymnesium parvum* Carter (Haptophyta). *Mar Drugs* 8(3):678-704

Marrs KA, Alfenito MR, Lloyd AM, Walbot V (1995) A glutathione-S-transferase involved in vacuolar transfer encoded by the maize gene *Bronze-2*. *Nature* 375:397-400

Martin JF, Casqueiro J, Liras P (2005) Secretion systems for secondary metabolites: how producer cells send out messages of intercellular communication. *Curr Opin Microbiol* 8:282-293

Martin JA, Wang Z (2011) Next-generation transcriptome assembly. *Nat Rev Genet* 12:671-682

Masuda S, Harada J, Yokono M, Yazawa Y, Shimojima M, Murofushi K, Tanaka H, Masuda H, Murakawa M, Haraguchi T, Kondo M, Nishimura M, Yuasa H, Noguchi M, Oh-oka H, Tanaka A, Tamiaki H, Ohta H (2011) A monogalactosyldiacylglycerol synthase found in the green sulfur bacterium Chlorobaculum tepidum reveals important roles for galactolipids in photosynthesis. *Plant Cell* 23(7):2644-2658

Masschelein J, Mattheus W, Gao LJ, Moons P, Van Houdt R, Uytterhoeven B, Lamberigts C, Lescrinier E, Rozenski J, Herdewijn P, Aertsen A, Michiels C, Lavigne R (2013) A PKS/NRPS/FAS hybrid gene cluster from *Serratia plymuthica* RVH1 encoding the biosynthesis of three broad spectrum, zeamine-related antibiotics. *PLOS One* 8(1):e54143

McGrath JP, Varshavsky A (1989) The yeast STE6 gene encodes a homologue of the mammalian multidrug resistance P-glycoprotein. *Nature* 340:400–404

McKey D (1979) The distribution of secondary compounds within plants. In: Rosenthal GA, Janzen DH (eds) Herbivores: Their Interaction with Secondary Plant Metabolites. Academic Press, New York, NY, p 6916-6921

Meldahl AS, Edvardsen B, Fonnum F (1994) Toxicity of four potentially ichthyotoxic marine phytoflagellates determined by four different test methods. *J Toxicol Environ Health* 42:289–301

Mendoza I, Rubio F, Rodriguiez-Navarro A, Pardo JM (1994) The protein phosphatase calcineurin is essential for NaCl tolerance of *Saccharomyces cerevisiae*. *J Biol Chem* 269:8792-8796

Metz JG, Roessler P, Facciotti D, Levering C, Dittrich F, Lassner M, Valentine R, Lardizabal K, Domergue F, Ya- mada A, Yazawa K, Knauf V, Browse J (2001) Production of polyunsaturated fatty acids by polyketide synthases in both prokaryotes and eukaryotes. *Science* 293:290–293

Moellering ER, Muthan B, Benning C (2011) Freezing tolerance in plants requires lipid remodeling at the outer chloroplast membrane. *Science* 330(6001)226-228

Moestrup O (1994) Economic aspects, blooms, nuisance species, and toxins. In: Green JC, Leadbeater BSC (eds) The Haptophyte Algae, Systematics Association Special Vol. 51. Clarendon Press, Oxford, UK, p 265-285

Moisander PH, McClinton E, Paerl HW (2002) Salinity effects on growth, photosynthetic parameters, and nitrogenase activity in estuarine planktonic cyanobacteria. *Microb Ecol* 43:432

Monroe EA, Johnson JG, Wang Z, Pierce RK, Van Dolah FM (2010) Characterization and expression of nuclear-encoded polyketide synthases in the brevetoxin-producing dinoflagellate *Karenia brevis*. *J Phycol* 46:541-552

Monroe EA, Van Dolah FM (2008) The toxic dinoflagellate *Karenia brevis* encodes novel Type I-like polyketide synthases containing discrete catalytic domains. *Protist* 159:471-482

122

Moore BS, Hertweck C (2001) Biosynthesis and attachment of novel bacterial polyketide synthase starter units. *Nat Prod Rep* 19:70-99

Moreau P, Brandizzi F, Hanton S, Chatre L, Meiser S, Hawes C, Satiat-Jeunemaitre B (2007) The plant ER-Golgi interface: a highly structured and dynamic membrane complex. *J Exp Biol* 58(1):49-64

Morey JS, Monroe EA, Kinney AL, Beal M, Johnson JG, Hitchcock GL, Van Dolah FM (2011) Transcriptomic response of the red tide dinoflagellate, *Karenia brevis*, to nitrogen and phosphorus depletion and addition. *BMC Genomics* 12:346

Moroney JV, Bartlett SG, Samuelsson G (2001) Carbonic anhydrases in plants and algae. *Plant Cell Environ* 24:141-153

Mortimer JC, Laohavisit A, Macpherson N, Webb A, Brownlee C, Battey NH, Davies JM (2008) Annexins: multifunctional components of growth and adaptation. *J Exp Biol* 59:533-544

Moseley JL, Chang C-W, Grossman AR (2006) Genome-based approaches to understanding phosphorus deprivation responses and PSR1 control in *Chlamydomonas reinhardtii*. *Euk Cell* 5:26-44

Mulroth A, Keshuai L, Rokke G, Winge P, Olsen Y, Hohmann-Marriott MF, Vadstein O, Bones AM (2013) Pathways of lipid metabolism in marine algae, co-expression network, bottlenecks and candidate genes for enhanced production of EPA and DHA in species of Chromista. *Mar Drugs* 11:4662-4697

Murakami-Murofushi K, Nishikawa K, Hirakawa E, Murofushi H (1997) Heat stress induces a glycosylation of membrane sterol in myxoamoebae of a true slime mold, *Physarum polycephalum*. *J Biol Chem* 272:486–489

Murata M, Yasumoto T (2000) The structure elucidation and biological activities of high molecular weight algal toxins: maitotoxin, prymnesins and zooxanthellatoxins. *Nat Prod Rep* 17:293–314

Nakahara T, Yokochi T, Higashihara T, Tanaka S, Yaguchi T, Honda D (1996) Production of docosahexaenoic and docosapentaenoic acids by *Schizochytrium* sp. isolated from Yap islands. *J Am Oil Chem Soc* 73:1421-1426

Neumann U, Brandizzi F, Hawes CR (2003) Protein transport in plant cells: in and out of the Golgi. *Ann Bot* 92:167-180

Nickel W (2010) Pathways of unconventional protein secretion. *Curr Opin Biotechnol* 21:621–626

Niewiadomski P, Knappe S, Geimer S, Fischer K, Schulz B, Unte US, Rosso MG, Ache P, Flugge U-I, Schneider A (2005) The Arabidopsis plastidic glucose 6-phosphate/phosphate translocator GPT1 is essential for pollen maturation and embryo sac development. *Plant Cell* 17(3):760-775

Nightingale TD, Cutler DF, Cramer LP (2012) Actin coats and rings promote regulated exocytosis. *Trends Cell Biol* 22(6):329-337

Nikolau BJ, Ohlrogge JB, Wurtele ES (2003) Plant biotin-containing carboxylases. *Arch Biochem Biophys* 414:211-222

124

Niu X, Bressan RA, Hasegawa PM, Pardo JM (1995) Ion homeostasis in NaCl stress environments. *Plant Physiol* 109:735-742

O'Fallon JV, Busboom JR, Nelson ML, Gaskins CT (2007) A direct method for fatty acid methy ester synthesis: Application to wet meat tissues, oils, and feedstuffs. *J Anim Sci* 85(6):1511-1521

Ohlrogge J, Browse J (1995) Lipid biosynthesis. *Plant Cell* 7:957-970

Ojangu EL, Jarve K, Paves H, Truwe E (2007) *Arabidopsis thaliana* myosin XIK is involved in root hair as well as trichome morphogenesis on stems and leaves. *Protoplasma* 230:193-202

Oliver DJ, Nikolau BJ, Wurtele ES (2009) Acetyl-CoA - Life at the metabolic nexus. *Plant Sci* 176:597-601

Olli K, Trunov K (2007) Self-toxicity of *Prymnesium parvum* (Prymnesiophyceae). *Phycologia* 46:109-112

Otterstrom CV, Steelmann-Nielson E (1940) Two cases of extensive mortality in fishes caused by flagellate *Prymnesium parvum* Carter. *Reports of the Danish Biological Station* 44:4-24

Paasche E (1998) Roles of nitrogen and phosphorus in coccolith formation in *Emiliania huxleyi* (Prymnesiophyceae). *Eur J Phycol* 33:33–42

Padan E, Schuldiner S (1996) Bacterial Na$^+$/H$^+$ antiporters: molecular biology, biochemistry, and physiology. In: Konings WN, Kaback HR, Lolkema JS (eds) Handbook of Biological Physics. Elsevier Science, Amsterdam, the Netherlands, p 501-531

Pal D, Khozin-Goldberg I, Cohen Z, Boussiba S (2011) The effect of light, salinity, and nitrogen availability on lipid production by *Nannochloropsis* sp. *Appl Microbiol Biotechnol* 90:1429-1441

Pao SS, Paulsen IT, Saier MH (1998) Major facilitator superfamily. *Microbiol Mol Biol Rev* 62:1-34

Paster Z (1973) Pharmacology and mode of action of prymnesin. In: Martin DF, Padilla GM (eds) Marine Pharmacognosy: Action of Marine Biotoxins at the Cellular Level. Academic Press, New York, NY, p 241-263

Paulsen IT, Brown MH, Skurray RA (1996) Proton-dependent multidrug efflux pumps. *Microbiol Rev* 60:575-608

Pearson LA, Hisbergues M, Borner T, Dittman E, Neilan BA (2004) Inactivation of an ABC transporter gene, *mcyH*, results in loss of microcystin production in the Cyanobacterium *Microcystis aeruginosa* PCC 7806. *Appl Environ Microbiol* 70(11):6370-6378

Peer WA (2011) Plasma membrane protein trafficking. In: Murphy AS, Peer W, Schulz B (eds) The Plant Plasma Membrane, Vol. 19. Springer-Verlag, Berlin Heidelberg, Germany, p 31-56

Perez-Prat E, Narasimhan ML, Binzel ML, Botella MA, Chen Z, Valpuesta V, Bressan RA, Hasegawa PM (1992) Induction of a putative Ca^{2+}-ATPase mRNA in NaCl-adapted cells. *Plant Physiol* 100:1471-1478

Pfeifer BA, Khosla C (2001) Biosynthesis of polyketides in heterologous hosts. *Microbiol Mol Biol Rev* 65(1):106-118

Pick U, Ben-Amotz A, Karni L, Seebergts CJ, Avron M (1986) Partial characterization of K^+ and Ca^{2+} uptake systems in the halotolerant alga *Dunaliella salina*. *Plant Physiol* 81:875-881

Plaxton WC, Carswell MC (1999) Metabolic aspects of the phosphate starvation response in plants. In: Lerner HR (ed) Plant Responses to Environmental Stresses: From Phytohormones to Genome Reorganization. Marcel Dekker, Inc., New York, NY, p 350-372

Pokotylo I, Pejchar P, Potocký M, Kocourková D, Krčková Z, Ruelland E, Kravets V, Martinec J (2013) The plant non-specific phospholipase C gene family. Novel competitors in lipid signalling. *Prog Lipid Res* 52:62–79

Popov KM, Kedishvill NY, Harris RA (1992) Coenzyme A- and NADH-dependent esterase activity of methylmalonate semialdehyde dehydrogenase. *Biochim Biophys Acta* 1119(1):69-73

Poste G, Allison AC (1973) Membrane fusion. *Biochim Biophys Acta* 300:421-465

Putman M, van Heen HW, Konings WN (2000) Molecular properties of bacterial multidrug transporters. *Microbiol Mol Biol Rev* 64:672-693

Qi B, Beaudoin F, Fraser T, Stobart AK, Napier JA, Lazarus CM (2002) Identification of a cDNA encoding a novel C18-Δ9 polyunsaturated fatty acid-specific elongating activity from the docosahexaenoic acid (DHA)-producing microalga, *Isochrysis galbana*. *FEBS Lett* 510:159–165

Quist TM, Sokolchik I, Shi H, Joly RJ, Bressan RA, Maggio A, Narsimhan M, Li X (2009) HOS3, an ELO-like gene, inhibits effects of ABA and implicates a S-1-P/ceramide control system for abiotic stress responses in *Arabidopsis thaliana*. *Mol Plant* 2(1):138-151

Rausch C, Bucher M (2002) Molecular mechanisms of phosphate transport in plants. *Planta* 216:23-37

Raymond CK, Howaldstevenson I, Vater CA, Stevens TH (1992) Morphological classification of the yeast vacuolar protein sorting mutants- evidence for a prevacuolar compartment in class E *vps* mutants. *Mol Biol Cell* 3:1389-1402

Rea PA, Li ZS, Lu YP, Drozdowicz YM, Martinoia E (1988) From vacuolar GS-X pumps to multispecific ABC transporters. *Annu Rev Plant Physiol Plant Mol Biol* 49:727-760

Read BA, Kegel J, Klute MJ, Kuo A, Lefebvre SC, Maumus F, Mayer C, Miller J, Monier A, Salamov A, Young J, Aguilar M, Claverie JM, Frickenhaus S, Gonzalez K, Herman EK, Lin YC, Napier J, Ogata H, Sarno AF, Shmutz J, Schroeder D, de Vargas C, Verret F, von Dassow P, Valentin K, Van de Peer Y, Wheeler G, *Emiliana huxleyi* Annotation Consortium, Dacks JB, Delwiche CF, Dyhrman ST, Glockner G, John U, Richards T, Worden AZ, Zhang X, Grigoriev IV (2013) Pan genome of the phytoplankton *Emiliana* underpins its global distribution. *Nature* 499:209-213

Reggiori F, Tucker KA, Stromhaug PE, Klionsky DJ (2004) The Atg1-Atg13 complex regulates Atg9 and Atg23 retrieval transport from the pre-autophagosomal structure. *Dev Cell* 6(1):79-90

Reich K, Bergmann F, Kidron M (1965) Studies on the homogeneity of prymnesin, the toxin isolated from *Prymnesium parvum* Carter. Toxicon 3:33-39

Reis VM, Oliveira LS, Passos RMF, Viana NB, Mermelstein C, Sant'Anna C, Pereira RC, Paradas WC, Thompson FL, Amado-Filho GM, Salgado LT (2013) Traffic of secondary metabolites to cell surface in the red alga *Laurencia dendroidea* depends on a two-step transport by the cytoskeleton. *PLOS One* 8(5):e63929

Renaud SM, Parry DL (1994) Microalgae for use in tropical aquaculture II: Effect of salinity on growth, gross chemical composition and fatty acid composition of three species of marine microalgae. *J Appl Phycol* 6:347-356

Rezanka T (1989) Very-long-chain fatty acids from the animal and plant kingdoms. *Prog Lipid Res* 28:147-187

Robert SS, Petrie JR, Zhou XR, Mansour MP, Blackburn SI, Green AG, Singh SP, Nichols PD (2009) Isolation and characterisation of a Δ5-fatty acid elongase from the marine microalga *Pavlova salina*. *Mar Biotechnol* 11:410– 418

Roessler PG (1990) Environmental control of glycerolipid metabolism in microalgae: commercial implications and future research directions. *J Phycol* 26:393-399

Robinson MD, McCarthy DJ, Smyth GK (2009) edgeR: a Bioconductor package for differential expression analysis of digital gene expression data. *Bioinformatics* 26(1):139-140

Romantsov T, Guan Z, Wood JM (2009) Cardiolipin and the osmotic stress responses of bacteria. *BBA– Biomembranes* 1788(10):2092-2100

Roze LV, Chanda A, Linz JE (2011) Compartmentalization and molecular traffic in secondary metabolism: a new understanding of established cellular processes. *Fungal Genet Biol* 48(1):35-48

Sacher M, Barrowman J, Wang W, Horecka J, Zhang Y, Pyapaert M, Ferro-Novick S (2001) TRAPP I implicated in the specificity of tethering to ER-to-Golgi transport. *Mol Cell* 7:433-442

Saeed AI, Sharov V, White J, Li J, Liang W, Bhagabati N, Braisted J, Klapa M, Currier T, Thiagarajan M, Sturn A, Snuffin M, Rezantsev A, Popov D, Ryltsov A, Kostukovich E, Borisovsky I, Liu Z, Vinsavich A, Trush V, Quackenbush J (2003) TM4: a free, open-source system for microarray data management and analysis. *Biotechniques* 34:374-378

Salgado LT, Viana NB, Andrade LR, Leal RN, de Gama BAP, Attias M, Pereira RC, Amado Filho GM (2008) Intra-cellular storage, transport and exocytosis of halogenated compounds in marine red alga *Laurencia obtusa*. *J Struct Biol* 162:345-355

Sambrook J, Russell DW (2006) Purification of nucleic acids by extraction with phenol:chloroform. *Cold Spring Harb Protoc* Doi:10.1101/pdb.prot4455

Sarig S (1989) Introduction and the state of art of aquaculture. In: Shilo M, Sarig S (eds) Fish Culture in Warm Water Systems: Problems and Trends. CRC Press, Boca Raton, FL, p 1-19

Sayanova O, Haslam RP, Caleron MV, Lopez NR, Worthy C, Rooks P, Allen MJ, Napier
JA (2011) Identification and functional characterisation of genes encoding the
omega-3 polyunsaturated fatty acid biosynthetic pathway from the
coccolithophore *Emiliana huxleyi*. *Phytochemistry* 72:594-600

Sayed OH (2003) Chlorophyll fluorescence as a tool in cereal crop research.
Photosynthetica 41:321-330

Schapire AL, Voigt B, Jasik J, Rosado A, Lopez-Cobollo R, Menzel D, Salinas J,
Mancuso S, Valpuesta V, Baluska F, Botella MA (2008) Arabidopsis
synaptotagmin 1 is required for the maintenance of plasma membrane integrity
and cell viability. *Plant Cell* 20:3374-3388

Schneider CA, Rasband WS, Eliceiri KW (2012) NIH Image to ImageJ: 25 years of
image analysis. *Nat Methods* 9:671-675

Schubert H, Fulda S, Hagemann M (1993) Effects of adaptation to different salt
concentrations on photosynthesis and pigmentation of the cyanobacterium
Synechocystis sp. PCC 6083. *J Plant Physiol* 142:291-295

Schwer B, Bunkenborg J, Verdin RO, Andersen JS, Verdin E (2006) Reversible lysine
acetylation controls the activity of the mitochondrial enzyme acetyl-CoA
synthetase 2. *Proc Natl Acad Sci USA* 103(27):10224-10229

Sengco MR, Hagstrom JA, Graneli E, Anderson DM (2005) Removal of *Prymnesium
parvum* (Haptophyceae) and its toxins using clay minerals. *Harmful Algae* 4:261-
274

Sharma KK, Schuhmann H, Schenk PM (2012) High lipid induction in microalgae for biodiesel production. *Energies* 5:1532-1553

Shen B (2003) Polyketide biosynthesis beyond the type I, II and III polyketide synthase paradigms. *Curr Opin Chem Biol* 7:285-295

Shilo M (1967) Formation and mode of action of algal toxins. *Bacteriol Rev* 31:180-193

Shilo M (1971) Toxins of chrysophyceae. In: Kadis S, Ciegler A, Ajl SJ (eds) Microbial Toxins. Academic Press, New York, NY, Vol. 7, p 67-103

Shin OH, Han W, Wang Y, Südhof TC (2005) Evolutionarily conserved multiple C2 domain proteins with two transmembrane regions (MCTPs) and unusual Ca^{2+} binding properties. *J Biol Chem* 280:1641-1651

Silva P, Geros H (2009) Regulation by salt of vacuolar H^+-ATPase and H^+-pyrophosphatase activities and Na^+/H^+ exchange. *Plant Signal Behav* 4(8):718-726

Simonsen S, Moestrup O (1997) Toxicity tests in eight species of *Chrysochromulina* (Haptophyta). *Can J Bot* 75(1):129-136

Singh A, Nigam PS, Murphy JD (2011) Mechanism and challenges in commercialization of algal biofuels. *Bioresour Biotechnol* 102:26-34

Singh SC, Sinha RP, Hader DP (2002) Role of lipids and fatty acids in stress tolerance in cyanobacteria. *Acta Protozool* 41:297

Sirikantaramas S, Yamazaki M, Saito K (2008) Mechanisms of resistance to self-produced toxic secondary metabolites in plants. *Phytochem Rev* 7:467-477

Smith S, Tsai SC (2007) The Type I fatty acid and polyketide synthases: a tale of two megasynthases. *Nat Prod Rep* 24(5):1041-1072

Sokatch JR, Sanders LE, Marshall VP (1968) Oxidation of methylmalonate semialdehyde to propionyl coenzyme A in *Pseudomonas aeruginosa* grown on valine. *J Biol Chem* 243(10):2500-6

Stabell OBK, Pedersen K, Aune T (1993) Detection and separation of toxins accumulated by mussels during the 1988 bloom of *Chrysochromulina polylepis* in Norwegian coastal waters. *Mar Environ Res* 36(3):185-196

Steinke M, Wolfe GV, Kirst GO (1998) Partial characterization of dimethylsulfoniopropionate (DMSP) lyase isozymes in 6 strains of *Emiliana huxleyi*. *Mar Ecol Prog Ser* 175:215-225

Subramaniam S, Fahy E, Gupta S, Sud M, Byrnes RW, Cotter D, Dinasarapu AR, Maurya MR (2011) Bioinformatics and systems biology of the lipidome. *Chem Rev* 111(10):6452-6490

Summers PS, Nolte KD, Cooper AJL, Borgeas H, Leustek T, Rhodes D, Hanson AD (1988) Identification and stereospecificity of the first three enzymes of 3-dimethylsulfoniopropionate biosynthesis in a chlorophyte alga. *Plant Physiol* 116:369-378

Sun Y, Zhou X, Dong H, Tu G, Wang M, Wang B, Deng Z (2003) A complete gene cluster from *Streptomyces nanchangensis* NS3226 encoding biosynthesis of the polyether ionophore nanchangmycin. *Chem Biol* 10(5):431-441

Sunkar R, Bartels D, Kirch HH (2003) Overexpression of a stress-inducible aldehyde dehydrogenase gene from *Arabidopsis thaliana* in transgenic plants improves stress tolerance. *Plant J* 35:452-464

Sutter JU, Sieben S, Hartel A, Eisenach C, Thiel G, Blatt MR (2007) Abscisic acid triggers the endocytosis of the Arabidopsis KAT1 K^+ channel and its recycling to the plasma membrane. *Current Biol* 17:1396-1402

Sze H, Li X, Palmgren MG (1999) Energization of plant cell membranes by H^+-pumping ATPases: regulation and biosynthesis. *Plant Cell* 11:677-689

Sztul E, Lupashin V (2006) Role of tethering factors in secretory membrane traffic. *Am J Physiol Cell Physiol* 290:C11-26

Takabe T, Incharoensakdi A, Arakawa K, Yokota S (1988) CO_2 fixation rate and RuBisCO content increase in the halotolerant cyanobacterium, *Aphanothece halophytica,* grown in high salinities. *Plant Physiol* 88:1120-1124

Talebi AF, Tabatabaei M, Mohtashami SK, Tohidfar M, Moradi F (2013) Comparative salt stress study on intracellular ion concentration in marine and salt-adapted freshwater strains of microalgae. *Nat Sci Biol* 5(3):309-315

Teo SS, Ho CL, Teoh S, Rahim RA (2009) Transcriptomic analysis of *Gracilaria changii* (Rhodophyta) in response to hyper- and hypoosmotic stresses. *J Phycol* 45:1093-1099

134

Teshima S, Yamasaki S, Kanazawa A, Hirata H (1983) Effect of water temperature and salinity on eicosapentaenoic acid level of marine *Chlorella*. *Bull Jpn Soc Sci Fish* 549:805

Theodoulou FL, Eastmond PJ (2012) Seed storage oil catabolism: a story of give and take. *Curr Opin Plant Biol* 15:322-328

Thompson GA (1996) Lipids and membrane function in green algae. *Biochim Biophys Acta* 1302:17-45

Thorpe C, Kim JJ (1995) Structure and mechanism of action of the acyl-CoA dehydrogenases. *FASEB J* 9(9):718–725

Thorvaldsdóttir H, Robinson JT, Mesirov JP (2013) Integrative Genomics Viewer (IGV): high-performance genomics data visualization and exploration. *Brief Bioinform* 14:178-192

Tuteja R (2005) Type I signal peptidase: An overview. *Arch Biochem Biophys* 441:107-111

Ulitzur S, Shilo M (1970) Procedure for purification and separation of *Prymnesium parvum* toxins. *Biochim Biophys Acta* 201:350–363

Ulitzur S, Shilo M (1964) A sensitive assay system for determination of the ichthyotoxicity of *Prymnesium parvum*. *J Gen Microbiol* 36:161–169

Valentin HE, Lincoln K, Moshiri F, Jensen PK, Qi Q, Venkatesh TV, Karunanandaa B, Baszis SR, Norris SR, Savidge B, Gruys KJ, Last RL (2006) The *Arabidopsis* vitamin E pathway gene5-1 mutant reveals a critical role for phytol kinase in seed tocopherol biosynthesis. *Plant Cell* 18:212–224

Van Dolah FM, Lidie KB, Monroe EA, Bhattacharya D, Campbell L, Doucette GJ, Kamykowski D (2009) The Florida red tide dinoflagellate *Karenia brevis*: New insights into cellular and molecular processes underlying bloom dynamics. *Harmful Algae* 8:562-572

Van Dolah FM, Zippay ML, Pezzolesi L, Rein KS, Johnson JG, Morey JS, Wang Z, Pistocchi R (2013) Subcellular localization of dinoflagellate polyketide synthases and fatty acid synthase activity. *J Phycol* 49:1118-1127

Viso AC, Marty JC (1993) Fatty acids from 28 marine microalgae. *Phytochemistry* 34:1521-1533

Volkman JK, Smith DJ, Eglinton G, Forsberg TEV, Corner EDS (1981) Sterol and fatty acid composition of four marine Haptophycean algae. *J Mar Biol Assoc UK* 61:509-527

Walczak HA, Dean JV (2000) Vacuolar transport of the glutathione conjugate of *trans*-cinnamic acid. *Phytochem* 53:441-446

Wallis JG, Browse J (1999) The Δ8-desaturase of *Euglena gracilis*: An alternate pathway for synthesis of 20-carbon polyunsaturated fatty acids. *Arch Biochem Biophys* 365(2):307-316

Wamer J, McIntosh K (2009) How common are extraribosomal functions of ribosomal proteins? *Mol Cell* 34:3-11

Warmka J, Hanneman J, Lee J, Amin D, Ota I (2001) Ptc1, a type 2C ser/thr phosphatase, inactivates the HOG pathway by dephosphorylating the mitogen-activated protein kinase Hog1. *Mol Cell Biol* 21:51-60

Weisiger RA (1996) When is a carrier not a membrane carrier? The cytoplasmic transport of amphipathic molecules. *Hepatology* 24(5):1288-1295

Weissbach A, Legrand C (2012) Effect of different salinities on growth and intra- and extracellular toxicity of four strains of the haptophyte *Prymnesium parvum*. *Aquat Microb Ecol* 67:139-149

Whyte JRC, Munro S (2002) Vesicle tethering complexes in membrane traffic. *J Cell Sci* 115:2627-2637

Wilkinson BM, Esnault Y, Craven RA, Skiba F, Fieschi J, Kepes F, Stirling CJ (1997) Molecular architecture of the ER translocase probed by chemical crosslinking of Sss1p to complementary fragments of Sec61p. *EMBO J* 16(15):4489-4795

Winsor B, Schiebel E (1979) Review: An overview of the *Saccharomyces cerevisiae* microtubule and microfilament cytoskeleton. *Yeast* 13:399-359

Wurch LL, Haley ST, Orchard ED, Gobler CJ, Dyhrman ST (2011) Nutrient-regulated transcriptional responses in the brown tide-forming alga *Aureococcus anophagefferens*. *Environ Microbiol* 13(2):468-481

Wutipraditkul N, Waditee R, Incharoensakdi A, Hibino T, Tanaka Y, Nakamura T, Shikata M, Takabe T, Takabe T (2005) Halotolerant cyanobacterium *Aphanothece halophytica* contains NapA-type Na$^+$/H$^+$ antiporters with novel ion specificity that are involved in salt tolerance at alkaline pH. *Appl Environ Microbiol* 71:4176-4184

Xie Z, Klionsky DJ (2007) Autophagosome formation: core machinery and adaptations. *Nat Cell Biol* 9:1102–1109

Yaguchi T, Tanaka S, Yokochi T, Nakahara T, Higashihara T (1997) Production of high yield of docosahexaenoic acid by *Schizochytrium* sp. strain SR21. *J Am Oil Chem Soc* 74:1431-1434

Yang I, Beszteri S, Tillman U, Cembella A, Uwe J (2011) Growth- and nutrient-dependent gene expression in the toxigenic marine dinoflagellate *Alexandrium minutum*. *Harmful Algae* 12:55-69

Yariv J, Hestrin S (1961) Toxicity of the extracellular phase of *Prymnesium parvum* cultures. *J Gen Microbiol* 24:165–175

Yasumoto T, Underdahl B, Aune T, Hormazabal V, Skulberg OM, Oshima Y (1990) In: Granéli E, Sundström B, Edler L, Anderson DM (eds) Toxic marine phytoplankton. Elsevier Science Publishers, New York

Yazaki K (2006) ABC transporters involved in the transport of plant secondary metabolites. *FEBS Lett* 580:1183-1191

Yorimitsu T, Klionsky DJ (2005) Atg11 links cargo to the vesicle-forming machinery in the cytoplasm to vacuole targeting pathway. *Mol Biol Cell* 16:1593–1605

Young AJ, Collins JC, Russell G (1987) Solute regulation in the euryhaline marine alga *Enteromorpha prolifera*. *J Exp Bot* 38:1309-1324

Zhang H, Hou Y, Miranda L, Campbell DA, Sturm NR, Gaasterland T, Lin S (2007) Spliced leader RNA trans-splicing in dinoflagellates. *Proc Natl Acad Sci USA* 104:4618–4623

Zhang J, Ruhlman TA, Mower JP, Jansen RK (2013) Comparative analyses of two Geraniaceae transcriptomes using next-generation sequencing. *BMC Plant Biol* 13:228

Zhang Y, Frohman MA (1997) Using rapid amplification of cDNA ends (RACE) to obtain full-length cDNAs. *Meth Mol Biol* 69:61-87

Zhang H, Zhai J, Mo J, Li D, Song F (2012) Overexpression of rice sphingosine-1-phosphate lyase gene OsSPL1 in transgenic tobacco reduces salt and oxidative stress tolerance. *J Integr Plant Biol* 54(9):652-662

Zheleznova EE, Markham P, Edgar R, Bibi E, Neyfakh AA, Brennan RG (2000) A structure-based mechanism for drug binding by multidrug transporters. *Trends Biochem Sci* 25:39-43

Zhila N, Kalacheva G, Tatiana V (2011) Effect of salinity on the biochemical composition of the alga *Botryococcus braunii Kütz* IPPAS H-252. *J Applied Phycol* 23(1):47-52

Zhou XR, Robert SS, Petrie JR, Frampton DM, Mansour MP, Blackburn SI, Nichols PD, Green AG, Singh SP (2007) Isolation and characterization of genes from the marine microalga *Pavlova salina* encoding three front-end desaturases involved in

docosahexaenoic acid biosynthesis. *Phytochemistry* 68:785–796

Zhu G, LaGier MJ, Stejskal F, Millership JJ, Cai X, Keithly JS (2002) *Cryptosporidium parvum*: the first protest known to encode a putative polyketide synthase. *Gene* 298-79-89

Zhu L, Zhang X, Ji L, Song X, Kuang C (2007) Changes of lipid content and fatty acid composition of *Schizochytrium limacinum* in response to different temperatures and salinities. *Process Biochem* 42:210-214

Vita

Aimee Elizabeth Talarski was born in Hartford, CT. Following graduation from Lewis S. Mills High School in Burlington, CT in 1995, Aimee entered Central Connecticut State University in New Britain, CT. In 1996, she transferred to the University of Connecticut in Storrs, CT and received a Bachelor of Science with a major in Diagnostic Genetic Sciences in 1999. For her final semester at the University of Connecticut, she relocated to New Orleans, LA to participate in a clinical cytogenetics rotation at the Tulane University Hayward Genetics Center in New Orleans, LA. For the following 5 years (2000-2005), she was employed as a cytogenetic technologist at Children's Hospital of New Orleans. In 2002, she entered graduate school at Louisana State University Health Sciences Center in New Orleans, LA. She attended classes part-time while still working full-time, and obtained her Master of Science in Genetics in 2006. Following Hurricane Katrina, she relocated to Austin, TX in 2006, and obtained employment at the University of Texas at Austin in the lab of Dr. John W. La Claire, II. The following year (2007), she began graduate studies at the University of Texas at Austin.

Permanent email address: aimeetalarski@hotmail.com

This dissertation was typed by Aimee Elizabeth Talarski.

141